TECHNISCHE UNIVERSITÄT MÜNCHEN

Fakultät für Maschinenwesen
Lehrstuhl für Mikrotechnik und Medizingerätetechnik

A New Postoperative Adjustable Middle Ear Prosthesis: Design and Validation Aided by a New 3D Printed Functional Middle Ear Model

Ismail Kuru

Vollständiger Abdruck der von der Fakultät für Maschinenwesen der Technischen Universität München zur Erlangung des akademischen Grades eines

Doktor-Ingenieurs (Dr.-Ing.)

genehmigten Dissertation.

Vorsitzender: Prof. Dr.-Ing. Veit Senner

Prüfer der Dissertation:

1. Prof. Dr. rer. nat. Tim C. Lüth
2. Prof. Dr.-Ing. Werner Hemmert
3. Prof. Dr. phil. nat. Hannes Maier

Die Dissertation wurde am 12.11.2018 bei der Technischen Universität München eingereicht und durch die Fakultät für Maschinenwesen am 16.05.2019 angenommen.

Acknowledgments

I thank to Prof. Dr. Tim Christian Lüth for giving me this opportunity. Not only during my doctorate, but from much earlier on, his encouragement has driven me to take challenges and to overcome them by scientific thinking and tinkering.

I was most fortunate to work with Prof. Dr. Hannes Maier from Hannover Medical School. I thank him for being a second supervisor. His guidance helped me to push this work beyond its boundaries. I also thank to Mathias Müller for his contributions to this project.

Of course, this work could not be possible without the professional and personal support of my dear colleagues Eva Graf, Daniel Roppenecker, Johannes Coy, Konrad Entsfellner, Jan Gumprecht, Yannick Krieger, Sandra Brecht, Suat Cömert and Mattias Träger. Also many thanks to Renate Heuser, Cornelia Härtling, Gerhard Ribnitzky and Markus Wörl, who were the backbones of MiMed and of this project as well.

Furthermore, I thank to Thomas Maier-Eschenlohr for initiating this project, to Prof. Dr. Thomas Lenarz for involving Hannover Medical School and to DFG for financing it for four years. In addition, I thank to Prof. Dr. Werner Hemmert and Prof. Dr. Veit Senner for being in my defense committee.

The great impact of my students on this work cannot be left unsaid, which is why I thank to William Bittner, Fernando López Ferrer, Natalia Moreno-Arrones Fuentes, Alexandra Grün, Christina Harbauer, Keiji Higuchi, Mai Han Hoang, Sevan Mazaduryan, Thomas Merk and Martina Roth for their parts.

Moreover, I thank to my parents Nur and Habip Kuru, who encouraged me to pursue a doctorate, as well as my brother Mustafa Kuru and my closest friends in Munich, Maksut Dursun, Can Kuseyri, Zeynep Çokuğraş, Ilgın Eke, Gökçe Yavuz, Tuba Tuncer, Serhan Mercan and Nihan Mercan for their sincere support.

Finally, I thank to my wife Aslı Okur Kuru, who took this path with me. During this exciting journey we did our doctorates together, we got married and we had our son Efe. She was there for me during frustration and joy, for which I cannot be grateful enough.

dedelerime, ninelerime...

Abstract

The middle ear is a mechanically sophisticated organ, which is the bridge between the outer environment and the sensing organ, the inner ear. Its primary functions are to conduct sound from the eardrum to the inner ear and to protect the inner ear from excessive forces caused by ambient pressure variations or other factors. However, the fragile structures of the middle ear are sometimes prone to chronic infections and degeneration. Injuries of these structures lead to an decreased sound conduction, which is called conductive hearing loss and which can be cured by a variety of treatments. One of the most common treatment procedure for permanent injuries is the tympanoplasty type III, a surgical replacement of the ossicles with alloplastic passive prostheses. This is why these prostheses are called ossicular replacement prostheses (ORP).

The state of the art ORPs can restore the sound conduction with a high satisfaction. Nevertheless, their monolithic and rigid construction poses a structural contrast to the mobile and elastic ossicular chain. This structural difference leaves the inner ear without the needed protection, because the ORPs cannot adapt their length after the tympanoplasty. Therefore, the success of the tympanoplasty depends very much on the experience of the surgeon in adjusting the prosthesis length intraoperatively. This deficit results in unsatisfactory operational outcome, which is very common for tympanoplasty. A too loose or too tight prosthesis may result in weak sound conduction, a too short prosthesis might migrate and change position or a too long prosthesis might extrude and injure the eardrum and/or the inner ear. This may even result in an irreversible sensorineural hearing loss.

However, it was revealed during this research on ORPs that these deficits have been addressed by a variety of researchers without being able to test and validate their solutions even under laboratory conditions. The reason for that is the limitations of the environments available for developing new ORPs, which makes it hard to test new concepts in a systematic way.

Having these issues in mind, it was aimed in this thesis to develop a new type of ORP, the postoperative adjustable middle ear prosthesis (PAM). Yet this aim was engaged in a wider perspective by introducing a new method for developing ORPs and dedicated test environments for this method. Prior to PAM, a new 3D printed functional middle ear model

was introduced during this thesis, which allowed to test ORPs systematically during the development. To the best of author's knowledge, this middle ear model was the first of its kind.

After establishing the needed test environment, the PAM was designed and implemented according to the introduced development method and with the aid of the introduced testing environment in four iterations. PAM had an elastic spring-damper-element made of long-term implantable materials. Again to the author's knowledge, this kind of ORP was also not introduced before. By functional experiments on middle ear models and temporal bone preparations, it could be shown that compared to conventional ORPs PAM could compensate forces on the inner ear better and that it could conduct sound less dependent on its intraoperative adjusted length. As a result, it could be shown that PAM had a great potential to reduce both the migration and extrusion risks.

Keywords: Postoperative Adjustable Middle Ear Prosthesis, Ossicular Reconstruction, Tympanoplasty, Spring-Damper-Element.

Contents

List of Figures

List of Tables

CHAPTER 1

Introduction

Millions of people suffer annually from middle ear diseases, such as chronic otitis media (Monasta et al. 2012), which can cause irreversible injuries. One of the most common consequences of these injuries is the conductive hearing loss, which obstructs the ability of the middle ear to conduct sound waves from the outer ear to the inner ear. Being deprived from one of the intrinsic sense organs, needed not only for daily life but even for survival, led humans to investigate it since centuries. And, once the human middle ear was started to be investigated, it revealed itself to be such a unique anatomical structure of extremes, that it fascinated researchers from different backgrounds along the way.

The middle ear is a sophisticated and complex structure with elements of converse properties fulfilling opposed functions in a perfect harmony. It contains the smallest (ossicles) and the hardest bones (temporal bone) in the entire human body, but also softest membranes and ligaments with a thickness of tenth of a millimeter. Despite its delicate structures, it is a robust mechanism that can work under extreme circumstances. Due to its composite construction, it can react alternatively to different kinds of stimulation, although it is utilized with passive mechanical structures.

It is of great wonder how this kind of complexity level and such extreme properties are justified for such a small organ that fulfills supposedly a simple function of sound conduction. To answer this question, one should first understand the structures of the middle ear and its surrounding, but also the isolated functions of the structures and the functions of the middle ear as a whole. Having understood the healthy middle ear, this introduction will address the diseases and the effects of the diseases on the particular structures in the middle ear, especially the conductive hearing loss. This will be followed by a summary of state of the art methods to diagnose from which causes a patient suffers and which therapeutic

treatments for the conductive hearing loss are available. In particular the state of the art passive middle ear prostheses used for these procedures will be described in detail. However, these prostheses have some deficits and they cause severe complications posterior to the treatment, which will be focused in this chapter. Also, the reasons will be explained, why the pursuit to solve these deficits is not a trivial one. Finally, this chapter will end by mention the objectives and the structure of the thesis.

1.1. Anatomy of the Middle Ear

The middle ear (ME) is surrounded by the temporal bone (TB) in the skull, which has a outer hard shell and a hard spongy inner part called mastoid. The TB has four openings to the neighboring structures (see Figure 1.1). The first one is the auditory tube (also called tuba auditiva or Eustachian tube) that is located beneath the tympanic cavity and that opens to the nasopharynx and oval cavity. This opening makes the ME a unique structure, since it is the only organ in the human body with a closed air pocket containing stationary air, yet it is connected to outside and it can be ventilated if necessary. The largest opening is the connection to the ear canal (EC), which is enclosed by the tympanic membrane (TM) and which marks the border to the outer ear (OE). On the opposite side of the TM, the TB has two small openings called oval window (OW) and round window (RW), both are closed by a thin membrane and both are at the border to the inner ear (IE). The OW and the RW have a direct connection through the double spiral of the cochlear filled with a viscous fluid called perilymph, such that pushing the OW inwards results in RW being pushed outwards.

At the border between the OE and ME, the edge of the TM is fixed to TB at the end of the EC with an approx. 45° tilt, so that the surface of the TM is elliptical and bigger than the cross-section of the EC. This is essential for protecting the TM with a narrow EC, while the TM can have a large surface to gather enough sound pressure (SP) waves. The TM itself is an almost transparent membrane with approx. $100\ \mu m$ thickness and a unique funnel-like form. The central part of the TM (the tip of the funnel) is called umbo, which is tented inward and held by the tip of the malleus. Although under optical observation the smooth TM seems tightened, it is a flaccid membrane with a complex pattern of stiff fibers. These fibers are aligned in radial and circular formations around umbo.

The TM and the OW are connected via a chain of three small bones: malleus, incus and the stapes. These small bones are called the ossicles and these three ossicles form the ossicular chain. The malleus is shaped like a hammer, which has a long manubrium (handle), a head and a neck connecting these two. A tiny limb called lateral process protrudes from

the manubrium at the neck. The malleus is connected to the TM along the manubrium and it is connected to the incus through the saddle shaped incudomalleolar joint (IMJ) at the hammer head. The incus, the largest of ossicles, has an anvil shaped body connected to malleus and two limbs protruding from its body. The lenticular process is located at the end of the longer limb, which connects to the stapes through the incudostapedial joint (ISJ). The stirrup shaped stapes is the smallest of the ossicles and of all the bones in the human body. Just like a usual stirrup, the stapes has two branches starting from the oval tread and merging at the tip. The tip of the stirrup and its merging branches are called the stapes superstructure (SSS). The tip of the SSS is connected to the lenticular process of incus. The stirrup tread is called the stapes footplate (SFP), which covers most of the OW and which is connected to the TB through the annular stapedial ligament (short: annular ligament).

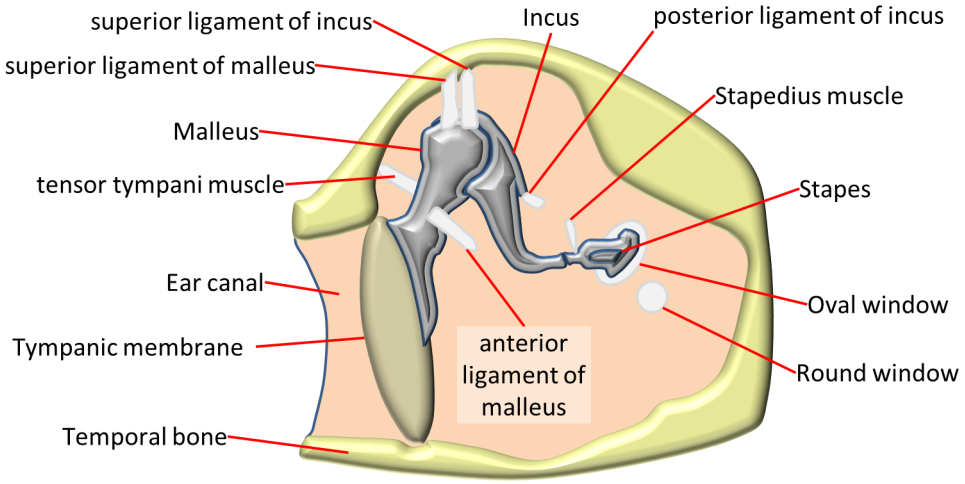

Figure 1.1.: The anatomy of the middle ear.

The ossicular chain of a healthy human is attached to the TB through a complex ligament and muscle formation. A healthy ossicular chain is free of tension, if the air pressure in the ME is equal to the ambient pressure. The malleus is attached to the TB at four points: at the head through superior ligament of malleus, at the lateral process through tensor tympani muscle, at the neck through anterior ligament of malleus and at the notch through lateral ligament of malleus. The Incus is attached to the TB at the top of its body through the superior ligament of incus and at the tip of the short process through posterior ligament of incus. Because the IMJ and the ligaments connect the malleus and the incus very tightly together, this formation is called the malleus-incus-complex (MIC). The superior ligaments

of incus and malleus extend side by side parallel to each other and anchor the MIC to the upper wall of the TB. The posterior ligament of incus and the anterior ligament of the malleus are located collinear and form a pivotal axis around which the MIC rotates. The stapes is attached to the TB through annular ligament at the SFP and through stapedius muscle close to the ISJ.

1.2. Functions of the Middle Ear

The ME has two main functions, which are the protection of the IE from excessive forces and the sound conduction from OE to the IE. To understand the main functions of the ME one must understand its two major modes of motion. First mode is the static mode characterized by the quasi-static pressure changes in the ambient pressure. These pressure differences reach up to kPa-range, they induce macroscopic motions at the TM and ossicles of up to $1\ mm$ and they have a frequency of up to around $1\ Hz$. The dynamic mode is characterized by the SPs in the range of $10\mu Pa$ (hearing threshold) to $1Pa$ ($94dBSPL$) that induce microscopic motions of TM with a magnitude of up to $1\ \mu m$ and with a frequency range of $20 - 20,000\ Hz$. The TM and the ossicles have very complex motion patterns under dynamic mode, depending on the amplitude, speed and the frequency of the forces applied to TM. This section will stay focused on the major motion modes, however, more detail about the motion modes of the TM and ossicles can be found in the literature. An overview of these findings from the research can be found in the following chapters as well as in the previous publications of Kuru et al. (2014) and Kuru et al. (2016a).

Generally speaking, muscles and ligaments of a healthy ME act like tension or torsion springs with viscoelastic properties and they hold the ossicular chain together without preload. Depending on the stiffness and configuration of the springs, they also define the direction as well as the magnitude of the motions of each ossicle. Since these elements act as mechanical elements, we can describe the ossicular chain as a mechanism. Using kinematics to describe and analyze the ME is not only useful as a bridge between the medical and technical aspects of the issue, but it is necessary to understand the deficits of the ossicular chain reconstructions in the later sections, as these procedures are mechanical reconstructions of the ossicular chain.

1.2.1. Static mode

The static mode is predominated by the muscles and ligaments with lower rotatory or linear stiffness, because only higher compliances allow macroscopic motions. In contrast, the

stiff structures allow only a limited freedom of motion and such low compliances become insignificant for the resulting macroscopic motions. Based on the research of Hüttenbrink (1988), the ossicular chain in static mode can be roughly simplified to a mechanism with one DoF. As seen in Figure 1.2, this mechanism transforms the large inward-outward motion of the TM under high ambient pressure changes to a small upward-downward motion at the stapes, which protects the IE from pressure differences that could stress the TM.

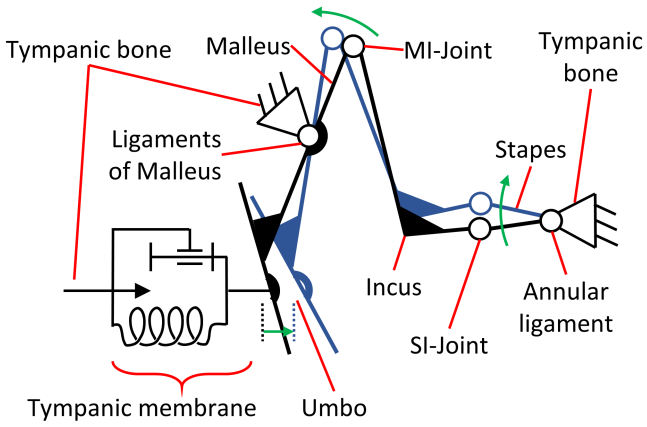

Figure 1.2.: Kinematic model of the ossicular chain as a four bar linkage. The black links show the starting position and the blue links show the tilted position. The green arrows mark the motion direction of the joints.

Analyzing from a kinematic standpoint reveals that this mechanism is a four bar linkage. Just like every four bar linkage, the ossicular chain has a ground link (frame), an input link, a floating link (coupler) and an output link which are the TB, malleus, incus and the stapes respectively. Again, like every four bar linkage this mechanism has four joints, which are all rotating joints in this case. In this configuration, the input link (malleus) is attached to the frame (TB) by a joint pivoting around the axis defined by the collinear posterior ligament of incus and the anterior ligament of malleus. Additionally, TM acts as a bedstop between the malleus and the TB due to its stiff fibers. The saddle formed incudomalleolar joint connects the input link (malleus) to the coupler (incus), which can be modeled as a rotatory joint with a strong torsion spring. The incudostapedial joint couples the coupler (incus) to the output link (stapes). The annular ligament links the output link (stapes) back to the frame (TB). Actually, the annular ligament has multiple DoFs, but its major axis of motion in the static mode rotates the stapes around the long axis of the SFP.

An interesting feature of this joint formation is that all the major axes of motions are

almost parallel to each other in an anterior-posterior direction. Therefore, this mechanism can be further simplified to a planar quadrilateral linkage (also called $4R$- or $RRRR$-linkage). We can show that the ossicular chain has only one DoF by applying Chebychev-Grübler-Kutzbach criterion as seen in Equation 1.1:

$$M = T \cdot (N - 1 - j) + \sum_{i=1}^{j} f_i \tag{1.1}$$

where N is the number of links, j is the number of joints and f_i is the number of DoF each joint has. T gives the number of DoF of an object in space. T is 6 for $3D$ mechanisms, whose links can translate in and rotate around three different spatial axes. T is 3 for spherical mechanisms, whose all joint axes cross in one single point, or for planar mechanisms, whose joint axes are all parallel to each other. In the case of a $4R$-linkage, the links can translate in two directions in the motion plane and rotate around an axis perpendicular to the motion plane.

An increase of the ambient pressure pushes the TM and thus the input link (malleus) inwards. Although the MIC rotate mainly as whole, a less significant relative motion between the input link (malleus) and the coupler (incus) draw them closer. The coupler (incus) tilts the output link (stapes) upwards around the long axis of the SFP. The inward motion of the input link (malleus) comes to a halt, when the TM's strong fibers take up the load. The redirection and limitation of the inward motion result in a tilting of the stapes around the long SFP-axis rather than a inward-outward motion of the SFP. Therefore, the motion component perpendicular to the OW is minimized and the compression on the IE is limited. To conclude, the four bar linkage characteristic of the ossicular chain is ME's primary protection mechanism of the IE against ambient pressure variations.

1.2.2. Dynamic mode

The microscopic high frequency motions of the ossicles in dynamic mode look very different from the $4R$-kinematic with a single DoF in static mode. The main reason for this incoherent change of mode is the non-linear viscoelastic properties of the ligaments. When the SP waves start to vibrate the ossicular chain with a high frequency, the stiff structures and the mass of the structures start to predominate the motion in total. In contrast to the static mode, the whole chain moves almost as a monolithic part rotating around the MIC's main axis of rotation. Although relative motions between ossicles do exist, they are negligibly small and the motion redirection via $4R$-kinematic (from inward-outward motion to stapes tilting) diminishes. Thus, the ossicular chain converts the small inward-outward

motion of the TM to an even much smaller inward-outward motion of stapes, but with a force amplification.

The amplified force transmission is a crucial function of ossicular chain, because this is how the ME conducts the sound waves from the OE to the IE. If the ME would be cut off and the naked OW would gather the sound waves, the $99.9\ \%$ of the sound waves would be reflected at the surface between air and perilymph due to the abrupt change of acoustic impedance, which would demand a much higher sensitivity of the cochlear.

ME achieves the force amplification mainly through three effects. First and most dominant of them is the amplification through area difference between the TM and the SFP, where the area of the TM is roughly 15 times larger than the area of the SFP. The SP wave is gathered and converted into a force oscillation at the TM, which is conducted through the ossicular chain to the SFP. This force oscillation is then focused on a much smaller area of SFP, which causes a much higher SP in the IE.

The second effect is the increased force absorption by reduced acoustic impedance difference at the TM. In fact, this is not a direct amplification, but a reduction of the reflected SP. Since the sound impedance of the TM is much closer to the sound impedance of air and much lower compared to the sound impedance of perilymph, the sound absorption is increased. The third effect is a pure kinematic amplification of force by leverage arm. The line of action of the resulting force by SP lays at the umbo, the tip of the TM. Since the distance between the main axis of the MIC and the umbo is about $1.3 - 2$ times longer than the distance between the main axis of the MIC and the ISJ, the resulting force is amplified by this ratio (Zwicker & Fastl, 2013, p. 25; Schünke et al., 2006, p. 146).

However, there is more than a simple force amplification to it. As described above, the TM has a very unique form and fiber formation. Therefore, the TM has a very unique motion pattern depending on the frequency of the SP, which gives it a mechanical frequency filter property. This phenomenon, which was first introduced by Tonndorf & Khanna (1972) and later agreed by later researchers such as Cheng et al. (2010), shows that up to the first resonance frequency around $1\ kHz$ the TM vibrates inward-outward as a whole membrane. After the resonance frequency its two anterior-posterior halves starts to vibrate in opposite directions. In higher frequencies this phenomena is observed with four quadrants, where the diagonal quadrants vibrate in same phase and the adjacent quadrants vibrate in opposite phases. After $8 - 10\ kHz$ the picture gets very chaotic and does not show a significant pattern, where numerous local vibrations can be observed across the surface of the TM in different incoherent phases.

The motion pattern of the TM has a great effect on hearing, because this phenomenon effects the characteristic transfer function of the ME, which was first investigated by

Rosowski et al. (1990) and standardized as the ASTM Standard F2504.24930-1 (ASTM 2005). The transfer function of the ME is defined as the transformation of the sound pressure level (SPL) at the TM measured in $[dB\ SPL]$ to a displacement of the SFP measured in $[\mu m]$, so that the abscissa of the transfer function is the frequency in $[Hz]$ or $[kHz]$ (in logarithmic order) and the ordinate is the displacement normalized by the SPL in $[dB\ re\ \mu m/Pa]$. The SPL is measured relative to $20\ \mu Pa$, where the minimum SP that can be heard by a human ear at $1\ kHz$ is $3\ dB$. The transfer function has two main regions: the plateau region and the roll-off region. The plateau region is the frequencies up to the first resonance frequency around $1\ kHz$, where the transfer is mostly constant over the frequency range. After the resonance frequency the transfer function declines with a roughly constant gradient. More detailed description including the experimental setup can be found in the Section 3.2.1.

Besides the sound conduction with amplification and filtering, the dynamic mode enables also a protection function in addition to the motion redirection via $4R$-kinematic in the static mode. If the sound is so loud that the nerves in the IE are stimulated excessively, the muscles of the ME at the malleus and stapes pull tight. This reflex decouples the ossicular chain to some degree and reduces the transmission in lower frequencies ($< 2\ kHz$) in order to protect IE.

1.3. Middle ear's Weaknesses and Conductive Hearing Loss

The ME is a robust mechanism that can work under extreme situations, such as $30\ m$ deep under the water or $5000\ m$ above the sea level. However, ME has its own weak points that can effect its structures and therefore its sound conducting function.

First vulnerability of the ME is the infections. Since the auditory tube connects ME to the outside of the body through nasopharynx and oral cavity, which carry infectious bacterial and viral microorganisms by their nature, there is a high risk that these microorganisms can reach the ME cavity (Lenarz & Boenninghaus 2012). Once reached there, ME cavity is a very pleasant medium for microorganisms to reproduce, since the cavity is always wet and it is kept to constant temperature of approx. $36.8\ C$ by the body heat.

Furthermore, the latest findings show that there is a one more effect in play. Patients with auditory tube dysfunction cannot open their auditory tube frequently enough to let air into the ME cavity for ventilation, which is a muscle activated function. As described above, the air can still leave the ME by itself, because the auditory tube functions as a passive valve system as long as it is not activated by the muscles. This one-way air flow leads to a lower air pressure and a lower oxygen level in the ME cavity, which is especially

suitable for reproduction of some bacteria types.

A characteristic case is the infant otitis media, because children have a tight and short auditory tube as well as a weak immune system. Since the ME cavity is very suitable for microorganism migration, it is also a serious risk factor that the infection becomes chronic, which causes the small structures in the ME to degenerate with time. Hence, the chronic ME infections are one of the leading causes for ME parts to change their properties and shape or even disappear altogether.

Another weakness of the ME is its small sized elements, which are packed very dense together. Especially with growing age, the tissues may go under alterations because of various and some times unknown reasons. In these cases, the ossicles but also the ligaments become stiffer, so that altered ossicles fuse with other ossicles and/or with the TB. First of two common cases is the otosclerosis of the MIC, where the superior ligaments alter to a point that the malleus head and incus body start to develop a bony connection to the upper wall of the TB, thus leaving the malleus and the incus immovable. Second case is the immovable stapes, whose annular ligament altered to a point that the SFP is almost incorporated to the OW. Both cases block the ossicular movement and thus the sound conduction.

Of course, infections and ossifications are not the only reasons for an incomplete or immovable ossicular chain and TM. There are countless other causes including alterations, effusions, diseases, pathologies or traumata in ME, which disrupt its abilities such as force amplification and reduction of sound reflection. The patients suffering from these complications loose their ability to hear as a result of the lacking sound conduction in the ME. Therefore, it is called the conductive hearing loss (CHL). To be clear, the CHL patients have intact IEs, which are able to transform mechanical vibrations to electrical signals. Patients with sensorineural hearing loss (SNHL), on the other hand, have a defect IE. Of course, a combination of CHL and SNHL is also possible, since the degeneration and alteration can spread to or occur simultaneously at multiple locations. From this section on, this thesis will focus on the CHL as well as its diagnosis and treatment.

1.4. Diagnose of Conductive Hearing Loss

A central term for describing the diagnose of the CHL is the Air-Bone-Gap (ABG). The ABG is the hearing level difference between the air conduction and the bone conduction. The air conduction is the usual way of hearing of a healthy person. Here, the TM captures the sound waves propagating through the air and vibrate the ossicular chain, which in turn amplifies and conducts the vibrations to the IE. The bone conduction is the stimulation of

the IE directly by vibrating the surrounding bones of TB and skull (e. g. with a tuning fork). This is a known phenomena, which makes us hear all the vibrations in our skull, such as chewing noises while eating a crunchy food. Bone conduction is even utilized by some bone conduction devices to bypass ossicular chain. The perception differences between these two hearing paths help understand which part of the ear is defect.

One of the first developed and still widely used methods to identify CHL is the Rinne Test (Lenarz & Boenninghaus 2012). Here, the physician places a vibrating tuning fork against the mastoid bone of the patient. The patient signalizes the moment, when the vibration of the tuning fork is so weak that it cannot be heard anymore via bone conduction. The physician positions the still vibrating tuning fork quickly in front of the patient's ear. Despite the weaker vibration, a healthy person can once more hear the tuning fork, because the air conduction is normally stronger than the bone conduction. However, a CHL patient cannot hear the tuning fork when it's positioned in front of the ear, because the IE can be stimulated by vibrations (evidence of bone conduction) but the ME is not able to gather and conduct enough SP from air to IE (weak or lost air conduction). Today, Rinne test is not enough to conclude the CHL diagnose, but it is still one of the first choice of physicians for the start. Since it is an easy procedure that can be carried out with a simple tuning fork, even general practitioners or neurologists conduct this test occasionally.

A more modern and comprehensive method to measure the ABG is the audiometry, which has various forms to differentiate between numerous sources of hearing losses by utilizing complex tone and speech tests. The pure tone audiometry (PTA) is a very common objective audiometry test, which measures the hearing levels and loudness discomfort levels of the patients in a wide range of frequencies and levels. Since it is aided by electronic devices, it is not only possible to detect the ABG, but also to measure the intensity of it in $[dB]$ relative to the patient's own hearing (e. g. comparing left and right ears) or relative to an absolute value (e. g. as SPL) and even separately at right and left ears at distinct frequencies.

The tympanometry is a different approach to diagnose CHL, but also other dysfunctions. The aim of this diagnostic procedure is to find out, if the patient's TM has a healthy compliance and if the air pressure in the ME is in balance with the ambient pressure. Both criteria can be tested by changing the air pressure in the isolated EC from -300 dPa to $+300$ dPa, while tone pulses with a frequency of 226 Hz are sent periodically to the TM and the reflected tone pulses are measured simultaneously. Since, the highest TM compliance provides the maximum sound absorption (or the minimum reflection) at the TM surface, the tympanogram can detect at which pressure difference this maximum is reached. A healthy TM should have no tensions under 0 dPa pressure difference, thus it

would have the highest compliance at $0\ dPa$ difference, and it has a maximum compliance of up to $1.5\ ml$. It is important to note that $1.5\ ml$ is a commonly used unit in medical devices describing the equivalent volume, although the physical unit for the compliance is the acoustic $[mho]$, which is "Ohm" written backwards and equals to $[1/Ohm]$.

This method is especially effective to find out dysfunctions in the auditory tube. For example, a minimum sound reflection at a negative pressure difference indicates that the pressure in the ME is lower than the ambient pressure and that the auditory tube evacuates the air more than it lets the air inwards. On the contrary, a minimum sound reflection at a positive pressure difference indicates that the tube is so tight that air cannot leave the ME cavity (e. g. auditory tube blocked by effusions). Here two cases are essential for the CHL: an abnormally high compliance of the TM indicates an ossicular luxation and a normal compliance without stapedius reflex (contraction of the stapedius muscle at sound perception) indicates otosclerosis.

These and other methods such as Weber-test and medical imaging techniques can be utilized to identify cause and degree of the hearing loss, which could not be all named here. This diversity of the diagnostic methods is needed, because there is also a large variety of treatment methods specialized in solving distinct problems. Therefore, it is very essential for the treatment to diagnose the illness accurately.

1.5. Treatment of Conductive Hearing Loss

1.5.1. Overview of the treatments for the hearing organ

The treatment depends very much on the stage and the type of the disease. Since numerous structures and biological mechanisms play a significant role for the ME, there are numerous causes for CHL including complications of biological nature (e. g. infections) or pathological nature (e. g. otosclerosis) as described in the Section 1.3. Hence, various treatments are available for physicians and surgeons to treat almost every complication or disease, from simple conservative methods to high-tech implants. However, the stage of the disease is a more decisive factor for the treatment's complexity and invasiveness. For example, effusion can be treated with decongestant nasal drops and antibiotics at an early stage, but in later stages the effusion becomes a thick glue-like fluid (also called "glue ear") and cannot be evacuated through the auditory tube anymore (Lenarz & Boenninghaus 2012). In this case, a tympanostomy tube is inserted to the TM, which maintains the lacking ventilation of the ME cavity and allows the effusion to be evacuated through it.

A detailed synopsis of the conventional and invasive treatment procedures for management of CHL and SNHL (including mixed hearing loss) was described by Mankekar (2014, p. 26-27) in his book, which helps to get an overview of the whole spectrum of treatments in an iterative arrangement according to the stage of the hearing loss. CHL can be diagnosed by a surgeon (clinical diagnosis) and by using PTA (audiological diagnose). Usually, conservative methods are prioritized in the first treatment attempts, which are mainly medication or wearable hearing aids with sound amplification function. Unfortunately, if the structures of the ME are permanently damaged and it is not possible to recover them, conservative methods cannot reconstruct patient's hearing anymore. At this stage of hearing impairment, patients need reconstructive surgical interventions including ossicular reconstruction surgery with passive implants. If the surgery does not recover the hearing sufficiently, next steps can be using hearing aids in addition to the passive implant. In more severe cases, the OE and ME can be bypassed by inserting an active ME implant, which can vibrate the ossicles or the mastoid actively.

However, a more complicated algorithm must be followed at presence of SNHL, where a large variety of hearing aids and implants as well as their combination can be utilized depending on the severity as well as the progression of CHL and SNHL. In extreme cases cochlear implants can be inserted into the IE or brain stems and mid-brain implants can be inserted into the auditory cortex for direct electrical stimulation of the nervous system, thus bypassing all the mechanical components of the ear. Although this iterative arrangement covers the whole spectrum, the surgeon is not obligated to follow it from its start to end. Considering the stage and progression of the disease but also patient's unique situation (e. g. other medical conditions), the surgeon may start at an arbitrary point and end the treatment even without reconstructing sufficient hearing (e. g. due to old age).

1.5.2. Treatments for conductive hearing loss

Despite the variety of the causes for hearing loss and their treatments, this thesis will focus on the treatment of CHL cases with a level of severity that they cannot be treated with conservative methods but also do not necessitate active implants. One of the oldest and still most widely used standard treatment technique in such cases is the tympanoplasty. This is a surgical procedure, during which the tympanic cavity is opened, the ME structures are reconstructed and the TM is closed back again at the end. Both inspection and surgery are carried out after the TM is opened up and the main objective is to restore the ME functions as well as to cure acute diseases by direct intervention. Tympanoplasty is preferred especially for the treatment of otosclerosis and chronic otitis media, the two most frequent

diseases causing injuries on TM and ossicles. Although tympanoplasty was known since early 20th century, its first systematical classification was introduced by Wullstein (1956, p. 1082), where five cases were distinguished from type I to type V.

Of great interest for this thesis is the tympanoplasty type III, which is carried out, if parts of the patient's ossicular chain is defect, but the SFP is intact and mobile. In general, the tympanoplasty aims to reconstruct the ossicular chain via columella effect by bridging the TM and the SFP through a single column, which is a similar construction to the ossicular chain of the birds. Depending on the stapes' condition, type III is further classified as type IIIA, where the ossicular chain is reconstructed with an intact stapes, and type IIIB, where the SSS is missing or removed during the reconstruction and only the SFP stays intact. Since different factors influence the surgical outcome of the Tympanoplasty, it is difficult to answer the question, whether type IIIA is audiologically better than IIIB (Mankekar 2014, p. 14).

Preparation for surgery and access to middle ear structures

In preparation for the surgery, the spectrum of the pathogenic germs is tested to choose a suitable ear drop and antibiotic. Additionally, the EC is cleaned thoroughly. These steps are especially important for ears with secretion and effusion, so that the amount of germs can be kept at a minimum. If there are polyps in the EC, these can be removed preoperatively for better sight and access to the tympanic cavity.

First step of the surgery is to prepare the OE and TM to access the tympanic cavity. The three incision approaches are called transmeatal, endaural and retroauricular. The transmeatal approach, being the least invasive of three, is the conduction of the surgical procedure through a funnel, so that the EC is not traumatized. Endaural approach allows an easy access to the tympanic cavity and the necessary incisions do not cause a large traumatization of the OE, which shortens the postoperative treatment and aims good esthetic outcome. Furthermore, incisions allow to harvest autografts for reconstructive procedures. The retroauricular approach enables the best sight and access to all ME structures by creating a large flap, which shortens the path to the TM. Since the endaural approach is usually preferred for ossicular reconstructions, this approach will be explained in detail.

The endaural approach begins with an vertical incision between the helix and the tragus (icisura intercartilaginea) and intercartilaginous incision at $12:00$ o'clock position (see Figure 1.3). These incisions are extended by a third circular incision around the EC, in order to create a meatotympanal flap. The circular incision of the meatotympanal flap should be around $2-4mm$ away from the periphery of the TM. While a too wide flap can

become too voluminous for handling intraoperatively, a too narrow flap area may not allow to cover the reconstructed canal wall sufficiently during postoperative EC reconstruction. The circular incision should begin at $6:00$ o'clock position, reach the intercartilaginous incision and go on until $1:00$ o'clock (approx. $210°$). This results in a triangular incision. The incisions are followed by the mobilization of the skin to create an EC skin flap. The canal walls can be drilled for better sight and access. If needed, a U-shaped incision can be placed at the $6:00$ o'clock position to create a skin flap. This incision allows to flap the skin on to the TM and drill the anterior canal wall for canal enlargement.

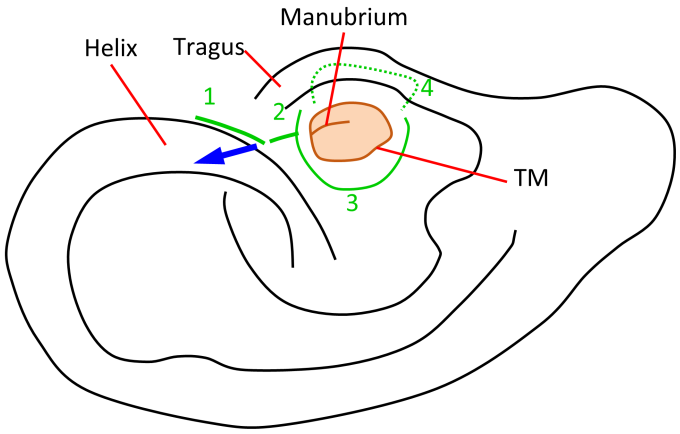

Figure 1.3.: The green lines show the vertical (1), the intercartilaginous (2) and the circular (3) incisions for the endaural approach on the right ear. The dotted green line shows the optional U-shaped incision (4). The blue arrow points the 12 o'clock direction.

The second step of the surgery is to open the tympanic cavity, for which mainly two techniques are available. First approach is called Canal-Wall-Down, where the posterior canal wall and the lateral attic wall are removed to have an optimal access to the ME cavity. The main advantage of this technique is that it allows TM to stay intact. The removed parts of the attic and canal wall are not reconstructed. The second approach is called the Canal-Wall-Up (CWU) or Intact-Canal-Wall (ICW). This technique aims a minimal trauma at the canal wall and attic wall. If the narrow EC does not allow surgeons to operate through it, parts of the attic and canal wall may be removed, yet they are reconstructed afterwards. An incision in the TM allows surgeons to operate in the tympanic cavity.

Ossicular reconstruction

As described by Theissing et al. (2006, p. 376-380), the standard tympanoplasty type III procedure is the reconstruction of the ossicular chain by using autografts (patient's own ossicles) or by using alloplastic implants (made of biocompatible materials). For reconstruction with autografts, a bent pick is used to drill into the IMJ and luxate the incus. Depending on the intact parts of the ossicles, the incus body or the malleus head can be prepared for the reconstruction. If the malleus and the body of incus are both intact, malleus is left untouched for TM stabilization. Both processes of the incus are cut off and a shallow hole is drilled into the stump of the long process (lenticular process) for placing at the stapes head. If the malleus is intact but not the incus, the head of the malleus is removed with a malleus nipper and a hole is drilled into the stump of the manubrium. The manubrium itself is left intact for TM stabilization. The malleus head or the incus body is held with a suction tube at the round head, so that the drill hole on the other end can be placed at the stapes head. If the malleus is left intact and the incus body was used for reconstruction, incus body can be leaned to the malleus. If necessary, a small notch can be drilled on the incus body for a more robust contact between malleus and incus.

As the researchers gain more experience with alloplastic materials for ossicular reconstructions, it seems like different materials are suitable for different cases (Theissing et al., 2006, p. 370; Strutz & Mann, 2017, p. 352-353). For example, Sennaroglu (2016) and his group uses glass ionomer cement for reconstructions from smaller incus defects up to building a complete columella. Nevertheless, the standard ossicular reconstruction with alloplastic implants is carried out with ossicular replacement prostheses (ORP). While partial prostheses (PORP) are used for type IIIA cases with intact stapes, total prostheses (TORP) are used for type IIIB cases with direct contact to SFP. Similar to the above described standard procedure, the tympanic cavity is opened and the defect parts of the ossicular chain are removed. Then, the prosthesis foot is placed on the stapes head (type IIIA) or the SFP (type IIIB). In case of an immovable ossified SFP, the SFP can be perforated for directly driving the IE with a piston protheses (TORP). The prosthesis foot of the ORPs can be secured by a cartilage shoe or special connectors. After the reconstruction, a cartilage layer is placed on the prosthesis head and the TM is flapped back loosely on the cartilage layer. If needed, the prosthesis can be stabilized by filling the tympanic cavity with absorbable gelfoam. Some details will be described in the Section 1.6.

There are some important measures that must be taken during ossicular reconstructions with ORPs. First of all, the length of the prosthesis has a great impact on the surgical outcome, which will be described in detail in the Section 1.7. Therefore, a great effort

is made for a precise intraoperative measurement of the prosthesis length, which can be carried out by using special measurement instruments, by using instruments with known length for the scaling (e. g. circular knife with a diameter of $2.5\ mm$) or by prosthesis dummies. The prosthesis dummies are usually provided as a set with different known lengths and made of plastic material with a similar shape like the real prosthesis. The surgeon can try out different dummies in order to find the best fitting length. Depending on the measured length, the surgeon picks a ready prosthesis with the desired prosthesis length or picks an adjustable prosthesis and adjusts its length intraoperatively.

Another crucial measure is to harvest a thin cartilage layer of $100 - 400\ \mu m$ to place it as an interface between the prosthesis head and the TM as mentioned above. This measure enables a broader contact surface and a tent shaped fixture of the TM. Finally, the angle between the prosthesis shaft and the SFP should be as close to perpendicular as possible. Otherwise, a great portion of the applied force is lost as a radial component, which can be eliminated by the annular ligament.

Since there are various types of PORPs and TORPs with different materials and shapes, the ORPs will be described in the following section.

1.6. Ossicular Replacement Prostheses

In Germany, about 2700 PORPs and TORPs are implanted yearly (Statistisches Bundesamt 2014), whose shapes and materials are familiar to the surgeons. However, the history of ORPs is as long as the history of tympanoplasty itself (Emmett 1989) and there has been a tremendous development over the past decades. First trials began in the late 1950s by Shea (1958*b*), who also introduced a vein graft for TM closure, and they were carried on by Austin (1963), who used an umbrella-like columella. After its introduction, countless alloplastic prostheses were introduced by researchers around the world in order to overcome some drawbacks of autogenous materials. Throughout the following decades, almost every known implantable and biocompatible material was tested for this purpose, including ceramics, plastics and metals. However, first attempts were mostly unsuccessful due to material failure and extrusion. Theoretical work, such as the patent of Hurst (1973), shows that ORPs the failures led the researchers to introduce more sophisticated solutions that went beyond a simple material research even in very early stages of the ORP development.

1.6.1. Materials for ossicular replacement prostheses

Early trials with implant materials were carried out with vinyl acrylic (Wullstein 1952), polyethylene (Shea 1958*a*), PTFE (polytetrafluoroethylene) (Austin 1963) and stainless steel (Palva et al. 1971). The success rates of these attempts were so low that the general consensus of the early 1970s was to abolish the alloplastic prostheses altogether, especially the ones that were made of hard materials. Ironically, first commercial alloplastic ORP was introduced in the same decade by Shea (1976), which was made of a semi-soft white sponge of high-density polyethylene called plastipore. Although its success rates are debated, this material is still favored by some surgeons.

Another material family for ORP is the ceramics, such as aluminum oxide (Jahnke et al. 1979) or Ceravital (Reck 1983). The most successful member of this family is the hydroxyapatite (HA), which was first introduced by Grote (1984) as a ORP material. Due to its highly biocompatible properties, it is possible to place a prosthesis head made of HA in direct contact with the TM without the need of a cartilage layer. This enables also hybrid combinations with other materials for better handling (Hildmann & Sudhoff 2006).

Latest breakthrough in ORP development was the introduction of titanium in early 1990s by (Dalchow et al. 2001). Titanium is a lightweight, highly biocompatible material and its metallic properties makes it a useful material for prosthesis design and production. As titanium can be forged into thin and complicated yet strong structures, prosthesis heads can be perforated for sight and prosthesis feet can be equipped with clipping mechanisms. As a result, titanium dominates today's choice of alloplastic material for ORP, especially in Europe (Theissing et al. 2006, Strutz & Mann 2017).

1.6.2. Forms of ossicular replacement prostheses

Decades of trials with ORPs narrowed the large spectrum of their form mainly to above mentioned two prosthesis types of PORPs and TORPs (see Figure 1.4). Both have a similar structure with a flat elliptical or round head and a long body. After the implantation, the prosthesis head contacts the cartilage layer that covers the inner side of the TM. Since they differ at the connection point to the stapes, they have different kind of prosthesis feet. PORPs are used for type IIIA tympanoplasty cases, where the stapes is intact. Therefore, its prosthesis foot has a cuplike opening that covers the stapes head. On the other hand, TORPs are used for type IIIB tympanoplasty cases, where the stapes is injured but the SFP is intact. Hence, the prosthesis foot of TORP is attached to the SFP and it has a cylindrical form for a better centering on the SFP.

Although the prosthesis head and foot are characteristic for all PORPs and TORPs, the

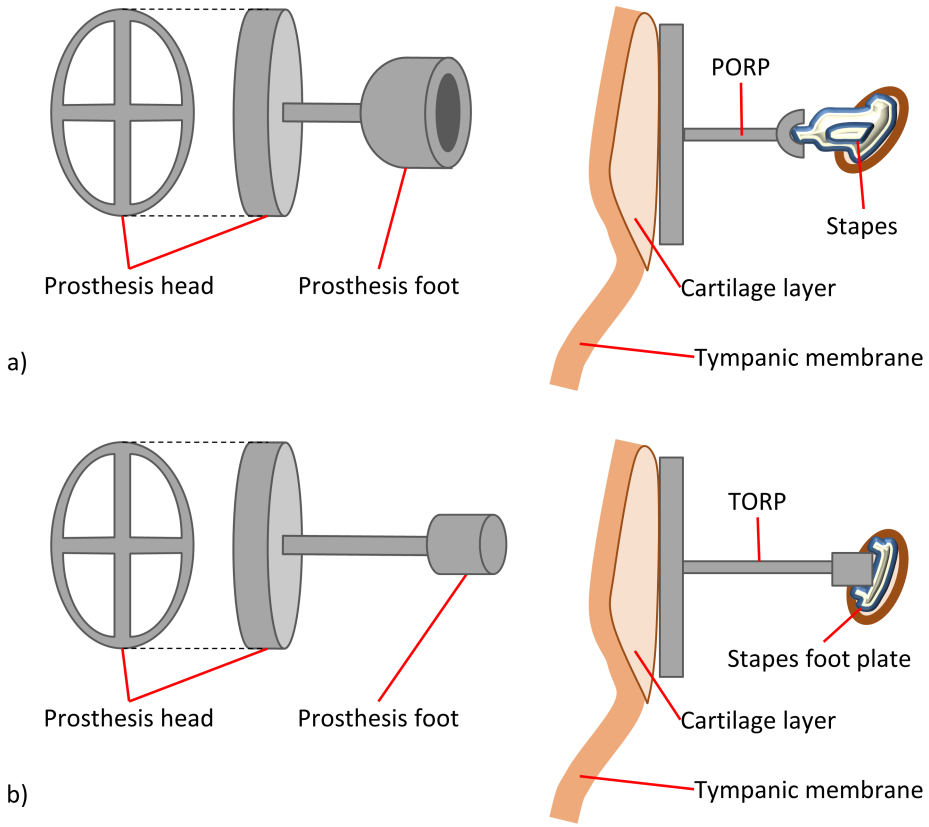

Figure 1.4.: Both PORPs and TORPs have an oval or round prosthesis head, which are placed on the TM with a cartilage layer serving as an interface. a) The prosthesis foot of a PORP has a cuplike shape and it is placed on the SSS. b) The prosthesis foot of a TORP is cylindric and it is placed on the SFP.

physical properties of the prosthesis material results in a variation of shape and surgical handling. For example, mechanical material properties of plastipore or HA necessitate a thick prostheses shaft. Therefore, the handling of these thick prostheses is similar to autografts, where the surgeon cuts and drills the prosthesis to fit it to the anatomy of the patient.

In contrast, the titanium prostheses have a very thin shaft connecting the prosthesis head and the foot. The prosthesis head and the foot have specific forms, which were enhanced throughout the years. Hence, titanium prostheses cannot be cut or drilled arbitrarily. The length adjustment of a titanium prosthesis is carried out by two ways. The surgeon may choose a ready prosthesis with the desired length from a set of prostheses. Second option

is to use an intraoperative adjustable prosthesis with a special clamping mechanism at the prosthesis head. The shaft can be slid along the head to set the prosthesis length and the remaining part of the shaft protruding the prosthesis head can be cut. In contrast to plastipore and HA prostheses, the shaft of a titanium prosthesis can be bent and formed repeatedly during the surgery to adapt its shape to the anatomy of the patient. An exception to this kind is a metal-PTFE-hybrid prosthesis introduced by Fisch et al. (2004) whose shaft can be both bent and cut to adapt it to the anatomy.

1.7. Deficits of the Passive Middle Ear Implants

1.7.1. Deficits of the graft materials

Especially in the early years of the tympanoplasty, surgeons preferred allografts and autografts for ossicular reconstructions. This approach gained further acceptance due to the material related failures of the first alloplastic prostheses as mentioned above. However, the allogeneic transplants proved themselves to be a poor choice very fast, because it was not possible to prevent some infections from spreading through ossicular bone grafts, such as HIV. In contrast, the autografts are still widely in use due to their biological acceptance by the patient's body and due to their suitable material properties for sound conduction. However, autografts show the characteristic deficits of biological materials. For instance, the surgeon must clear the possibility of a contact with the bony walls of the ME, otherwise the autogenic ossicles may develop ankylosis and lose their mobility by merging themselves with the surrounding tissue (Hildmann & Sudhoff 2006, p. 50). Furthermore, the CHL is often caused by chronic infections that degenerate ossicles. If the infections continue or recur after the surgery, they can degenerate the autografts as well and result in poor long-term hearing outcome.

1.7.2. Deficits of the passive middle ear prostheses

The deficits of the autografts made it necessary to develop prostheses made of alloplastic materials. However, to abandon the autogenic materials means to abandon their advantages too. Since an alloplastic material cannot be biologically restructured by the body, it cannot adapt to its surrounding anymore. Therefore, the greatest challenge of the ossicular chain reconstruction with an alloplastic prosthesis, is the determination of the optimal prosthesis shape and its adaptation to the patient's anatomy.

The reconstruction of the ossicular chain with a columella structure removes the DoF of the natural ossicular chain mentioned in the Section 1.2.1. The reduction of DoF obscures

the compensation of static tension, which occurs as a result of the changes in the anatomy (e. g. swellings of the mucosa) or in the external circumstances (e. g. ambient pressure variations). Since the columella made of alloplastic material, which is the largest part of the ossicular reconstruction, cannot react to these changes like the ossicular chain, the surrounding tissues may try to compensate these changes in an undesired way. This is the natural biological mechanism of the body, which ties to minimize the tension.

Especially, the determination of the appropriate prosthesis length becomes a very challenging step (Theissing et al., 2006, p. 378; Strutz & Mann, 2017, p. 352). For example, the surgeon might select the prosthesis length slightly longer than needed to secure the prosthesis grip on the TM as well as SFP and to provide a stronger sound conduction between them. It should not be forgotten that the tissues of the patient's ME are probably weakened prior to the surgery due to infection and/or degeneration. Therefore, this might cause tension on the tissues that is too high in the long term. The tension may trigger further traumatization of the tissues, which typically results with an extrusion through TM, SFP or both. The extrusion refers to the perforation of the TM or SFP by the prosthesis, where the prosthesis head protrudes into the EC or the prosthesis foot protrudes into the IE. Approx. 5% of the patients suffer from this complication (Hess-Erga et al. 2013, Vassbotn et al. 2007), whereas approximately one fifth of the extrusions end up in an irreversible SNHL. The critical tension for extrusion was determined by Zahnert (2011) as low as $5\ mN$, which can be easily exceeded by postoperative changes, even if the length was set right during the surgery.

Nevertheless, an ossicular chain reconstruction free of tension cannot be achieved just by setting the prosthesis length slightly shorter than needed. This approach is not safe and does not secure better surgical outcome, because a loose grip may cause prosthesis migration. The prosthesis migration refers to a postoperative change of the prosthesis position, usually at the prosthesis foot. Typical results of prosthesis migration is a weak contact to the stapes or even lost of contact altogether, because the prosthesis may slip all the way into the ME cavity. Furthermore, the migrated prosthesis foot may contact the medial wall of the ME at the side of the OW, which may cause immobility of the prosthesis. Approximately another 5% of the patients suffer from this kind of complication (Mardassi et al. 2011, Meulemans et al. 2013, Schmerber et al. 2006).

Furthermore, the operational outcome may still be unsatisfactory, if the tension on the TM and SFP is not optimal (Morris et al. 2004). Since the sound conduction is the conduction of an oscillating force, the sound conduction of a particular frequency depends very much on the tension. If the tension is lower than an optimal tension, generally the conduction becomes weaker in all frequencies, because the force cannot be conducted to the SFP

sufficiently. If the tension is higher than optimal, the higher frequencies may be conducted slightly better, but the lower frequencies are conducted significantly weaker, because the higher tension starts to block the prosthesis mobility by saturating the annular ligament.

Including all the cases of extrusion and migration as well as the cases with an ABG greater than 20 dB, approx. 40% of the postoperative outcome is rated as unsatisfactory (Offergeld 2013, Yu et al. 2013). This issue becomes more prominent, if it is considered that these unsatisfactory results include revision operations, which means a second surgery cannot guarantee a better outcome than the first one. Therefore, the options left for the treatment of these cases are more invasive methods such as circumvention of the ME structures by active ME prostheses.

1.8. Developing New Ossicular Replacement Prostheses

1.8.1. Background and state of the art for developing ORPs

Even though, above mentioned challenges with the alloplastic prostheses stayed prominent for the last five decades, there is still no commercially available prosthesis, that can help the surgeons to adjust the tension postoperatively. As mentioned by Emmett (1989) and Hildmann & Sudhoff (2006), prosthesis related complications such as extrusion were already known in the 1950s. Since then, the improvement efforts were focused on the alloplastic material research for better biocompatibility with the ME structures and on new surgical handling methods as well as optimization of known surgical methods. A good example is the invention and improvement of using cartilage interface as a cushion between the TM and the alloplastic prosthesis as well as the dedicated instruments to carry out this step with less effort but higher precision. Hence, the audiological function of the commercial prostheses stayed very much limited to the columella effect.

In contrast, countless ideas have been published aiming the utilization of the passive ME implants with postoperative length adjusting functions. For instance, one of the first patents for more sophisticated solutions to adjust postoperative ORPs was filed in as early as 1970 (Hurst 1973). It is remarkable that following this patent, new ideas came out without interruption throughout the decades until today. The amount of publications in form of research articles, patents or doctoral theses is so high, that all of them could not be possibly cited in this work. Even so, a short review of the proposed solutions will be presented in the Chapter 2, for it is essential in this thesis to highlight the focus of the research groups around the world and the pitfalls of developing a new postoperative adjustable ORPs. For this section, it is important to point out that there is a great barrier between

the ideas and their realization. The alarming fact, that only a few of the countless ideas for postoperative adjustable ORPs could even make it to laboratory tests and literally none of them reached to the level of clinical study is a long lasting discussion in the research community (Hoffstetter 2011).

In order to understand this dilemma, first the circumstances of the prosthesis development for ORPs must be understood. As mentioned above, the highly complex acoustic properties of ME are characterized by various factors and it is very hard to reproduce these factors. This complexity limits the availability of reliable utilities for experiments. Therefore, since Rosowski et al. (1990) could show that the acoustic properties of the human TB preparations from cadavers are close to the ones of the living humans, TB preparations became the only accepted state of the art environment for purposes of testing ME implants (both active and passive).

Research on environments for developing ORPs reveals that there is no other solution that can remotely capable of competing with TB preparations. Of course, there are a variety of solutions proposed by a variety of researchers, which will be presented and discussed in the Chapter 3. However, these solutions lack one or more aspects of the TB preparations and they stay as a part of the state of the research rather than the state of the art.

1.8.2. Deficits of the temporal bone preparations and other limitations

The primary issue with developing ORPs is the lack of suitable experiment environments that supports systematic functional testing of new prostheses with length adjustment capability. Although the TB preparations are the only choice for experiments that the researchers have, they are not necessarily very suitable for reproducible testing of prostheses. The temporal bone preparations provide varying transmission characteristics between individuals (Huber et al. 2001) and their properties change with time. Therefore, a systematic development with temporal bone preparations requires a great deal of effort and time (Stieger et al. 2007). Additionally, both the preparation and the utilization of harvested TBs need experienced personnel with expert level anatomy knowledge, dedicated instruments and conservation infrastructure as well as strict hygiene measures against potential infections.

Another challenge with the testing and validation of new postoperative adjustable ORPs is the complex biological mechanisms in the ME of the patient that designate the success of the surgery in the long term. Although the TB preparations are sufficient for the validation of a new prosthesis' functionality right after the ossicular reconstruction, they cannot simulate the biological aspects for the final and long term validation. Since it is known

that even a small unnatural tension as low as $5\ mN$ is capable of triggering traumatization of the tissues surrounding the prosthesis, the long term effects cannot be precisely investigated with the aid of the TB preparations, which cannot simulate biological mechanisms.

Here, other methods, such as tests on living animals or using integrated sensors with TB preparations and animals, may come in play, which has been used for different purposes such as biocompatibility tests according to ISO 10993. The former one allows detailed evaluation of material biocompatibility under constant conditions from a biochemical perspective. Yet one must consider the deviations between different species in terms of their ME anatomy and physiology, which makes it hard to deduce long term results from stationary animal tests for human patients living under dynamic circumstances. Thus, the risk for inflicting a new unknown type of injury by a new ORP cannot be excluded easily. Integrating sensors is possible and it is used for e.g. said ASTM Standard (ASTM 2005). Nevertheless, due to anatomic discrepancies between the TB preparations, it is not trivial or in some cases not even possible to integrate sensors for measuring physical parameters in $[mN]$ or $[nm]$ range on tissues with highly viscoelastic properties in a reproducible way.

Of course, from a pure scientific standpoint these risks and limitations may not be uncommon for the development of new type of prostheses in general. However there is one more aspect characteristic to developing ORPs, which does not allow to solve this issue just by introducing a new ORP concept. As mentioned above, approx. $3,000$ prostheses are implanted annually in Germany, which makes a total annual revenue of approx. $500,000$ € for a population of approx. $80,000,000$ people. On the one hand, the tests for validating new adjustable ORPs cost in an order of 6-digit numbers without being able to exclude all risks of permanent injuries such as SNHL. On the other hand, there are various methods accepted as standard to enhance the unsatisfactory surgical outcome with commercial ORPs, such as combination of ORPs with hearing aids or substituting ORPs with active ME implants. As a result, the chances of inflicting irreversible injuries to a patient with an unknown complication as well as its legal and financial burden become too large a risk for the ORP manufacturers.

Since this aspect is a financial matter and not scientific, this thesis will not focus on it. However, it is clear that the environments for developing new ORPs do not provide enough safety for ORP developers or manufacturers and it is clear that the difficulties for solving the issue of developing a new postoperative adjustable ORP is not limited to the novelty of the prosthesis design. On the contrary, it is very crucial to underline that a new concept for a postoperative adjustable ORP can only be successful first by solving the issues with the development environment for ORPs with a whole package of new concepts for developing tools tailored for the introduced ORP concept. Thus,

insufficient development environments bring this issue back to the realm of science and therefore it will be a core part of this thesis.

1.9. Objectives and Structure of the Thesis

Considering the deficits of the standard procedures and prostheses as well as the barriers in developing new prostheses, it is of great importance to point out that creating a successful postoperative adjustable ME prosthesis (PAM) must be considered in a wider perspective. This task needs a full concept of prosthesis development, right tools for systematic testing and a new concept idea that can exclude the causes of new complications right at the beginning of the conception as well as that would not jeopardize the uniqueness of the clinical application of the conventional ORPs by introducing a new technical solution.

Therefore, first the issues with the ORP development must be solved, so that the time and effort needed for developing a new ORP can be reduced and the ORP related complications can be predicted more safely. Second, reproducible synthetic functional ME models are needed for systematic testing of new types of ME implants, which allow integration of sensors for different measurements, integration of equipment to simulate different physical situations and modeling of different anatomies including pathological cases.

With these motivations, the Chapter 2 will present the technical requirements that should be met by a new postoperative adjustable ORP and the concept of a process to develop such an ORP. This chapter will include an overview for the state of the research regarding the postoperative adjustable ORPs to distinguish the scientific novelty of proposed prosthesis concept and to present different focuses of the researchers.

Having laid the fundament of this thesis, the Chapter 3 will portray the conception, realization and validation of a new FEM model for the ORP concept and of a new functional ME model, since the first challenge with developing a new ORP is the lack of suitable testing environments. This chapter will give an overview for the state of the research regarding the ME models to underline the scientific novelty of proposed concept.

Next, a new postoperative adjustable PAM will be introduced in Chapter 4 that was developed according to the concept presented in Chapter 2 and tested with the aid of the models introduced in Chapter 3. This chapter will present experiments on TB preparations according to ASTM standards to show the sound conduction characteristics of PAM in comparison to conventional prostheses. Finally, the Chapter 5 will highlight the significant results reached in this work and give an overview of the future work.

CHAPTER 2

The Requirements and Concept

The purpose of this chapter is to lay the fundaments of this thesis by building a bridge between the medical and the technical aspects. Therefore, the first section will include an analysis of the medical problem from a technical perspective to identify the main requirements and further continue to describe and quantify requirements that originate from the medical application. In the second section, the main theoretical concept of this thesis will be introduced, which is proposed to meet the requirements defined in the first section.

2.1. Requirements

2.1.1. The need of postoperative length adjustment from a mechanical standpoint

As shown in Section 1.2.1 of previous chapter, the ossicular chain has a single DoF under quasi-static forces. Mathematically, this can be shown by applying the Chebychev-Grübler-Kutzbach criterion to a mechanism with four links and four parallel joints. However, if the ossicular chain is reconstructed with an ORP, the number of links and joints are reduced, because the prosthesis merges with the ME structures after a successful operation. Therefore, it is essential for this thesis to analyze the reconstructed ossicular chain from a mechanical standpoint to gain a deeper understanding for the deficits of the conventional prostheses and to define the mechanical requirements to overcome these deficits.

As described in the Section 1.5.2 of the last chapter, the classification of tympanoplasty to types IIIA and IIIB depends on which parts of the ossicular chain are intact or defect, alternatively, which portion of the ossicular chain should be reconstructed with the aid of

an ORP. Since the number of joints and links define the number of DoF of a kinematic mechanism, the cases of type IIIA and IIIB must be analyzed separately.

In case of a PORP and an intact stapes combination, the chain has three links (1 : the TB, 2 : the PORP merged with the malleus, 3 : the stapes) and three joints (1 : the TM, 2 : the PORP foot at the SSS, 3 : the annular ligament). With the help of the Equation 1.1, it can be shown that this mechanism has 0 DoF:

$$M = 3 \cdot (3 - 1 - 3) + \sum_{i=1}^{3} f_i = 3 \cdot (-1) + (1 + 1 + 1) = 0$$

for $T = 3, N = 3, j = 3$ and $f_i = 1$. Mechanisms without DoF are called isostatic mechanisms. Due to the kinematic constraints, the links of an isostatic mechanism cannot move relative to each other, although they are linked via moving joints. However, the ability of joint motion makes a crucial characteristic of isostatic mechanisms possible: isostatic mechanisms have no initial preloads. This characteristic can be visualized with an example of a triangular mechanisms with three linear links with same length, which are connected at the tips via rotatory joints (see Figure 2.1). If one of the links would be stretched or contracted, the other two links connected by a joint could move relative to each other and adapt their combined length to the third link. Therefore, best application for isostatic mechanisms can be seen at static structures such as bridges and buildings, where the structure can eliminate inner tensions by itself, for example tensions caused by changing link length due to temperature variations.

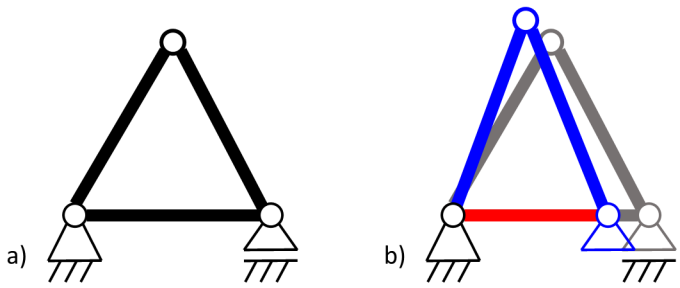

Figure 2.1.: An isostatic mechanism with three linear links with same length, which are connected at the tips via rotatory joints, can be seen a) in its initial configuration and b) during its adaptation to the change in the length of the lower link. In the subfigure b) the static structures are colored black, the initial positions of the structures grey, the length changing link red and the structures moving without geometric changes are colored blue.

However, there is an exception to this crucial property. If the joints are positioned along a straight line, alternatively, if the sum of the lengths of the two shorter links is equal to the length of the third and longest link, a kinematic singularity occurs. In this case, the two shorter links would build a column and act as if they were a singular link, so that a change in any one of the links would cause tension/contraction of the other two links. Since the reconstruction of the ossicular chain aims force conduction through a columella, the joints of the reconstruction with a PORP are aligned exactly in a singularity arrangement. Otherwise, e.g. if the anatomical limitations do not allow the PORP to be implanted coaxial with the stapes, a considerable portion of the conducted force is lost by tilting the stapes instead of moving it inwards/outwards. For the surgical outcome this would mean sound conduction loss or higher ABG. Thus, the intraoperative length adjustment of the PORP becomes very crucial for the surgical outcome, because preloads can occur in singularity arrangement and as explained in the previous chapter preloads may cause high ABG or extrusion.

In case of a TORP and a defect SSS combination, the prosthesis foot usually merges with the SFP and the prosthesis head merges with the TM after a successful surgery. This mechanism has two links (1 : the TB, 2 : the columella consisting of malleus, TORP and SFP) and two joints (1 : the TM and 2 : the annular ligament). By using the Equation 1.1, it can be shown that this mechanism has -1 DoF:

$$M = 3 \cdot (2 - 1 - 2) + \sum_{i=1}^{2} f_i = 3 \cdot (-1) + (1 + 1) = (-1)$$

for $T = 3, N = 2, j = 2$ and $f_i = 1$. Mechanisms with negative DoF are called hyperstatic mechanisms. Just like the isostatic mechanisms, the links of an hyperelastic mechanism cannot move relative to each other. However, their main difference to isostatic mechanisms is that preloads do occur in the hyperstatic mechanisms and the hyperstatic mechanisms cannot eliminate these tensions. The only way to build a hyperstatic mechanism without tension is to make the links the exact right geometry. For an ossicular chain reconstruction with TORP, this means that the length of the TORP must be exactly as long as the distance between the malleus and the SFP. Thus, reconstructions with TORPs are prone to preloads by nature, which occur in the length adjustment step.

As a result of this mechanical analysis, it can be mathematically shown that both PROPs and TORPs are unable to reconstruct the kinematic characteristic of the ossicular chain. Hence, a reconstructed ossicular chain cannot protect the IE from excessive forces. Of course, an experienced surgeon can increase the surgical success by preventing the initial preloads intraoperatively, however, forces caused by postoperative changes (e. g. ambient

pressure changes or scar tissue growth) cannot be avoided as long as the positive DoFs are missing. This issue cannot be solved by a better surgical procedure, but with a PAM.

The required range of motion can be determined by two means. First, the umbo displacement was reported as $610\ \mu m$ ($-207\ \mu m$ to $+403\ \mu m$) in a pressure range of $\pm 3.9\ kPa$ (Hüttenbrink 1988) and as $514\ \mu m$ ($-151\ \mu m$ to $+363\ \mu m$) in a pressure range of $\pm 1.6\ kPa$ (Dirckx & Decraemer 1991). Second, Schmerber et al. (2006) has reported that during revision operations the failed PORPs and TORPs were replaced with longer PORPs and TORPs, which were in average $1.22\ mm$ longer than the replaced ones. Although the higher than average migration rate may indicate a systematic error of the procedure applied in this study, it serves as a good reference value.

To conclude, the main objective is to enable the DoF for macroscopic motions under quasi-static pressure changes. This requires the new ORP to be either an elastic monolithic structure or a multi-body system instead of a rigid columella construction. An increase of at least one DoF for PORP and two DoF for TORP are needed. The range of the relative motion between the malleus and stapes should be at least $1\ mm$.

2.1.2. Maintaining the sound conduction under length adjustment

As mentioned in the Section 1.2.2, the ossicular chain acts as if the ossicles were a monolithic rigid body under dynamic motion, so that the SPs can be conducted from TM to the OW. Therefore, it is the best option so far to reconstruct the ossicular chain as a single columella to provide sufficient sound conduction with minimal losses and minimal ABG. Therefore, arbitrarily increasing the DoF of the reconstructed ossicular chain to positive values would not only eliminate the preloads on the tissues, but it may also eliminate the force conduction all together and thus, the sound conduction would be insufficient.

Indeed, the two functionalities require contrary properties. On the one hand the ultimate way to protect the IE from any preload would be to decouple it from TM or at least connect it through a possibly loosest linkage available. On the other hand, the ultimate way to conduct sound without loss would be to connect TM to IE via an infinitely stiff linkage. For decoupling IE from TM would result in total hearing loss, there would be no need for IE or to protect. Therefore, conventional prostheses tend to fulfill the sound conduction function and neglect the protection. The fact that the annular ligament's stiffness is approx. $3\ N \cdot mm^{-1}$ at the maximum strain (based on values published by Gan et al. (2011)) and the stiffness of a titanium prosthesis with a shaft of $5\ mm$ length and $0.2\ mm$ diameter made of grade 2 titanium (elastic modulus of $105 GPa$) is approx. $660\ N \cdot mm^{-1}$ supports the idea that the conventional solution is in favor of the ultimate sound conduction.

Therefore, the solution should be either a passive mechanism like ossicular chain itself, which reacts to static and dynamic stimulations differently, or it must be an active system, which can sense the type of stimulation and follow external length adjustment commands. Since the articulation of the mechanism is inevitable for both passive and active solutions, the joints separating the links must be combined with a form of force conduction. It is known from the basic mechanics that the options for force conduction are form closure, friction elements, damper elements, spring elements or their combinations. In case of an active length adjustment these options must be combined with a suitable type of actuation.

To achieve both protection and sound conduction functions, it is not enough to utilize the mechanism with a simple force conduction. Instead, the mechanism must react alternatively to different force modes. Referring to the classification of force modes from Section 1.2 Functions of the Middle Ear, the static forces must be compensated and the dynamic forces must be conducted, thus the mechanism should act as a mechanical high-pass filter. Although a certain cutoff frequency cannot be defined, it should be somewhere between $1\ Hz$, because ambient pressure changes occur in a period of approx. $1\ s$, and $20\ Hz$, because a healthy human being can hear a frequency range of $20\ Hz - 20,000\ Hz$. The frequency range that should certainly be conducted is $100\ Hz - 10,000\ Hz$, which is defined in the ASTM standard F2504.24930-1 (ASTM 2005) and which includes the speech relevant hearing range. However, of great interest is the frequency range of $300\ Hz - 3,400\ Hz$, which is accepted as the voice frequency band (or voice band).

2.1.3. Requirements and restrictions based on medical application

In addition to the above mentioned main requirements, there are some restrictions which are not requirements per se, but these restrictions can be seen as boundaries that are originate from the medical application of the PAM. Although narrowing down the scope of solutions at the beginning of concept layout may not be considered constructive in terms of general product development methods, these restrictions are crucial to understand the said barriers between the variety of ideas and the few realized prostheses.

To understand the importance of these restrictions, one must first understand their close relation to the unique position of the tympanoplasty in the large spectrum of procedures for treatment of CHL. If the treatment methods were to be prioritized from least invasive and most conservative to most invasive and least conservative, the tympanoplasty is the least invasive procedure among the surgical procedures and it is the last option, which still aims to reconstruct an ossicular chain. Thus, it is the first choice right after the conservative solutions, if an operation is inevitable. Since this positioning has its limits, a new solution

should not push the tympanoplasty out of this unique position, but rather minimize the deficits of the tympanoplasty and make it even more favorable.

To secure the unique role of the tympanoplasty, the good qualities of the state of the art prostheses and the standard tympanoplasty procedure should not be sacrificed for a new solution. On the one hand, the ossicular reconstruction is a complex procedure for several reasons. There is a huge variety of pathological cases, where one or more ME structures are injured, missing or even deformed, and usually the surgeon gets the full overview of the situation only after opening up the ME intraoperatively. The entrance of the ME is either through the narrow EC or a meticulously opened tunnel through the hardest bone in the body. The working space in the temporal space is also very limited and the operations must be conducted on or close to delicate structures. On the other hand, the surgeons must put up with reasonable amount of time and effort as well as tissue traumatization in order to implant a small and lightweight intraoperative adjustable prosthesis. Normally, the operation takes about $1-2$ hours and the patient is not hospitalized afterwards. Finally, both the surgical procedures and the prostheses stood the test of time and well known to the surgeons. Both were adapted to each other with time, so that a high level of sophistication, specialization and integration was achieved during last decades.

Therefore, a new PAM should not change the surgical or the postoperative procedures, especially the patient's behavior and life standard after healing. Primarily this requires that the new prosthesis should stay within the same geometrical and physical frame of the conventional prostheses for factors regarding both anatomy and surgical handling. A prosthesis larger than its conventional counterparts or a prosthesis system with multiple units increases the invasiveness of the surgery and requires more complicated procedures with special instruments. Such an increase in the complexity jeopardizes the authenticity of a PAM drastically. As mentioned in the Section 1.5 there is already a large spectrum of treatment solutions, especially with active middle ear implants. These implants have multiple units and require an invasive implantation, however, their functions are not limited to bridging the TM to the IE. Instead, they can stimulate the IE actively, which enables a stronger sound amplification compared to passive solutions and even postoperative adaptation of amplification for individual frequencies. Additionally, the current trend is to treat active ME prostheses as an alternative to the passive ORPs, if there is a risk that the patients may not recover their hearing with passive prostheses (e. g. risk of progressive SNHL). Following this line of thought, these restrictions can be formulated into quantified requirements.

The geometry of a new PAM should stay as similar as possible to a conventional ORP. First, the surgeons should be able to implant it as one piece. If the proposed solution should

be an active prosthesis, it should carry all its components (energy storage, actuation, etc.) in a single unit. If the solution is a passive one, the parts should stay connected and they should not necessitate an anchorage other than the TM or the stapes. The diameter of the prosthesis head should be around $4\ mm$, because this size has a suitable surface ratio to an average TM allowing a good stress distribution without blocking the TM mobility and without obstructing the sight to the situs. Any other part of the prosthesis should also be smaller than the prosthesis head, so that the implantation through a narrow opening is possible. The initial length should be adjustable to a range of $3.5\ mm - 7\ mm$, since this range includes the distance between the TM and the SFP for almost all of the patients. Based on the experiments of Mojallal et al. (2009), Nishihara & Goode (1994) and Zahnert (2003), the weight should be less than $50\ mg$, $40\ mg$ or $15\ mg$ respectively.

Since the patient does not need to change the prosthesis or go under any special intervention (besides usual examination) for $10 - 15$ years after a successful operation, the new prosthesis should not necessitate these either. Ideally, this requires a self-sustaining system that does not need an external device or at least a system that does not need the interaction of any person including the patient. The functionality of the prosthesis should survive a lifespan of at least fifteen years or approx. $30,000$ cycles (5 times a day for 15 years) of length adjustments after successful healing. A typical scenario for this is a patient that goes to work by railway and travels through tunnels on a daily basis. Going in and coming out of the tunnel causes both negative and positive pressure changes multiple times every day.

Another important aspect is the interface between the prosthesis and the tissues. The prosthesis head and the prosthesis foot went through an decades of immense optimization. The conventional ORPS are made of highly biocompatible materials and optimized surface structure for avoiding extrusion and migration. It is therefore only natural that these interfaces should be kept as they are. Furthermore, the material and the structure of the new prosthesis should allow the intraoperative manipulation of its shape by cutting or bending, so that the surgeon can adapt the initial prosthesis shape to the patient anatomy. For an easy intraoperative use, the manipulation of prosthesis shape and its implantation should be possible with the standard instruments and the prosthesis should be robust enough to carry out these procedures without additional care.

The last restriction regarding the medical application is the challenges with the ME as medium for implants. As mentioned in Section 1.3, the ME provides a unique habitat that is very suitable for reproduction of microorganisms. This results in excretion of mucosal secretions, effusions due to chronic infections and biofilm formations on prosthesis surface, which can make the ME a hostile medium for ORPs. Therefore, PAMs with me-

chanical joints are prone to mechanical failure. They can be clogged by effusions and biofilms or their mechanical properties (e. g. friction coefficient) can be changed by secretions. Especially, if the small size of the system is considered, the long-term robustness goes under a great risk due to unpredictable frictions and part wear. If such an ORP with joints and links should be proposed, it should be isolated from the tympanic cavity by means of elastic covers and sealing elements.

2.2. Concept

The analysis of the medical application was completed in the previous section by exhibiting the full range of requirements and restrictions. This section will continue with a theoretical exhibition of the possible mechanical elements for realization of the needed DoF and with the elimination the ones that cannot serve to fulfill these requirements or to comply with the restrictions.

2.2.1. Classification of approaches

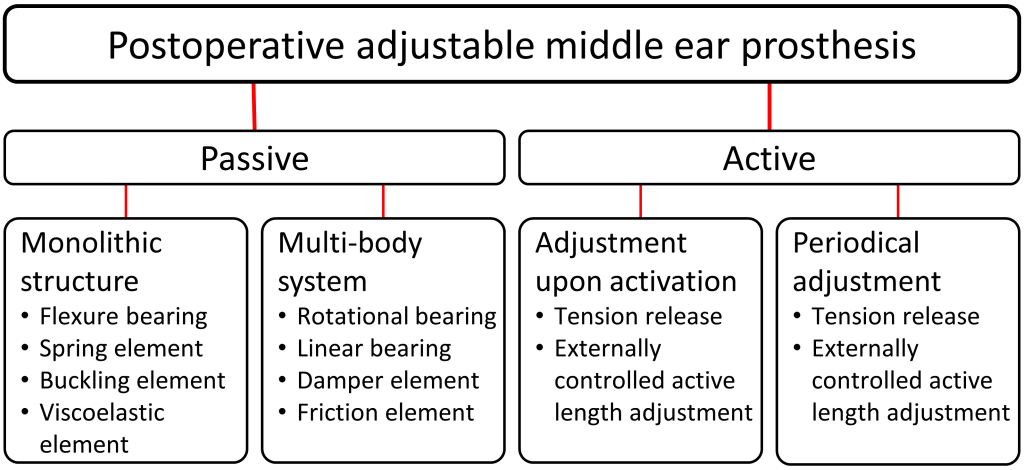

Figure 2.2.: The classification of the possible technical solutions for the postoperative middle ear prosthesis.

As seen in the Figure 2.2, main branching of the classification is the distinction between the active and passive solutions. In accordance with the general classification of the medical devices described by the Medical Device Directive (1993), any implant, which needs a source of power other than that directly generated by the human body or gravity (incl.

electricity), is an active implant. In contrast, if the length adjustment is activated solely by the motion of the TM under pressure difference or by the postoperative changes in anatomy, this implant would be a passive implant.

Approaches for active solutions

There can be four possible approaches to active implant concepts, which are combination of two approaches to activation timing and two approaches to activation mechanism. First approach for timing is to adjust the length of the prosthesis periodically. This approach aims to adjust the prosthesis length as often as possible to ensure a tension-free ossicular chain in order to minimize the long term effects of the tension on the tissues. It ignores the intraoperative length adjustment and tries to adapt the prosthesis length all the time. The second timing approach is the length adjustment upon activation, which aims a minimum wear on the length adjustment mechanism. This approach assumes that the intraoperative adjusted length to be close to optimum and aims length correction instead of constant adjustment.

The approaches to activation mechanism originate from the two sources of energy for the length adjustment. Since the TM is pushed in and outwards by the pressure differences or postoperative changes in anatomy, the length adjustment can be achieved by decoupling the prosthesis foot from the prosthesis head to release the tension and then coupling them back together in the new position. This approach aims a lower mechanism complexity. Technically this is an active approach, because the activation needs external energy, but the length adjustment itself could be considered as passive, because it relies on forces generated by the human body. The second approach relies only on external energy sources such as electricity. This approach aims full control of the length adjustment to keep the length close to optimal. Here, the prosthesis head and the prosthesis foot are coupled through an activated joint, which adjusts the distance between them.

Approaches for passive solutions

The passive solutions rely on the TM motions as their energy source. This includes both the activation of the length adjustment and the length adjustment itself. The main differences between the passive solutions are the types of articulation to enable the DoF.

A multi-body system consists of multiple rigid bodies that are articulated by rotational or linear bearings, where the bearings should be combined with force conducting elements for force coupling between the prosthesis head and the foot. The aim of this approach is to enable full control of the overall mechanical properties by coupling singular modules

with elementary functions to a mechanism, which can be laid out and adjusted separately. For example a rotational bearing is defined by its perfectly circular DoF or a spring can be defined by its linear stiffness with a particular spring coefficient. Basically, there are two types of bearings (linear or rotational) and three options for force conduction (spring, damper or friction elements). Of course, a combination of these are also possible to enable more complex mechanic properties. Joints can be combined to realize a kinematic mechanism with a parabolic trajectory. The parallel and serial combination of spring, damper and friction elements enable viscoelastic properties. The Maxwell model with a serial and the Kelvin-Voigt model with a parallel combination of one spring and one damper elements can be counted as basic viscoelastic modules.

An elastic monolithic structure consists of one single elastic body, however, portions of the single body can have different elastic properties. For example, some portions of the body can be even rigid, as long as the mechanism is compliant enough to enable relative motion of one portion to another. Therefore, this kind of mechanism is called a compliant mechanism. The primary aim of this approach is to eliminate the undesired effects due to backlash and friction of classical mechanical elements, which can change the overall mechanic properties of a system drastically. Thus, the classical mechanical parts are substituted with compliant elements, which usually have composite properties but not a defined and elementary property. Therefore, a total decoupling of elementary functions become impossible (e. g. a joint without spring behavior).

2.2.2. Evaluation of the approaches

Evaluation of active solutions

As mentioned above, there are four approaches to active solutions, which suppose to adjust the prosthesis length upon activation or automatically in certain periods and via tension release or actively.

To start with the first kind of approach, Wiens et al. (2013) introduced in his patent a TORP, whose prosthesis head and foot were coupled over a linear guide that can slide and change the distance between them. However, a clamping mechanism blocks the sliding of the linear guide, thus bridging the TM to SFP like a conventional TORP. The clamp mechanism stays closed until a person, for example a physician, opens it via a wireless activation apparatus. Opening the clamp mechanism starts a passive length adjustment by allowing a relative motion between the prosthesis head and the foot along the linear guide. After the length adjustment ends, the activation apparatus is turned off and the clamp mechanism closes again passively to block the motion. The blocked linear guide

starts conduct sound from TM to the SFP again.

If this solution is evaluated according to the requirements and restrictions described above, it becomes clear that the adjustment upon activation violates two restrictions. First, the patient would need additional interventions, because the prosthesis can adjust its length only when it's activated by a person. In contrast, patients treated with conventional prostheses do not need to go under any special intervention besides usual examination for $10 - 15$ years (see Section 2.1.3). Second, in some cases the patient might need up to $30,000$ cycles of length adjustment during the period of $10 - 15$ years. Since activating the prosthesis multiple times on a daily basis would require the patient to change his/her habits, this would reduce the life quality. Therefore, the approach of length adjustment upon activation cannot comply with this restriction either.

The main deficit of tension release is that the patient cannot hear during the length adjustment, because the prosthesis head and the prosthesis foot are temporarily decoupled from each other. This deficit becomes especially severe with the combination of tension release and periodic length adjustment, which would cause periodical temporary hearing loss. Since it is not possible to determine, when it is the suitable time to adjust the prosthesis length, it would significantly lower the life standard of the patient and it could even endanger the patient, if for example the patient cannot hear an alarm signal during a bad timed decoupling.

Therefore, the only possible active solution approach left is the periodical active length adjustment via an external control device that changes the prosthesis length automatically. Theoretically, this kind of a prosthesis could maintain hearing by a direct force conduction and adjust the prosthesis length without any special treatment or instrument. Thus, this approach could both fulfill the main requirements and comply with the direct restrictions of the application.

Here, the focus of the evaluation must move from a theoretical application evaluation to a more concrete technical feasibility study. Since the heart of the length adjustment would be the actuation mechanism, an overview of the possible micro-actuators is essential at this stage. According to Kohl (2002) the micro-actuators can be classified by their physical effects to five categories of Electrostatic, magnetic (reluctance), fluid (hydraulic), inverse piezoelectric and shape memory effects (see Table 2.1).

The electrostatic effect is very suitable for miniaturization because the electric field strength increases quadratically with the decreasing distance between the capacitor plates. The main disadvantage of this effect is the high supply voltage. For a actuator pressure of about $10^{-3}\ N/m^2$ and a gap of $1\ \mu m$ the voltage is approx. $150V$. In addition, electric fields interact with most materials, which must be reduced by suitable isolation from the

Table 2.1.: Micro-actuators by their type of physical effects and their characteristics. The column correlation of work density and size shows the relation of work (W) for a given volume (V) depending on the one dimensional scaling factor (r)

Physical effect	Max. work density	Correlation of work density and size	Typical supply voltage
Electrostatic	$10^5\ J/m^3$	$(W/V) \propto r^{0\ldots-1}$	$30V - 200V$
Magnetic	$4 \cdot 10^5\ J/m^3$	$(W/V) \propto r^{2\ldots-1}$	$1V \leq$
Hydraulic	$10^6\ J/m^3$	$(W/V) \propto r^{-1}$	-
Inverse piezoelectric	$1.2 \cdot 10^4\ J/m^3$	$(W/V) \propto r^{-1.75\ldots-1}$	$15V - 1000V$
Shape memory	$10^7\ J/m^3$	$(W/V) \propto r^{-2\ldots0}$	$1V \leq$

environment.

The hydraulic effect can achieve high working densities by applying pressure, which is ultimately limited by the pressure resistance of the chambers and supply lines. For example, a pressure limit of p_max of 10 bar corresponds to a working density of $10^6\ J/m^3$. However, such pressures cannot be reached by micro-structures. The generated pressure differences with micro-pumps are less than $1\ bar$. Therefore, an external pressure supply with macroscopic pumps is required for high work densities.

The magnetic effect allows to build actuators that can be operated with the lowest voltages. However, these actuators can only be miniaturized to a limited extent because the magnetic force decreases with the decreasing size. Faulhaber's smallest DL1900 commercial electric motor is only $1.9\ mm \times 1.9\ mm \times 5.5\ mm$ in size. This disadvantage can only be overcome by operating with high voltages and amperage.

The inverse piezoelectric effect allows to build actuators that can apply high forces and their work density is also preserved after miniaturization. In addition, they can be operated at high frequencies. However, the high operating voltages and the small travel way of approx. 0.1% of the original length of the piezoceramic oppose a great disadvantage.

The shape memory effect has a higher power density compared to the other principles. Since the actuator is cooled better with the decreasing size, miniaturization leads to an improvement of the action time. The most widely used shape memory alloy, nitinol, can stretch and compress up to 8% for a few cycles and up to 5% for several hundred cycles. For example, a $1\ cm$ nitinol wire can compress 5% in approx. $0.1\ s$ under a force of $1\ N$. Activation of the wire requires a voltage of approx. $1.3\ V$ and a current of $0.1\ A$. The main

disadvantage of shape memory materials is their weak dynamic operation. The action time of the actor is longer compared to the other principles and the actuation control is affected easily by the variations in ambient temperature.

From the comparison of actuator principles the shape memory effect emerges as the best suited actuator concept for a ME implant. The disadvantages of the principle have little effect on the functionality in ME, because the ambient temperature fluctuations are negligible in the ME medium and a highly dynamic system is not necessary for this application. Another advantage is that nitinol is very suitable for implant manufacturing, which is already implanted even in most critical parts of the body (e. g. coronary stents). In contrast, other effects cannot be miniaturized enough to realize a whole activation package in the given geometric constraints and/or they need very high supply voltages.

The second stage after the actuation concept is the energy source. Since the prosthesis must be one piece and lighter than $40\ mg$, it is not possible to integrate a long-lasting battery into it. Therefore, the energy must be transferred from a separate external source. However, the external energy source cannot have a physical contact with the prosthesis, because the implantation into the ME cavity or into the TB would make the surgery much more complicated than the conventional methods. Thus, the only option left is to transmit the energy from an external energy source to the prosthesis via a wireless coupling.

This approach has two fundamental deficits. First, this would contradict with our restriction not to necessitate an additional device or instrument other than the prosthesis itself. Second, it is technically a very challenging task, because the energy unit should be outside of the head, so that the sound path along the EC up to the TM is not obscured by any object. As a result, the external energy unit must send energy to the receiver in the prosthesis through at least $2\ cm$ thick layer of skin and bone. An exemplary calculation for inductive energy transmitting shows that only an energy flow in range of $[\mu W]$ can be achieved. As seen in the Equation 2.1, the reason for this is the ineffective transmission due to the distance d between the primary and secondary coils as well as the small radius r_s of the energy receiving secondary coil in the prosthesis.

$$M = \frac{\mu_0 \cdot n_p \cdot r_p^2 \cdot n_s \cdot r_s^2 \cdot \pi}{2\sqrt{\left[r_p^2 + d^2\right]^3}} \tag{2.1}$$

, where M stands for mutual inductance, μ_0 for the magnetic constant, n for number of turns, r for coil radius, p for primary, s for secondary and d for distance between the coils.

To conclude, non of the four active approaches can fulfill all the requirements and restrictions either because they are not suitable for the application or because they cannot be realized due to technical constraints.

Evaluation of passive solutions

As described in the previous section, there are two approaches to a passive solution: elastic monolithic structures or multi-body systems. Since these passive approaches are not separated by their functionality, as it was the case with the active solution approaches, but by the mechanical structures of elements that have complementary functions (e. g. viscoelasticity), the evaluation will focus first on the fundamental functions of the basic mechanical elements separately and then with more complex mechanisms of their combinations. The evaluation will include a short review of the state of research, where these mechanical elements were considered for a new postoperative adjustable ME prosthesis concept.

A **spring element** undergoes a certain deflection under a certain force (see Figure 2.3a). While a basic spring element has a linear correlation between the deflection and applied force called the spring constant, there are different types of springs that have a variable rate of deflection under a constantly increased force, such as progressive or degressive springs. Theoretically, force-deflection-curve of a spring element is a non-injective surjective function without a hysteresis behavior. So, if a certain force is applied to a spring, the certain force causes the same certain deflection every time, regardless of reaching to this exact force by increasing or decreasing the applied force and also regardless of the shape of the force-deflection-curve.

In the dynamic domain, the behavior of the spring is frequency dependent (see Figure 2.3b) and it has at least one particular resonance frequency depending on its force-deflection-rate. There are three important regions of the frequency-amplitude-graph for damped oscillations. At the frequency region lower than the resonance frequency, the oscillated object follows the oscillating drive with a low deflection. In the region around the resonance frequency, the oscillated object reacts with a higher amplitude than the oscillating drive. In the higher frequencies than the resonance frequency, the oscillating object reacts with a very low amplitude.

The regions of the frequency-amplitude-graph can be clarified with a thought experiment, where a spring with a spring constant k that was loaded with an undamped mass m is stimulated by a harmonic oscillation with input-deflection x_i and applied frequency of ω_A. If the spring was driven by a constantly increasing deflection (or constant velocity), so that the oscillation frequency became $0\ Hz$, the mass m would move to infinity without a deflection in regard to the spring. Therefore, the graph starts with a x_o-x_i-ratio of 1. If the frequency was increased to the resonance frequency ω_0, which can be described as:

$$\omega_0 = \sqrt{k/m} \tag{2.2}$$

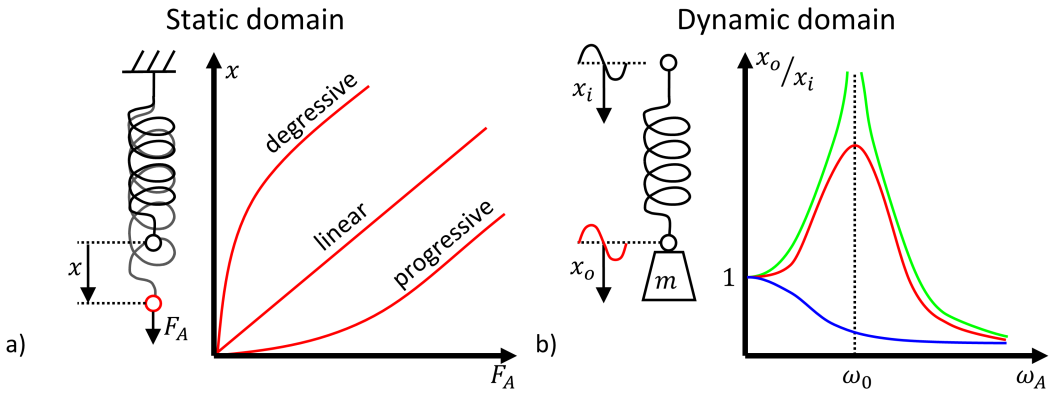

Figure 2.3.: Qualitative demonstration of the main characteristics of a spring element a) in static domain and b) in dynamic domain. In the dynamic domain, the red line shows a damped oscillation, the green line shows an extremely underdamped oscillation and the blue line shows an overdamped oscillation. F_A: applied force, x: deflection, x_i: input deflection, x_o: output deflection, m: damped mass, ω_A: applied frequency and ω_0: resonance frequency

, theoretically the undamped mass would reach an infinite oscillation amplitude. This is because the oscillation of the mass would be periodically accelerated by the stimulation. As a result, the graph has a vertical asymptote at ω_0 and the x_o-x_i-ratio becomes infinite. If the frequency was increased to infinity ($\omega_A = \infty\ Hz$), the mass would not move, because the stimulation would change the direction before the mass could be accelerated at all. Thus, the frequency axis becomes a horizontal asymptote and the x_o-x_i-ratio approaches to zero.

Spring element was proposed as a force coupling element between the TM and the SFP by Lenkauskas (1990), Magnan et al. (2001), Kraus (2011) and Bhansali (2012). However, a spring without viscoelastic properties, even a spring with a non-linear stiffness (e.g. shape memory alloys), has a particular stiffness under a particular elongation. Thus, it is unable to solve the dilemma of contrary requirements between the protection against static forces and sound conduction mentioned in Section 2.1.1 and Section 2.1.2. The dilemma can be clarified by referring to the diagram in Figure 2.3b. Since ideally the sound conduction requires a constant x_o-x_i-ratio in the range of $0.1 - 10\ kHz$, the resonance frequency should be way above $10\ kHz$ in order to stretch out the plateau region below the first resonance. Since the stiffness and the resonance frequency are proportional according to the equation 2.2 , the sound conduction requires a high stiffness in order to stretch out

the plateau region and maintain a constant ratio. In contrast, the quasi-static forces should be compensated or if possible they should not be conducted at all. This means that the force compensation requires a minimum spring stiffness, theoretically $0\ N/mm$. In other words, a spring element can only serve one of the functions at a time, because it is either too stiff to protect against static forces or too soft to transmit sound.

The conventional prostheses can be considered as a spring with very high stiffness, which fulfill the sound conduction and ignore the force compensation. Although it is not possible to construct a PAM with a basic spring element, the Magnan-Babighian telescopic total and partial prostheses manufactured by Audio Technologies (Milan, Italy) use a spring element for better handling of intraoperative length adjustment. In accordance with our assumptions, they too were reported as too stiff for postoperative length adjustment by Yamada & Goode (2010).

A **damping element** resists to motion with a force proportional to the velocity (see Figure 2.4a). While a basic damping element (also called Newtonian) has a linear correlation between the maximum reached deflection velocity and the applied force, there are different types of dampers that have a variable rate of resistance under a constantly increased velocity, such as dilatant or pseudoplastic (both non-Newtonian). Theoretically, the function between an applied constant force and the maximum velocity reached with that force is a non-injective surjective function without a hysteresis behavior. So, if a certain force is applied on an object and kept constant, it results in the same certain maximum velocity of the object every time, regardless of reaching to this constant force by increasing or decreasing the applied force. A major difference of the dampening element compared to spring element is that theoretically the spring element can store and release energy without losses, but the dampening converts the mechanic energy irreversibly into heat energy.

In the dynamic domain, the damping behavior is described by the damping ratio ζ, which can be visualized by referring to the Figure 2.4b. For a basic mass-spring-damper system with a mass m loaded on a spring with spring constant k and damped by a damping coefficient c, the damping ratio ζ can be calculated as:

$$\zeta = \frac{c}{2 \cdot \sqrt{k \cdot m}} \tag{2.3}$$

If the mass m is deflected from the equilibrium point by loading the spring and then let go, the mass m returns to its equilibrium point while one of four distinct cases occurs depending on the dampening ratio. If the damping coefficient c and thus the dampening ratio is set to zero, the system oscillates undamped with a constant amplitude about the equilibrium point (harmonic oscillation). If ζ is set to a value between 0 and 1, the system

oscillates underdamped. In this case the mass oscillates at least one time through the equilibrium point and turns back, while the amplitudes decrease exponentially throughout the cycles. In both undamped and underdamped systems, the frequency of the oscillation is not affected by the damping coefficient c. If the dampening ratio is set to higher than 1, the system becomes overdamped and it does not overshoot through the equilibrium point, rather it converges to the equilibrium point. Finally, if ζ is set exactly to 1, this system is critically damped and acts just like overdamped without overshooting through equilibrium point, only by converging to its equilibrium point in the shortest period of time possible.

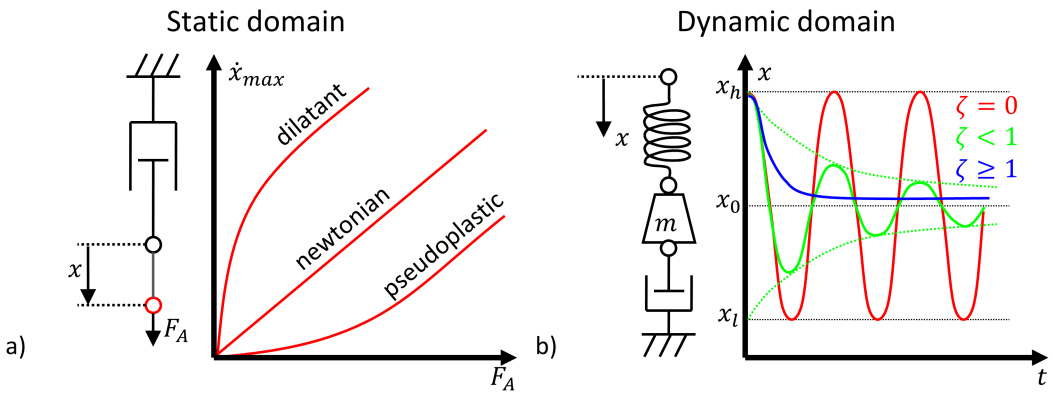

Figure 2.4.: Qualitative demonstration of the main characteristics of a damping element a) in static domain and b) in dynamic domain. In the dynamic domain, the red line shows an undamped harmonic oscillation, the green line shows a underdamped harmonic oscillation with the green dashed line marking the trend of the decreasing amplitude and the blue line shows an overdamped oscillation. F_A: applied force, x: deflection, $\dot{x}_{max}$: maximum velocity reached under constant force, x_h: higher endpoint of the oscillation, x_0: equilibrium point, x_l: lower endpoint of the oscillation, m: damped mass, t: time, ζ:damping ratio

Referring to the dilemma of sound conduction vs. force compensation, both requirements can be fulfilled by an overdamping element. Here, the Figure 2.4b can help understand this mechanism with a simplified analogy. The spring corresponds to the TM, x to oscillation of the TM stimulated by SP waves about its equilibrium point, the variable mass m to the quasi-static loads that change the equilibrium point, the base to IE and the damper is the PAM conducting forces caused by TM deflection by SP waves as well as

quasi-static loads to the IE.

Starting with the quasi-static loads, if x would stay constant and m would be increased abruptly, in analogy to abruptly increasing ambient pressure, the equilibrium point would shift downward. Initially, the overdamped system would conduct this load directly to the base, however, the damper would start to shrink with a velocity depending on the damping coefficient c. The shrinking damper would start to stretch the spring and distribute the quasi-static load to both IE and TM, until the system reaches the new equilibrium point. At the new equilibrium the quasi-static load would be taken solely by the spring element and the damper would apply no forces to the base. If the mass is returned to the initial value, the process would repeat in the opposite direction, ultimately applying no force to the base.

The dynamic loads can be represented by, a constant m and varying x as a harmonic oscillation. Here, the upper end of the spring starts to deflect. Since the system is overdamped, the damper element cannot shrink or stretch as much as the spring element, so that the lower end of the spring would only deflect at a much smaller scale and the deflection difference at the two ends of the spring element would load the spring by the factor of spring constant k. This dynamic load would be conducted to the base through the damper with a minimum loss.

Nevertheless, a damper element alone would not be enough for postoperative length adjustment of an ORP, because the overdamped prosthesis could not stretch its length by itself back to its original length. This poses a great risk of migration at the early stages after the surgery, when the prosthesis foot or head did not have the time to merge with the surrounding tissues. Referring back to the analogy, this would correspond to the damper having no connection to the base, so that it can be pushed against the base after the abrupt increase of the x however, if the x is decreased abruptly, it would pull the damper up and the damper would lose all contact to the base. In this case, an increase in the ambient pressure would shrink the prosthesis and a following pressure decrease would pull TM outwards, thus leaving the shortened prosthesis unsupported and prone to migration. To the best of authors knowledge, a damper element alone was not proposed as a solution for this task, but in combination with spring element, which will be evaluated later in this section.

The **friction element** consists of two contacting parts that conduct force through dry friction between the contacting surfaces (see Figure 2.5). In the static state, the static friction force $F_{R,s}$ is the multiplication of the normal force F_N, which is the perpendicular force on the contacting surfaces between the parts, and the static friction coefficient μ_S. When the friction element is set in motion by applying a horizontal force F_H greater than

the $F_{R,s}$, the friction coefficient μ decreases abruptly to a lower value than μ_S and the parts start to move relative to each other. In dynamic state, the dynamic friction force $F_{R,d}$ stays constant to $\mu \cdot F_N$, as long as the parts are in relative motion. If the relative motion stops, the friction coefficient rises abruptly back to μ_S. A characteristic property of the friction element is that the initial acceleration upon motion start cannot be arbitrarily low, because at the very moment when F_H surpasses $F_{R,s}$, the friction force decreases to $F_{R,d}$. A mass m can start its motion with the minimum acceleration $a_{min,s}$, which can be calculated as:

$$a_{min,s} = \frac{F_{R,s} - F_{R,d}}{m} \tag{2.4}$$

In contrast, once in the dynamic state the acceleration can be set arbitrarily depending on the horizontal force F_H, which is calculated as:

$$a_d = \frac{F_H - F_{R,d}}{m} \tag{2.5}$$

F_R, d causes irreversible energy lost, where the mechanical energy is converted into heat energy.

Besides the dry friction, there are three different types of friction. If the two contacting parts, such as described for dry friction, are separated by a thin fluid layer, this type is called lubricated friction. The lubrication can change the friction coefficient by multiple degrees of power. Especially μ_S can be decreased by lubrication very effectively, so that the minimum acceleration upon activation can be reduced for a milder transition from static to dynamic state, such as minimizing stick-slip-effect. The fluid friction is the friction between viscous fluid layers or the friction between a viscous fluid layer and a solid surface in relative motion to each other. If a laminar flow becomes turbulent, the components of fluid friction change their proportion to relative velocity from linear to parabolic. Fluid resistance of laminar flow is used for damping elements as described above. Another type is the internal friction, which occurs in solid bodies that undergo deformations. The behavior of the internal friction results in a similar effect to viscoelasticity.

The discontinuous behavior of the friction element makes it a great candidate for post-operative length adjustment of an ORP, which was proposed by different researchers such as Hurst (1973) and McGrew (1986). As mentioned in the Section 1.2, the magnitude of the quasi-static loads and the dynamic loads differ by multiple orders of power. If the activation force of the dry friction is set to a value between them, a quasi-static force higher than the activation threshold starts a relative motion between the contacting parts. TM deflects and take up the load. Since the load sinks under the threshold, the friction coefficient rises again. In the dynamic mode, the relative motion is blocked, because the usual sound

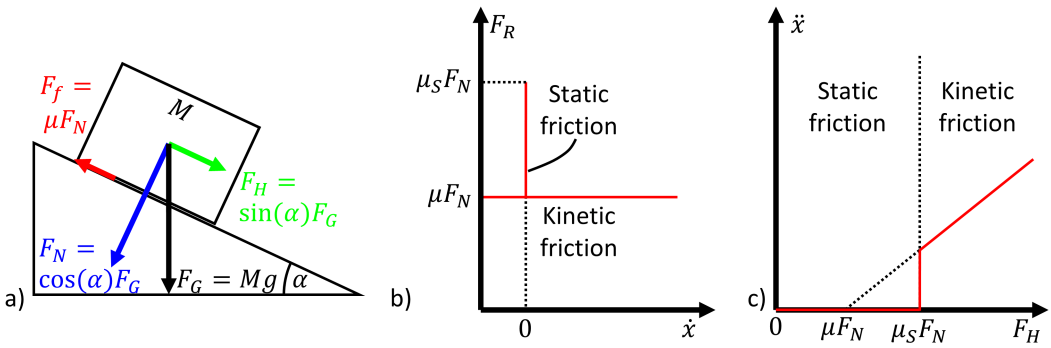

Figure 2.5.: Qualitative demonstration of the main characteristics of dry friction. a) Forces effecting a mass on an inclined plane with an angle, b) the relationship between the friction force and the velocity of an object and c) the relationship between the acceleration and the applied force. M: mass of object, g: gravitational constant, α: inclination angle, F_G: gravitational force, F_N: normal Force, F_H: horizontal force, F_f: friction force, μ: friction coefficient, μ_S: static friction coefficient, $\dot{x}$: velocity of the object and $\ddot{x}$: acceleration of object.

pressure waves cannot reach this activation force. Thus in the dynamic domain, the implant acts as a single body and conducts the dynamic forces caused by SP waves directly to the IE.

However, this application needs highly precise manufactured parts and a strong isolation from the ME environment, because the friction behavior is very sensible to the conditions of the surface contact. Since the prosthesis will be exposed to both axial and radial forces, it is a great challenge to keep the normal force between the contacting surfaces to a constant value, which determines the axial activation force directly. Furthermore, the wet environment of the ME can effect the contact condition drastically by changing the situation from a dry friction to a lubricated friction or from one lubricated friction to another one. Considering the variety of the fluids from saline water to glue-like secretes and effusions, the friction coefficient could change in multiple orders of power, especially in static state.

A **bearing** is a mechanical element that provides motion constraints between two parts, so that the relative motion between them can be limited to a predefined trajectory. Common bearings allow a linear or rotational motions. Although there is a variety of different bearings, mainly plain bearings and flexure bearings are the relevant types for this thesis due to the desired small size of the mechanism. Plain bearings consist of two parts con-

tacting each other by a circular or plain surface to realize a rotational or linear motion constraint respectively. Surfaces such as spherical or cylindrical can allow more DoF and even combinations of linear and rotational motion. The contact may have dry or lubricated friction behavior, whereas the activation force is normally minimized. The flexure bearings do not separate the parts like the plain bearings, rather it is a much more elastic portion of a monolithic structure that allows relative motion between the connected rigid portions. The flexure bearings usually have a viscoelastic behavior, which is dominated by the spring element. This behavior causes little to no resistance for small deflections, which makes flexure bearings suitable for mechanisms that are sensible to activation forces, which cannot be zeroized for the dry or lubricated friction behavior. In contrast, the flexure hinges have higher resistance to greater deflections due to spring factor and to higher velocities due to internal friction caused by the deformation.

This characteristic can be clarified by an example comparing a rotational bearing to a living hinge (see Figure 2.6). Theoretically, a rotational bearing enables a pure and endless rotational motion between two bodies without resistant. In contrast, if the living hinge is flexed more than a certain angle, the motion starts to deviate from a pure rotation and the force needed for further flexure increases with the angle by the factor of spring coefficient. In case of more complex behavior, the via rotational bearing connected parts can be coupled with a certain set of force conducting elements, where the mechanical properties of different elements can be changed individually. In contrast, monolithic structure design depends on both the form of the mechanism and the mechanical properties of the material, which effect the overall mechanical behavior simultaneously. A certain viscoelastic behavior can be achieved by using materials with known viscoelastic properties and a suitable flexure bearing form.

The small size of the prosthesis and the aggressive medium of the ME oppose a great risk for the classical plain bearing, because these bearings have two parts with a friction coupling. As mentioned above, friction become unpredictable due to factors of lubrication and backlash. If sediments leak between the parts, they could even clog the mechanism by blocking the motion or causing extensive part wear. This can be avoided by a strong isolation, however, it might be challenging for a $5\ mm$ long prosthesis that should be able to shrink about $1\ mm$. Therefore, the flexure bearings are favored for a passive approach. Focusing on the limitations of the flexure bearings, three aspects come to attention: undefined motion trajectory, complex mechanical properties and the large tensions at large deformations. These aspects are not disadvantages per se, however they must be considered carefully during the conception of the mechanism.

To conclude **the final evaluation of passive approaches**, the friction element and the

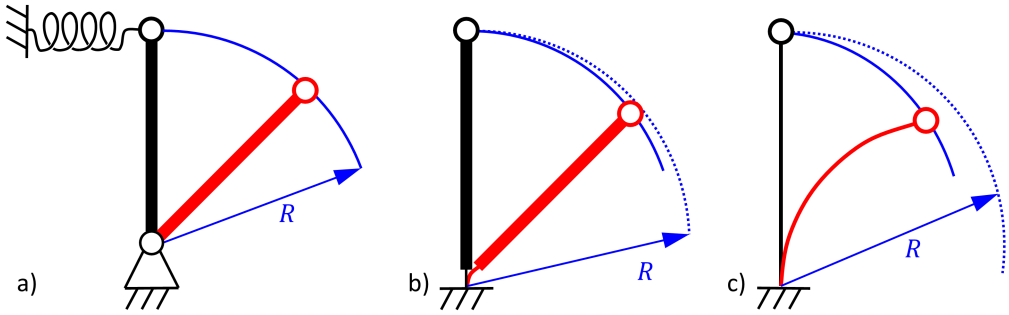

Figure 2.6.: a) a rigid body (black) mounted on a rotational bearing and supported by a separate spring. The rotational bearing allows the body (red) to move on a rotational track with radius R (blue line). The strength of the support depends on the stiffness of the spring. b) a rigid body (black) mounted on a flexure hinge. The trajectory (blue line) of the body in motion (red) and the strength of support depends on both shape and material of the flexure hinge. c) a flexible body (black) with a unique trajectory (blue line). Compared to the mechanism from b), the mechanism from c) is more compliant, but its trajectory deviates stronger from a rotational motion.

plain bearing were ruled out due to their unpredictable behavior under biological conditions in the ME. Nevertheless, the spring element, damper element or the flexure hinges cannot fulfill all the requirement by themselves. A composite structure with at least two of these must be combined to fulfill the requirements without contradicting the restrictions. The synthesis of such a mechanism will be described in the next section.

2.2.3. Closing in on the solution: an elastic Spring-Damper-Element

Last section provided a review of different approaches and their evaluation. The active solution approaches cannot be utilized for the postoperative length adjustment, because the length adjustment upon activation necessitate regular intervention, the periodical tension release fails even at the concept level and the only remaining approach of periodical active length adjustment does not match the requirements due to technical challenges. Furthermore, simple linear or rotatory joints, ratchet-like mechanisms, friction coupling and any other form of linkage with a contact of solid body to solid body were ruled out due to their unpredictable friction behavior and the risk of getting clogged by sediments between the parts.

In contrast, there are mechanical passive elements that can comply with restrictions and

fulfill the requirements at least to some level. A spring element can protect the IE or conduct sound, but cannot do both simultaneously. A damper element can adjust its length and conduct SP waves at the same time, but cannot stretch itself back to its initial length. Although singular mechanical elements cannot fulfill both functions of length adjustment and force compensation, they can be combined to a more complex mechanism. This section will describe the transition from the analysis of the above mentioned approaches to the synthesis of the fundamental concept of this thesis.

A promising combination is the parallel coupling of a spring and a damper element. The damping component stiffens under high frequency and it resists against persisting forces less with time. Hence, while the damper conducts the sound adequately, static pressures can compress it slowly. After the static pressure is gone, the spring can stretch the damper back to its initial length. Here, the spring should have a very low spring constant. Referring to the last section, it is utilized for its decoupled state in the upper frequency region and not for sound conduction. This approach has also found its place in the research. First solution for realizing such a prosthesis was introduced by Nishihara & Goode (1994), which utilizes a polyurethane sponge acting as a SDE due to its viscoelastic properties. Although this is a very straightforward idea, the material chosen for this purpose was not a biocompatible material. A follow-up work from the same group or a similar work from a different group is not known to the author.

Closest scientific theoretic work to polyurethane sponge solution was proposed by Bornitz et al. (2004), where a damping and a soft spring element was suggested as the ideal length variable prosthesis. In accordance with this idea, Abel & Abraham (2011) patented an implant made of a fluid filled linear piston with an elastic cover. In this configuration, the damping fluid transmits the sound and an elastic cover extends the prosthesis if needed. Both propose a classical damper element with a rotatory (Bornitz et al. 2004) or linear joint (Abel & Abraham 2011) and a fluid filled solid housing.

As mentioned in Section 2.2.2, these joints are prone to backlash and mechanical wear in the ME medium and therefore these solutions do not fulfill the mechanical requirements laid in this thesis. In addition, a single linear or rotatory joint with damping properties is not enough to realize the desired DoF according to the kinematic requirements mentioned in Section 2.1.1. The mechanism still needs other joints to achieve the amount of DoF, thus relies on further complexity. The challenges of such a complex construction are underlined and such a solution was described as impractical to realize by Bornitz et al. (2004). The absence of the publications regarding the realization of such an idea supports the assumption of its impracticability.

A slightly different concept was introduced by Hüttenbrink et al. (2005), which consists

of separate prosthesis head and foot coupled via a spherical joint covered by a viscoelastic silicone rubber layer. Similar to the ossicular chain, the sound is conducted by the direct physical contact in the joint and the viscoelastic cover, while the spring coupled kinematic compensates the static forces. Moreover, this prosthesis is made of biocompatible materials and does not necessitate additional instruments, thus fulfilling almost all of the requirements mentioned in prior sections. Another important point with this prosthesis is that this is probably the only prosthesis, which was tested with detailed realistic experiments on temporal bone preparations (Sauer 2016). A clinical study is not known to the author.

However, according to the kinematic analysis in Section 1.2.1, four joints and four links are needed for one DoF. The four joints in the reconstructed ossicular chain with the prosthesis of Hüttenbrink et al. (2005) are the TM, the joint in the middle of the prosthesis, an Omega-connector at the prosthesis foot and the OW. In contrast to the natural configuration of the ossicular joints, which tilts the stapes superstructure upwards-downward, this prosthesis aligns the joints on a linear configuration. Referring to the Section 2.1.1, this alignment is similar to the joint alignment of the reconstruction with PORP, where excessive forces along the prosthesis axis might be conducted with little or no loss due to the kinematic singularity. Finally, this concept uses a plain bearing, which does not comply with the restrictions due to friction behavior.

Despite the fact that a classical damper element does not comply with all restrictions, the damper-spring combination seems to be the only solution fulfilling all the requirements and restrictions. Therefore, the final concept should avoid a rigid damper element, but adopt the viscoelastic behavior of a spring-damper-element (SDE). Since the plain bearings are ruled out, both spring and damper elements should be integrated into a elastic monolithic structure. As described above, the flexure bearing has three issues, which should be evaluated for the purpose of the postoperative length adjustment.

The complex mechanical properties of a flexure hinge, which makes a total separation of the elementary mechanical functions impossible, is not contradictory to the requirements, as long as the desired viscoelastic properties can be implemented. It is important to enable a low spring and a high damping coefficient, which requires some level of distribution of these two functions to two separate parts, but not a total functional separation between them. This kind of functional distribution enables viscoelastic properties beyond the properties of existing materials.

As to the tensions in the system because of the large deformations and the inevitable spring behavior of the viscoelastic mechanism, the concept can be kept within the fulfillment of the requirements by setting the spring coefficient very low. Since the desired

spring part should have a very low spring coefficient in order to compensate the high static forces anyway, the deformations are not expected to generate excessive tensions.

Finally, the undefined motion trajectory is not an issue for the concept, because the natural ossicular chain allows motions besides strictly kinematic too. Although the ossicular chain was described as a $4R$-linkage in the Section 1.2.1, this is a simplified representation of the system. The ossicles are held together by elastic epithelium and ligaments, which allow an under-determined motion to some degree. Therefore, the concept can and should have more DoF than the minimum required 1 DoF for PORP and 2 DoF for TORP. This way, excessive preloads due to kinematic constraints can be avoided, which retard the adaptation to the changing anatomic situation. As long as the dynamic forces are conducted as desired, there is no risk of making the system under-determined.

2.2.4. The final concept for postoperative length adjustment

As mentioned in the last section, multiple DoF are required to design an under-determined mechanism, but an upper limit for DoF cannot be extracted from the medical application. Therefore, the mechanism can be designed as a 6 DoF, which includes 3 translations and 3 rotations. Having 6 DoF does not contradict any requirements or restrictions, but it is clear that not all of them might be necessary for the length adjustment and form adaptation. Consequently, this leads to a structure that is deformable in all directions and along all axes, which eventually must show different levels of resistance to deformations in different directions depending on the form and material of the structure. To sum it up, there is almost no limitation to the general structure, from the aspect of the spring element.

This leads the design to the specifications of the damper element. With a similar reasoning, we can conclude that the damper element should have the same 6 DoF. However, it is not practicable to implement multiple damper elements for all translational and rotational axes. This complexity can be reduced by a fluid mass that is kept between the prosthesis head and the foot, which resists all the relative motions between them by means of fluid friction as described above, but without necessitating a defined shape. Since the fluid cannot hold it self together, it must be kept in a cover. From the aspect of damping properties, there are no crucial requirements to the cover.

Combining the structural requirements of these two separate functional elements, we can conclude the central idea for the mechanical design of the PAM. The damper element is designed as a fluid mass that kept in place by a hermetically sealed cover between the prosthesis head and foot. Since there is no limits to the cover from the aspect of the damping properties and the spring element is allowed to have any structure, the cover

can be implemented as the spring element immediately. If the hermetically sealed cover is made of an elastic material, it creates a flexure hinge system that is deformable in all directions. Since the spring should be of a very low stiffness, the cover should have a very thin wall thickness. So to say, the core idea of the mechanical concept is balloon filled with a viscose fluid.

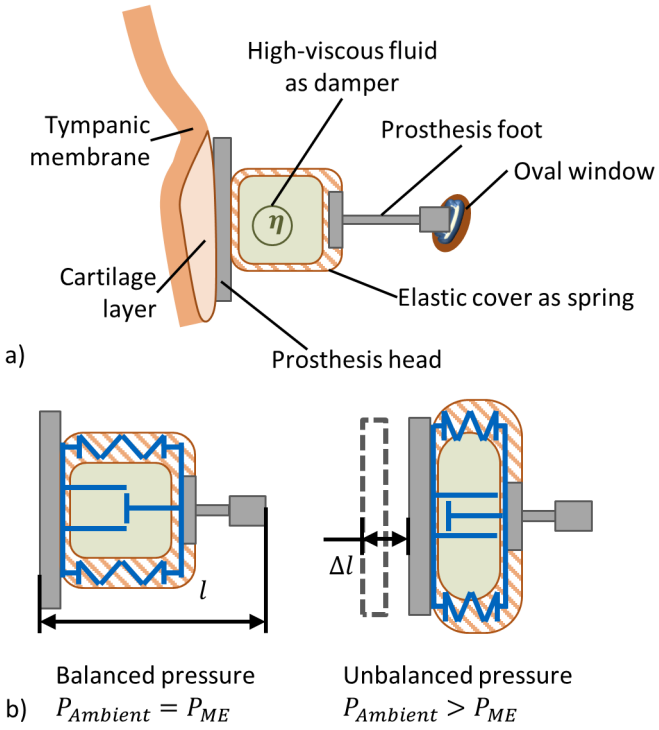

Figure 2.7.: a) The structure of the new prosthesis. b) schematic presentation of the elastic silicone cover as spring and the silicone gel fill as damper under balanced and unbalanced middle ear pressure.

Although, a balloon is made of a thin layer of material, it does not collapse under load, because the hydrostatic pressure that prevails the closed structure keeps the volume constant and the cover acts as an exoskeleton. Depending on the form of the balloon and the load applied to it, it can be bent, stretched, sheared or twisted, but it would eventually return to its initial form by the elastic cover after the load is gone. The returning to the initial form would take a certain period of time depending on the damping ratio, which is related to the ratio between the strength of the spring and the damping fluid. Moreover, because the fluid filled balloon has two components, the cover and the fluid filling can be made of variable materials to achieve different levels of spring strength and damping properties

respectively. Hence, a partially functional distribution is achieved (see Figure 2.7).

As explained before, the resistance of the damper stays minimum during slow displacements, such as the displacement of the TM during quasi-static pressure changes, but increases with the velocity, such as with the high frequency oscillations under the sound pressure (see Figure 2.8). Comparing this behavior to the medical disadvantages of the conventional prostheses, the damper is an ideal force coupling element, which closes the ABG by transmitting dynamic load and which could decrease the extrusion rate by compensating the quasi-static loads, while the spring element in a parallel combination could apply a defined pre-load, which is necessary for reducing the luxation risk.

Since an elastic balloon with a viscose fluid filling is a parallel combination of a spring and a damper element, from now on it will be called as spring-damper-element or short SDE in this thesis.

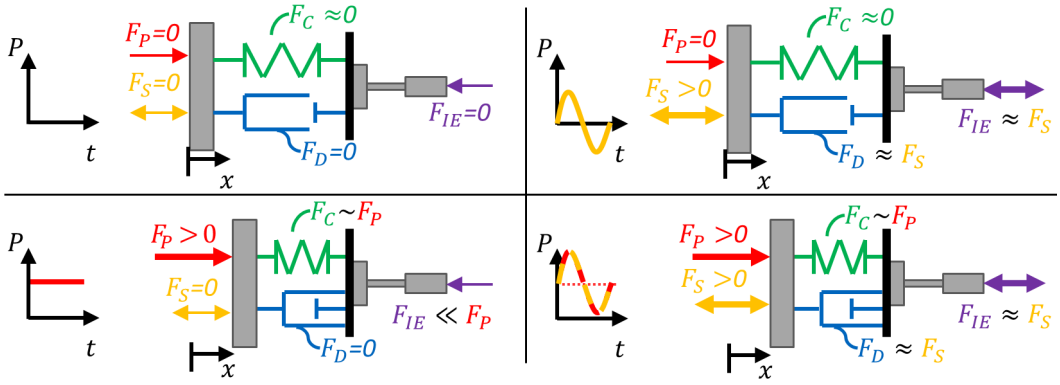

Figure 2.8.: The concept of a prosthesis with a SDE. While the quasi-static loads are compensated, the dynamic loads are transmitted to the IE. x: Deflection of the prosthesis head, t: time, P: Ambient pressure, F_P: Quasi-static load (unbalanced middle ear pressure), F_S: Dynamic load (sound), F_C: Spring force, F_D: Damper force and F_{IE}: Force transmitted to the IE via the prosthesis foot.

2.2.5. A concept for process of prosthesis development

As we mentioned earlier, designing a concept of a PAM is not sufficient for penetrating through the said barriers between the ideas and their realization. Since we laid the foundation of the concept in the previous subsections, this final subsection will conclude the chapter by introducing an iterative development process for a prosthesis with the proposed SDE as seen in Figure 2.9.

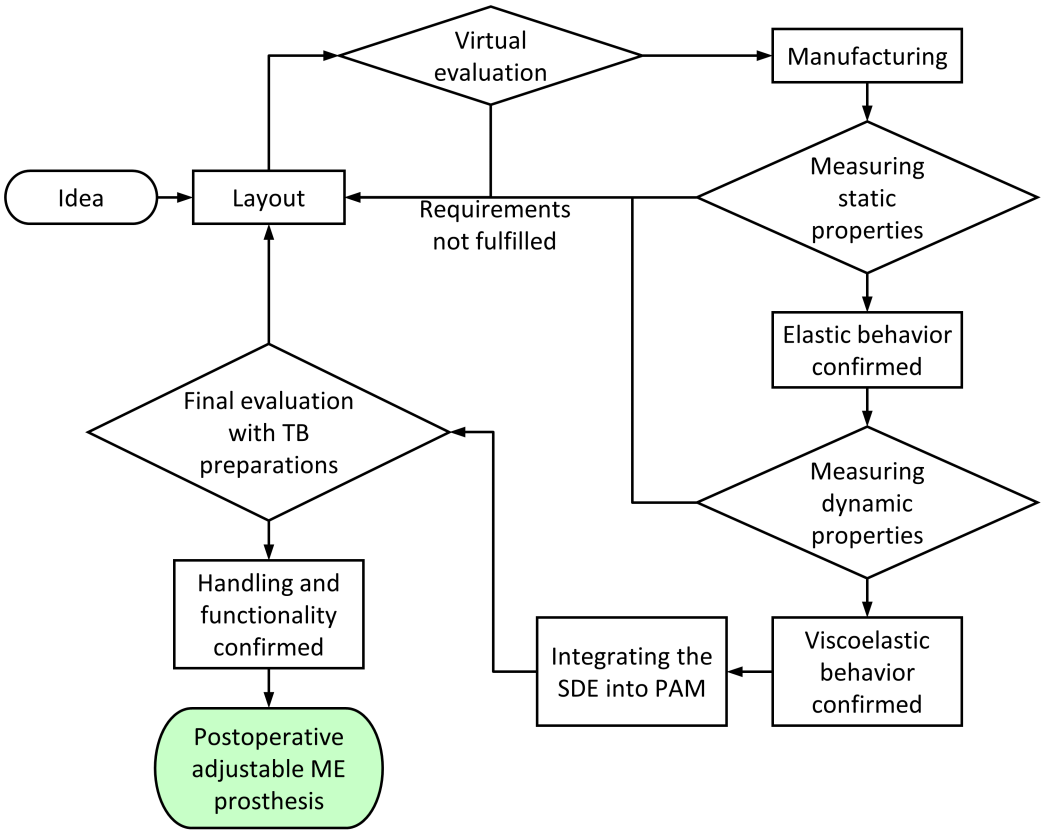

Figure 2.9.: The flow chart of the development process. TB: temporal bone, SDE: Spring-Damper-Element, PAM: Postoperative Adjustable Middle ear prosthesis

The proposed SDE is an elastic balloon, which has thin walls in order to minimize the stiffness, which is small in size because of space limitations and which has a non-linear deformation behavior due to its hermetically sealed structure with internal hydrostatic pressure. All these factors makes a virtual evaluation necessary for two reasons: the manufacturing new prototypes for every iteration would cost much time and effort and it would be impracticable, if not impossible, to measure physical parameters such as local stresses on such a small yet deformable object. Therefore, the elastic behavior of the SDE must be tested by a virtual evaluation for a first feasibility by calculating the maximum stresses and deformations due to forces and tensions applied on the elastic cover.

Once the virtual feasibility is passed, first functional models of the SDE can be manufactured. These functional models are then tested by means of different apparatuses in order to confirm the feasibility by means of virtual evaluation. If these measurements are satisfactory, the elastic behavior of the SDE under quasi-static forces can be confirmed, which is

crucial for the protection of IE through force compensation. This step is followed by a second series of measurements to test the dynamic behavior of the SDE. This should be done based on the ASTM standard F2504.24930-1 mentioned in the Section 1.2.2, which is the method for measuring the sound conduction of a ME. For both quasi-static and dynamic measurements, a realistic and functioning ME model is necessary, which should simulate the TM and the ossicular chain to test both sound conduction and force compensation.

If both static and dynamic behaviors are confirmed, the next step is to integrate the SDE into a prototype of PAM. It is necessary to evaluate the prototype with a TB preparation for functionality and handling. The functional part of this evaluation is the state of the art testing for ME implants (ASTM standard F2504.24930-1). The handling part is necessary to prove that the advantages achieved by the functional enhancement do not change or disturb the surgical procedure.

The Chapter 3 will describe the conception and realization of these virtual and physical models as well as their validation, the Chapter 4 will describe how these models are used for the development iterations and the final evaluation.

CHAPTER 3

Tools for Testing PAM

3.1. A Virtual Model of the Spring-Damper-Element for Testing the Static Behavior

For investigating the SDE's mechanic behavior under quasi-static deformation, the peak stresses in the elastic cover and the tension applied at the interfaces to tissues were of special interest. As mentioned in the Section 2.2.5 a virtual model was needed, because the SDE with its thin walled structure must be very small and elastic, whose mechanical behavior was not practical, if not impossible, to analyze by means of conventional sensors. Therefore, a model based on Finite Element Method (FEM) to test the PAM was created with the commercially available software ANSYS®. This section will only give a brief overview to the implementation of the simulation, whereas the detailed description of its development and implementation can be found in master thesis of Roth (2016).

Since the boundary conditions of a simulation has a great effect on its implementation, these must be defined. According to the requirements from Section 2.1.1 the maximum deflection of the TM was modeled as a $1\ mm$ long and $1\ mm/s$ fast relative motion between the prosthesis head and foot. According to the requirements from Section 2.1.3, the dimensions of the examined SDEs had a height of approx. $2\ mm$, a width of approx. $3\ mm$ and a wall thickness of $0.1mm$.

Different elements were selected for different parts of the prosthesis depending on the geometrical and material properties. The larger titanium prosthesis head was modelled with hexahedral SOLID186 elements. The thin bar of the titanium prosthesis foot needed to be meshed with denser tetrahedral SOLID1487 elements (prosthesis foot diam-

eter $0.2mm$). SOLID285 elements that can undergo very large deformations were used for modeling the elastic silicone cover. The enclosed fluid was modelled using tetrahedral HSFLD242 elements for modeling hydro-static effects.

Since silicone rubbers show a hyperelastic material behavior, special stress-strain tests for both tensile and compression loads were carried out on a selected silicone rubber. To optimize the simulation of the material's mechanical behavior, stress-strain measurements were mapped to different elastic material models, which can be employed in FEM. One of the most used among those models was the Mooney-Rivlin material, which was chosen for the simulation of the SDE in its five-term formulation (Kim 2014). This nonlinear analysis was solved using the full Newton-Raphson solution procedure.

3.2. A 3D-Printed Functioning Anatomical Human Middle Ear Model

As mentioned in the last chapter, a test environment is needed to verify the static and dynamic behavior of the proposed SDE. However, the ME is a sophisticated and complex structure with different functions which cannot be simplified to a linear indentation to simulate its quasi-static behavior or to a harmonic oscillation to simulate its dynamic behavior. Currently, human TB preparations are used as model for tests and experiments, which are not always easily accessible and which change their properties with time or between specimens. Therefore, an anatomically based and functional ME model is necessary to serve as a reproducible test environment. This section will give an overview of the state of the art for the testing environment and extend this overview with concepts from the research including their advantages and disadvantages. Next, a new concept for a ME model will be introduced and its realization as well as validation will be described. Final subsection will discuss its strengths and weaknesses as well as the possibilities to utilize it for the testing of the PAM.

3.2.1. Overview of the state of the art and research for middle ear models and their deficits

Today, human TB preparations harvested from cadavers are the state of the art for testing the ME implants, since these preparations do not differ significantly from the living human ME in their acoustic properties (Rosowski et al. 1990). This process is based on the PTA, which is one of the most widely conducted standard hearing test in the clinical practice. PTA determines, if the patient can hear sound tones of frequencies up to $8\ kHz$,

by asking the feedback of the patient at certain SPLs. Because it is not possible to get a direct feedback by measuring the reactions of the nervous system of a TB preparation, the tests with the TB preparations are conducted by measuring the stapes' response to sound according to the ASTM Standard F2504.24930-1, which describes a method for the output determination of Implantable Middle Ear Hearing Devices (IMEHDs) in human temporal bones (ASTM 2005).

For this measurement method, the TB must be prepared in a special way by the surgeons (see Figure 3.1). The EC of the TB preparation is sealed with an airtight tube, which allows connections for a loudspeaker and a microphone right in front of the TM. The loudspeaker is controlled by a computer to send sound signals at frequencies of $0.125,\ 0.25,\ 0.5,\ 1,\ 2,\ 3,\ 4,\ 6,\ 8$ and $10\ kHz$ with an intensity of $94\ dB\ SPL$, which is regulated by the microphone. Furthermore, a posterior tympanotomy was drilled in the TB to enable direct sight to the SFP. The direct sight is needed for measuring the SFP oscillation by a Laser-Doppler-Velocimeter (LDV), which is capable of measuring oscillations with amplitudes in range of sub-nanometers and frequencies up to $100\ kHz$ without contacting the measured object. Usually, a small retrospective reflector is placed on the SFP, because the LDV measures the phase shifts between the sent and reflected laser beams. A second reflector is placed on the TB close to the SFP in order to measure the background oscillation of the TB simultaneously. If the SFP oscillation does not have a significantly higher intensity compared to the TB oscillation, the sound conduction by the ossicular chain or the ME implant cannot be verified for that frequency. In addition to this, all measurements were checked for their signal-noise-ratio.

The measurements are performed in two steps. First, the natural sound conduction of the ME is measured with the intact and untouched ossicular chain. The measured values at different frequencies are compared to the values specified in the ASTM Standard, which defines an upper and a lower limit as well as a mean value for the whole frequency range. The detailed description of the transfer function of a healthy ME can be found at the end of the Section 1.2.2. If all measured values lay within the tolerances, this TB is accepted as normal for the experiments, otherwise it is rejected from analysis.

In the second part the natural ossicular chain is replaced by a ME implant. The same procedure of measurement is repeated with the implant to compare its sound conduction to the ME's natural sound conduction. However, the second part is not limited to measurements with a single implant. Once the natural sound conduction is recorded, same TB can be used repeatedly for multiple measurements with different implants and/or in different situations. Changing the coupling between the implant and the ME or manipulation of the anatomy by dissecting certain structures can be counted as examples to different situations.

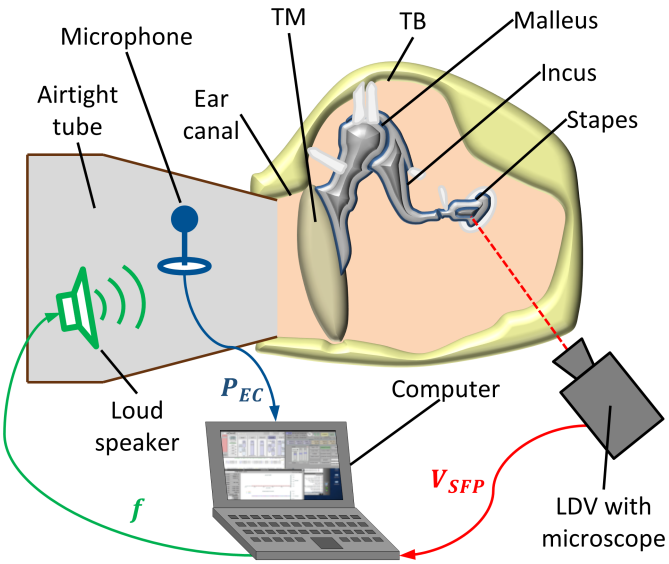

Figure 3.1.: The experimental setup for measuring the output determination of Implantable Middle Ear Hearing Devices according to ASTM Standard F2504.24930-1. TB: temporal bone, TM: tympanic membrane, LDV: Laser-Doppler-Velocimeter

Yet, TB preparations show a great variance in their transmission characteristics between individuals (Huber et al. 2001, Ahmad & Wright 2014) and their properties change with time. This phenomenon can be compared to the great variance of the face proportions of healthy individuals, which makes it possible for humans to distinguish between hundreds of individuals without needing unique markings for each of them. It is also clear that the state of the art process does not offer a solution to this deviation, rather it describes a method to deal with it in a specific way. Therefore, a systematic development of ME implants with the aid of the TB preparations requires a great deal of effort and time (Stieger et al. 2007, Buytaert et al. 2014). Additionally, the regulations become more complicated with time, which makes it more difficult to harvest TBs (Ahmad & Wright 2014). Finally, it is a difficult task for ME implant developers and researchers without medical background to use and maintain the TB, because its preparation needs the know-how of a surgeon as well as a special infrastructure and its anatomy allows a limited integration of sensors or other apparatuses for measuring or testing.

These challenges led researchers to introduce a variety of ME models, which reflect in a way the technological achievements of the last two centuries. First known functioning ME

model was a physical model introduced by Helmholtz (1868), which was made of wooden ossicles and a leather TM. With the achievements in the electronics, researchers started to develop circuit models, where the mechanical elements of mass, dampers and springs were substituted by resistances, coils and capacitors. Early examples for those were presented by Møller (1961) and Zwislocki (1962). With the introduction of the computer technology, this approach was followed by computer simulations starting in the late 1970s, e. g. Funnell & Laszlo (1978), Koike et al. (2002) Cai et al. (2010). Nevertheless, most of the time these numerous models aimed to model the ME itself and only a handful of them simulated functionality of a reconstructed ME by means of implants, such as simulations of Ferris & Prendergast (2000) and Bornitz et al. (2010).

Furthermore, various simplified physical models have been presented, which allow to conduct acoustic measurements of a reconstructed ossicular chain. Letens (1988) built an enlarged mechanical model with aluminum ossicles and an inner ear with electromagnetic impedance. Leysieffer et al. (1997) used a silicon mass to simulate IE and attached an incus to it in order to test a middle ear implant. Meister et al. (1997) simulated the TM and the IE by using two flat membranes with different properties and bridged them with a TORP to simulate the reconstruction. This concept was advanced by Mojallal et al. (2009), who introduced a flat animal skin as TM to model its viscoelastic properties and a small tube filled with saline solution as IE to model the perilymph. The most advanced ME model known to the author is the real sized physical model presented by Taschke et al. (2000). It consisted of ligaments and a flat TM made of silicone as well as ossicles made of epoxy resin. Its transfer function was reported to be in the tolerance range for most of the frequencies described by the ASTM. This model was used by Stieger et al. (2007) for experiments with ME implants.

However, some fundamental aspects of the ME anatomy and function as well as requirements for modeling a reconstructed ossicular chain were not taken into account by the presented ME models. To start with the virtual models, both circuit models and computer simulations are not suited for simulating implants. For one reason, it is a challenging task itself to simulate an implant, if it has a complex mechanism. Second, it is equally challenging to validate a simulation in a way that a simulation of a real prosthesis can be tested and the results can be transferred back to reality.

For understanding the deficits of the physical models, the anatomy and function of the ME must be described in more detail. The TM has a unique funnel-like form, which causes a complex frequency dependent displacement pattern across the TM surface (Tonndorf & Khanna 1972) and which has a significant effect on the acoustic characteristics of the ME (Rosowski et al. 2009, Cheng et al. 2015). The complex displacement pattern of TM

causes an additional functional aspect suggested by Eiber (1999). The linear and rotational components of the malleus oscillation is also frequency dependent. While the oscillations at low frequencies are almost linear in a medial-lateral direction perpendicular to the TM, the pattern becomes more complex at higher frequencies with both linear and rotational oscillation components in multiple axes. Furthermore, Cai et al. (2010) presented that the saddle-formed MIJ can act like a bevel-gear under rotational oscillations of the malleus at high frequencies, which leads to rotational oscillations of the stapes with multiple axes. Although these rotational components of the oscillations are of a lower magnitude compared to linear motions, Huber & Eiber (2011) could show that these rotations have in fact a significant impact on hearing with the aid of animal experiments.

Despite these facts, non of the presented physical models, known to the author, has an articulated MIJ or a TM with its unique funnel-like form. Instead the TM is simplified to a flat membrane, the MIJ is fixed and a fluid filled simulation of IE is usually missing. Another limitation of these approaches is that they are designed for one type of prosthesis and models a single ME anatomy.

3.2.2. Aim and Concept Overview of the Middle Ear Model

There are three aims to fulfill for a ME model to investigate the effects of a reconstructed ossicular chain. First aim is to enable a test environment for all kinds of implants and anatomies. This aim can be achieved by modeling all the essential structures of the ME in a realistic way, but not only a single anatomy, instead a variety of anatomies including pathological anatomies. The second aim is the reproducibility and validity of the experimental conditions. Only a ME model that provides realistic and reproducible properties between the individual models can overcome the limits of the TB preparations. The third aim is to reduce the effort needed to prepare the TB for the experiments. This includes a better sight and access to the essential parts of the ME as well as an easier integration of the sensors and apparatuses for the experiment.

With the motivation of creating a ME model for investigating the effects of a reconstructed ossicular chain with the aid of the state of the art measurement processes, a new functioning human ME model is introduced in this thesis. The structures of the proposed ME model are realistic and anatomical in form and functionality. The forms of the ME structures that are essential for the functionality of the ME model were segmented from micro computed tomography (μCT) data of a TB preparation. To realize the segmented forms with the utmost fidelity, the ME model was manufactured by 3D-printing with selective laser sintering (SLS). The bony parts were modeled by 3D-printed parts and the soft

structures were modeled by silicone rubber press molding with 3D-printed press forms. To the best of the authors' knowledge, this is the first real size 3D-printed middle ear model, which has fully articulated ossicles, a TM with a unique realistic funnel-like form, a fluid filled IE simulation and sound transmission similar to a human middle ear.

The approach presented in this thesis does not aim to model a single anatomy, rather a method to model all the essential anatomical structures of a given ME. 3D-printing is therefore essential to this concept, because it allows to model and even modify anatomical structures in a digital environment and then to 3D-print them, so that it is possible to model both healthy anatomies and pathologies and integrate modifications for better handling with the measurement devices right at the design phase.

3.2.3. General concept and design considerations

The first aspect for the conception of the ME model is the distinction between the parts of the ME that are essential for the sound conduction and the ones that are not. This is a crucial distinction, because the ME model can only be realistic by modeling essential parts that have a direct impact on the sound conduction as close to the original as possible, but at the same time manipulating other parts to make the model more adaptable to the needs of different experiments.

Regarding the analysis of the static and dynamic functions of the ME in the last chapters and the details described in this chapter, we can classify the ME structures in three groups. The most essential parts of the ME are the TM and the ossicles, because these structures collect and conduct sound pressures from outer ear to the inner ear. Therefore, these structures must be modeled as similar as possible to their original forms and should represent the kinematic functions. A second class is composed of ME structures that must be included in the model, but that do not need to be reproduced with a high geometrical fidelity. These are the EC, the ligaments as well as the epithelium that hold the ossicles together, the TB and the IE. These structures can be designed with artificial forms to adapt the model to the experiments. Other structures such as the labyrinth-shaped mastoid or tuba auditiva, which normally stays closed except short periods of muscle contractions, and functions such as the contraction of tensor tympani can be neglected for the experiments that are needed for the ossicular reconstruction.

Another aspect of developing the ME model is its manufacturing technique, which allows to fulfill the aims. As mentioned above, an anatomical functional model is needed as a realistic environment for reproducible experiments, but also for different experiments and implants. Therefore, it is required not to develop a single ME model, instead a process

that would allow to model healthy and pathological scenarios in a fast and reproducible way. Since conventional manufacturing processes cost much time and effort, especially for small series and complex anatomical forms, a rapid prototyping method should be used for manufacturing. This is easily applicable for the bony structures such as ossicles and TB. However, most of the elastic materials for 3D-printing technologies do not meet the requirements of the soft tissue manufacturing, because they can only endure small elongations and they are not suitable for printing thin structures such as membranes. Thus, a conventional method of manufacturing and conventional elastic materials must be used for soft tissue models such as TM and ligaments. A hybrid solution is proposed for this issue, which is using press molding of conventional materials into mold forms that are 3D-printed. This way the advantages of rapid prototyping can be utilized with a wide selection of elastic materials to reproduce soft tissues.

Bringing these two aspects together establishes the core idea of the concept. The geometry of the essential ME structures should be segmented from 3D-images of a patient or a cadaver in order to extract their real forms in digital media. These structures can either be 3D-printed directly or their negative forms can be created in digital media to print the mold forms for press molding. Rest of the ME structures can be designed with CAD software. Their design must take the interaction with the essential parts and the needs of the experiments into consideration. For example, the TB must hold the TM, the ossicles and the IE in the anatomically correct position, even though it is designed artificially to make the access to ossicles easy.

3.2.4. Materials, tools and realization

Two separate graphical user interfaces (GUI) were implemented in MATLAB 2013a (Mathworks, Natick, MA, USA) for segmentation of the anatomic form of the soft and bony ME structures from a μCT-data of a human TB with a voxel size of $18 \times 18 \times 18\ \mu m^3$. In the first GUI, the bony structures were automatically segmented by an intensity based algorithm depending on the high contrast in the scan as seen in the Figure 3.2. The TM, which was the only essential soft ME structure, could not be segmented directly by applying this method. Therefore, the TM was segmented in another GUI by visualizing the cross-sections of the μCT-data in the MATLAB and by marking the borders of the TM manually.

The obtained 3D images were exported as STL and post-processed with Materialise Magics software with Version 15.01 (Materialise NZ, Belgium; short: Magics) if needed. A selective laser sintering (SLS) machine (Formiga P100, EOS, Kreiling, Germany) was

used for 3D-printing the bony structures (the ossicles, the TB casing, the EC and the IE simulation) and molds for soft structures (TM and the epithelium layer of the ossicular chain). A white polyamide (PA) powder PA2200 was used as 3D-printing material. The SLS-machine could print structures with a layer thickness of $0.1\ mm$ in the vertical dimension z and with a minimum wall thickness of $0.5\ mm$ in the x-y-plane, whereas its laser positioning accuracy in the x-y-plane was $0.05\ mm$.

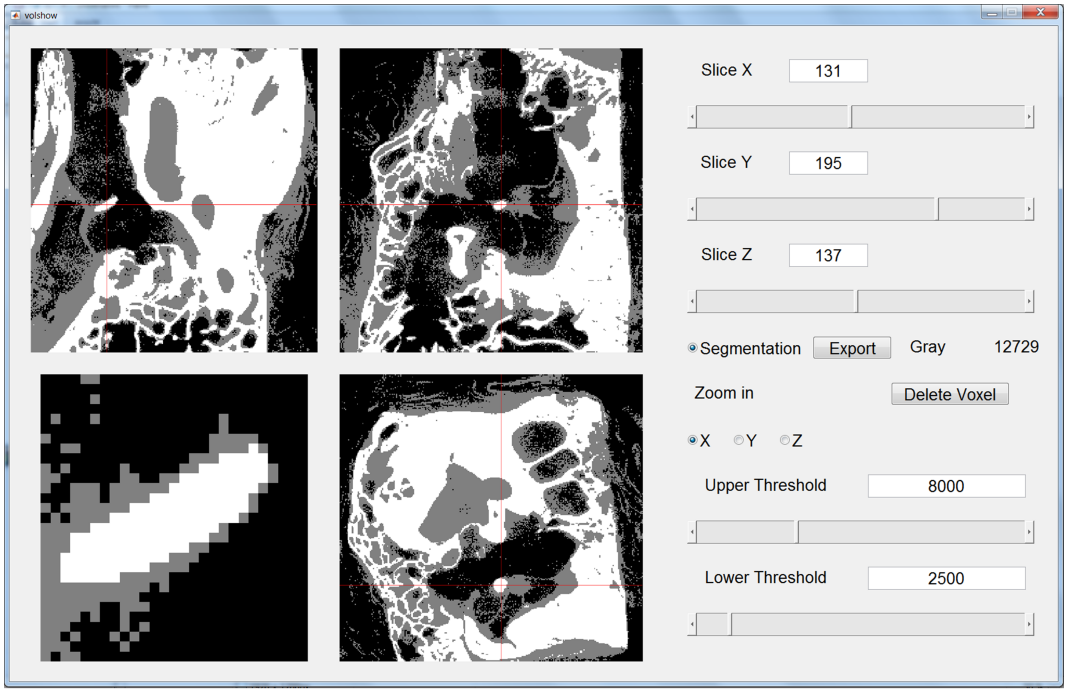

Figure 3.2.: The segmentation software implemented in MATLAB. Four views on the left show the cross-section of the DICOM-data in three spatial planes, where the bottom far left view is a zoomed view magnified by ten times. The red cross shows the position of the current voxel in the cross-sections.

For the soft tissues, three different types of two component silicone rubbers (Feguramed, Buchen, Germany) were used such as the TM, the ligaments, the oval window, the round window and the epithelium on the ossicles. These silicone rubbers had Shore $10A$, $20A$ and $40A$ hardness, which correspond to a Youngs' modulus of $0.4\ MPa$, $0.7\ MPa$ and $1.7\ MPa$ respectively.

Ossicles

The relative motion between the malleus and the incus reaches to macroscopic levels under static loads, e. g. by pressure differences on the TM, but stays in microscopic levels at high frequency oscillations (Cai et al. 2010). To reproduce these effects, the epithelium layer that holds the ossicles together as an ossicular chain must be the mimicked. Therefore, the ossicular chain was articulated by printing the ossicles separately (see Table 3.1) and covering them by a thin layer of silicon rubber coating with an approx. $0.2\ mm$ thickness and Shore $40\ A$ hardness ($SH40A$) A press mold form was created for this purpose (see Figure 3.3, top, published by Kuru et al. (2016a)).

Table 3.1.: Dimensions and masses of the 3D printed ossicles. LP: long process, SP: short process, SFP: stapes foot plate, $\varnothing$: diameter, m: mass, m_e: mass with epithelium, l: length, w: width

Malleus		Incus		Stapes	
$\varnothing_{Head}$	$3.3\ mm$	l_{SP}	$5.9\ mm$	w_{SFP}	$1.6\ mm$
$\varnothing_{Neck}$	$1.3\ mm$	l_{LP}	$6.7\ mm$	l_{SFP}	$3.2\ mm$
$\varnothing_{Manubrium}$	$0.9\ mm$	$\varnothing_{LP}$	$1.0\ mm$	l_{Stapes}	$3.9\ mm$
m	$13.1\ mg$	m	$17.9\ mg$	m	$4.3\ mg$
m_e	$26.2\ mg$	m_e	$36.1\ mg$	-	-

To cover the ossicles with an evenly thick layer without fixing them together, a special press mold was designed. This was also the first opportunity to use the advantages of combining digital 3D modelling and 3D printing. First, the digital model of the whole ossicular chain was segmented from the $\mu CT-$Data and converted to STL-format in MATLAB. This ossicular chain model was offset by $0.2\ mm$ outwards in Magics to create a similar shape like the outer surface of the epithelium around the ossicles. This shape was subtracted from a block by using Boolean-tools to create a hollowed out form inside a block. The block was then separated to four pieces to create the digital models of the single parts of the press mold.

The digitally created parts were 3D-printed. The inner surfaces of the hollow structures were lubricated with a silicone release agent that doesn't allow the silicone rubber to adhere on the 3D-printed parts. This was especially important, since the laser sintered parts have a rough and porous surface, which can intensify the adherence. Afterwards, the hollow structures were covered with fluid silicone rubber mixture (before the vulcanization) and the ossicles were placed into the mold. When the mold parts were pressed together, the

ossicles were laid into the silicone mixture. When the parts were pressed all together, the ossicles were positioned automatically by the mold, whereas a thin layer of silicone rubber vulcanized around the ossicles after approx. 30 min at room temperature.

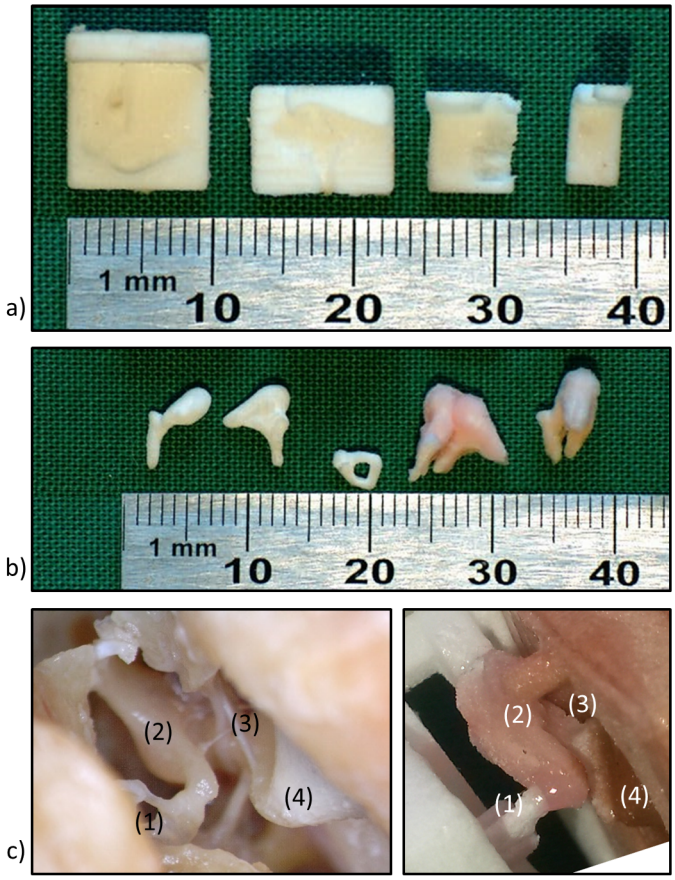

Figure 3.3.: a) 3D-printed molds for the ossicular chain. b) 3D-printed ossicles and silicone rubber covered malleus-incus-complex after casting (from two different angles). c) The ossicular chain of a human middle ear (left) and of the model (right): Stapes (1), incus (2), malleus (3) and TM (4).

In the earliest stages of the development of the ME model, the whole ossicular chain was molded into the silicone rubber epithelium. After first trials, molding of ossicular chain was limited to the MIC. The stapes was connected in a separate step in the assembly process, which will be described in the Section 3.2.4. This is also the reason, why there is no “mass with epithelium” was given for stapes in the Table 3.1.

Tympanic membrane and ear canal

Modeling the TM's unique form was not as straight forward as modeling the ossicles, because the contrast of the softer material of the TM in the $\mu CT-$data was not as high as the contrast of the bony material of the ossicles (see Figure 3.4. Furthermore, the TM had almost the same contrast like the contrast of the oily residuals on the outer side of the TM. Therefore, the segmentation of the TM was not possible to carry out by automatic algorithms in a trivial way. This issue was overcome by a manual segmentation routine implemented in MATLAB, which allowed to go through the cross-sections of the TM and mark the inner surface of the TM manually as well as exporting the markings as a 3D surface in STL-format.

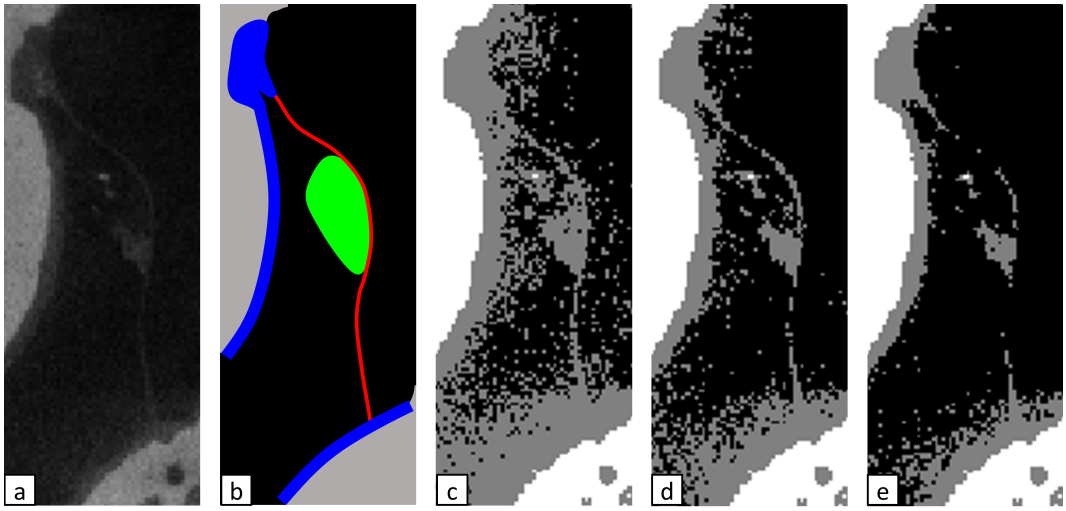

Figure 3.4.: Subfigure a shows the real $\mu CT-$data showing a cross-section of the TM. b) shows a simplified visualization of the structures seen in the subfigure a (black: air, grey: bone, blue: mucosa of the EC, red: TM, green: residuals on the outer side of the TM). The subfigures c-e show the intensity based segmentation at different segmentation thresholds, which fail to differentiate TM from residuals.

A mold form for silicon rubber casting was designed by TM's exported inner surface (see Figure 3.5 published in (Kuru et al. 2016a)). The manually segmented surface was supported by a block and the edge of the TM was marked with a circumferential thickening ($1\ mm$). Accordingly a negative form was created for the outer surface of the TM. The molds were 3D-printed in a vertical position, so that the TM surface was minimally

affected by the layer edges, which are a characteristic surface distortion in 3D-printing.

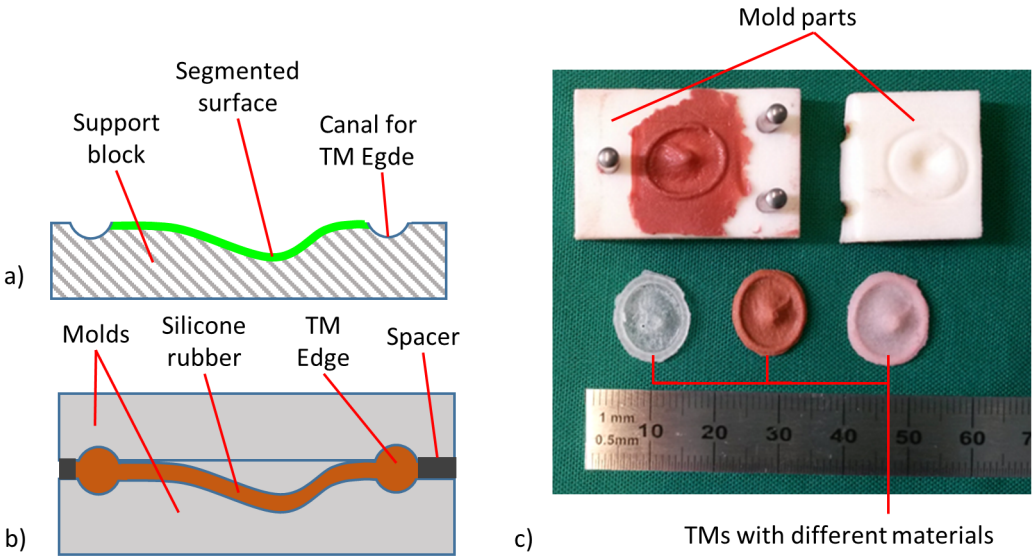

Figure 3.5.: a) The shape of the mold parts were created by segmenting the TM's surface and supporting it with a block. b) The mold parts were kept apart by a spacer and filled with silicone rubber mixture to manufacture the TM. c) 3D printed mold parts right after the silicone rubber casting and casted TMs with different materials.

The surfaces on the 3D printed mold form were smoothed and freed from loose PA powder with a sand paper and sprayed with silicone release agent. Prior to press molding, the mixture of the two-component silicon rubber was degassed under vacuum and spread thickly on the mold parts. The mold parts were pressed together, while they were separated by a spacer of $0.1\ mm$ thickness during vulcanization.

As the vulcanized TM was freshly taken out of the mold, it was a very thin membrane with numerous microscopic holes due to the rough surface of the laser sintered powder. To make the TM airtight, a very small amount of the same silicon rubber mixture was dropped on the outer surface of the TM and spread out with pressured air flow via an air pistol. By this the porosity of the TM was sealed without making the TM significantly thicker. The resulting TM has an elliptic form of approx. $9\ mm \times 11\ mm$ (without the circumferential thickening) and a thickness of approx. $0.2\ mm$ thickness at the thinnest spot.

The EC was designed as a cylindrical tube with an inner diameter of $10\ mm$ and an outer diameter of $15\ mm$. A rectangular EC frame was integrated to the proximal end of the EC for attaching the TM into it and attaching the EC to the casing (also see Section

3.2.4). The EC frame was $45°$ inclined to the EC axis just like in the natural ear (see Figure 3.6). To fix the TM into the EC frame, a TM frame was designed, which had the same outer dimensions as the inner dimensions of the EC frame, in order to press the TM frame into the EC frame, thus fixing the TM between the frames. Furthermore, a pin was placed on the TM frame for attaching the short process of the incus via posterior ligament of incus and a notch at the inner edge, so that the manubrium could be attached close to the circumferential thickening of the TM.

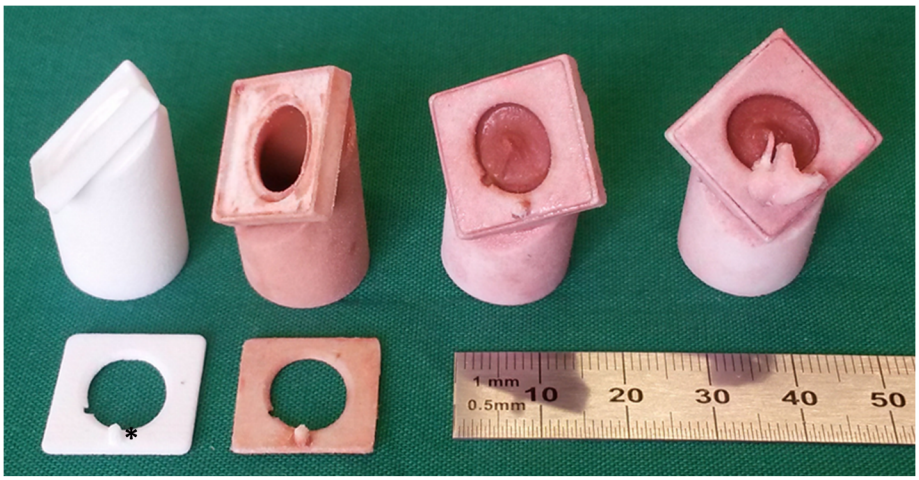

Figure 3.6.: From left to right: The EC and the TM frames right after 3D printing, EC and TM frames after sealing with silicone rubber, TM mounted between the TM and EC frames, the airtight outer ear canal with MIC attached on the TM. *: The pin for the attachment of the posterior ligament of the incus.

Both frames had a canal with the negative form of the circumferential thickening, which helped to fix the TM to the frame without any stress. The circumferential thickening is covered by the frames from both sides after the assembly of the EC. To seal the porous EC and TM frame for making the OE airtight, they were dipped into the silicon rubber mixture in a vacuum chamber to suck out the air out of their pores. As the air was let back into the vacuum chamber, the pores sucked the fluid mixture back in. The airtight design of the OE enabled us to conduct tympanograms on the ME model.

Oval window and inner ear

The design of the IE and OW had artificial forms, because their forms have less effect on the functionality and because IE needs to be manipulated for sensor integration. The

double spiral space of the IE filled with perilymph was modeled as a thin hollow L-shaped tube filled with saline water (see Figure 3.7). The OW was modeled as an elliptical hole ($2\ mm \times 4\ mm$) and it was sealed with a $0.1\ mm$ thick silicone rubber membrane. Similar to TM fixation, OW membrane was fixed between a rectangular OW frame and a IE frame, whereas the OW frame was built into the IE frame and IE frame was attached to the casing (see also Section 3.2.4). Both frames had the said elliptical hole for the OW in the middle covered by the OW membrane. The OW frame had also a pin next to the OW opening that allowed to build the superior stapedial ligament between the pin and the stapes.

The RW was modeled as a round hole of $1\ mm$ diameter and sealed with a $0.1\ mm$ thick silicone rubber membrane. It was made as a separate part that could be clipped at the end of the L-shaped tube. This clipping mechanism allowed to extend the initial IE volume (IEV) of approx. $20\ mm^3$. The length of the L-shaped tube, thus the volume of the IE fluid, could be changed by unplugging the RW part, clipping extension rings with same inner diameter like the L-shaped tube and then plugging the RW part on top of the extension rings. By adding different volume extensions to the IE, its volume could be changed between $20 - 27\ mm^3$. A hard plastic window was integrated into the IE phantom to measure the displacement of the SFP by a Laser-Doppler-Velocimetry (LDV) from the backside. The window was inclined by $15°$, to avoid reflections from this interface, affecting the measurement results of the LDV.

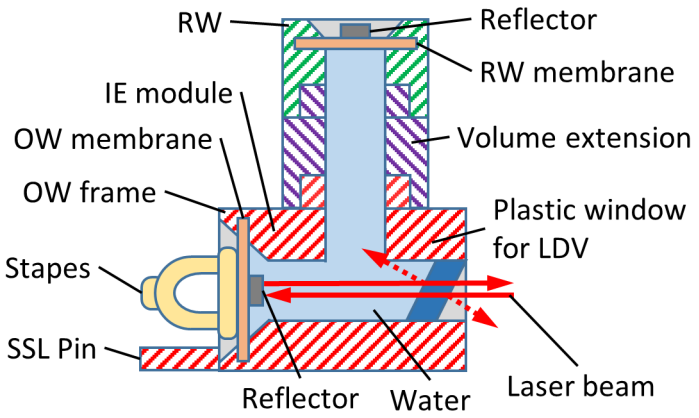

Figure 3.7.: The structure of IE and the direction of the laser beams travelling during the LDV measurement. The laser beam is reflected on the OW reflector and sent back to the LDV (red arrows). The plastic window deflects the undesired reflections by its angle (dashed red arrows). SSL: Superior stapedial ligament.

Casing

The primary function of the casing was to keep the anatomical structures in the right position and orientation, determined from the μCT-data. The casing had dedicated nests to fit in the frames of the TM and the IE in a defined position. Furthermore, a pin was added for the attachment of the ligaments of the MIC made of silicone rubber.

Another function of the casing was the absorption of unwanted resonance vibrations, which was a problem in earlier versions of the model (Kuru et al. 2014). Eight screws were mounted on the casing in a radial arrangement and their surrounding was filled with plasticine to dampen unwanted vibrations. The vibration dampening was achieved passively and an active adjustment of the screws was not necessary. Practically, the plasticine mass consumed the vibrations due to inner friction. We have also built a top cover with a window that can be attached to the casing to enclose the ME cavity. When the top cover was attached to the casing, the ME cavity was approx. $3\,ml$. The anatomical structures can be accessed by demounting the top cover, which allows an easy access for the manipulation of these structures.

Assembly of the middle ear model

The assembly had a great impact on the biomechanics of the model, which we had to improve throughout the different versions. A healthy ME usually has no tension on its structures as long as the pressure difference is equalized by the tuba auditiva. Live tissues can adapt themselves and adjust their elements structurally and geometrically to nullify the static forces. Since a synthetic ME model cannot adapt itself, it was crucial to minimize the initial stresses in the assembly, in order to enable realistic behavior.

As explained in this section, the assembly began with building the anatomical structures separately such as the EC with the TM, the MIC and the IE with the OW. Next, the EC was attached to the casing by placing EC frame in the dedicated nest on the bottom part of the casing and applying superglue between them. Since the shape of the nest let the attachment of the EC frame in a single defined position, no manual effort was needed to position them correctly.

The casing was fixed on a table, so that the TM was in a horizontal position while the tip of the TM was looking upward. The MIC was placed on the TM in a such way, that the manubrium was on the TM and the tip of the manubrium was at the said notch in the TM frame. The short process of the incus. The heads of the malleus and incus were attached to the pin on the casing via the superior ligaments of the malleus and incus. Here, all ligaments were made of silicone rubber and the superior ligaments were modeled as a

single merged ligament. At this point the TM was not attached to the manubrium. After the silicone rubber at the ligament attachments were fully vulcanized, the ME model was fixed to a table, so that the axes of the malleus and incus were in a vertical alignment. In this vertical position, the manubrium of the malleus was attached to the TM by applying silicone rubber.

The IE was then glued to the casing by placing the IE frame into the dedicated nest on the casing and applying super glue between them. Finally the stapes was attached to the tip of the long process of the incus and to the oval window membrane by applying silicone rubber. Because the silicone rubber was still fluid during the application, it ensured that there was no tension built up during the assembly of the ossicular chain. The resulting gap between the SFP and the elliptic hole in the OW frame was approx. $0.4\ mm$, which was closed by the silicone rubber of the OW membrane and formed the annular ligament.

3.3. Experiments with the Middle Ear Model

3.3.1. Objectives of the experiments

For the determination of the ME model's auditory properties during its development and for validating the final version of the model, two kinds of experiments have been conducted, which were chosen according to the two main functions of the ME. While the SFP's response to sound can give insight to the dynamic behavior of the ME model as a whole, the tympanometry can do the same for the static behavior. Moreover, these tests were chosen because they are standard tests, which are conducted in clinical practice since decades.

3.3.2. Stapes foot plate's response to sound

Expected results from the SFP's response to sound

There are two primary acoustic functionalities of the ME: the amplified sound transfer from the OE to the IE and the sound filtering based on frequency. The biggest impact on the transfer intensity is the TM's ability to gather sound from the surrounding air, meaning that the TM absorbing the maximum and reflecting the minimum amount of sound energy. The ratio of the absorbed to the reflected sound energy depends mainly on the difference between the sound impedances of the air (the medium) and the complex ME structure (especially the TM as interface). Therefore, a softer TM material should lead to a higher absorption as well as a higher sound transfer in overall, whereas a harder TM material

should lower the transfer intensity.

The frequency based filtering depends much on the natural frequency of a mechanical system, which is in our case the ME's resonance frequency. The resonance frequency depends on the compliance and the mass of a mechanical system. Since the soft tissue material (silicone rubber) is app. 10 times more compliant than the material PA2200, the combined compliance of the ME depends more on the softer tissues. Thus, a higher mass in the ME system through an increased IEV and a higher compliance through softer materials for the TM as well as the ossicular joints should push the natural frequency to lower values, increase the stimulation at lower frequencies and decrease the stimulation at higher frequencies. A lower IEV (lower mass) and harder materials for soft structures should affect reversely.

Experimental setup for measuring SFP's response to sound

PTA is maybe the most significant standard hearing test in the clinical practice to determine, if a person can hear all the isolated frequencies up to $8\ Hz$. However, PTA needs the feedback of the patient, which is not applicable in the case of a TB preparation. The stapes' response to sound according to ASTM standard F2504.24930-1 (ASTM 2005) allowed to carry out measurements complementary to the PTA, which was described in Section 1.2.2 and Section 3.2.1.

In the experiment series, the stapes vibration of the ME model was measured by applying an SPL of $94\ dB\ SPL$ to the TM with a loudspeaker (DT-48, Beyer Dynamics, Heilbronn, Germany) driven by a buffer amplifier (SA1, Tucker Davis Technologies, FL, USA) while the SPL at the TM was measured by a probe microphone (ER-7C, Etymotics, IL, USA) (see Figure 3.1). For signal generation and data acquisition a commercial $16-$bit, 4-input-channel data acquisition system and software (DMSystem and VibSoft 4.81, Polytec, Waldbronn, Germany) was used. A custom multi-sine signal having equal amplitudes (approx. $-30\ dB\ re\ 1Vrms$) at $0.125,\ 0.25,\ 0.5,\ 1,\ 2,\ 3,\ 4,\ 6,\ 8$ and $10\ kHz$ or a frozen pseudo random white noise was used to drive the loudspeaker, both generated at $25.6\ kHz$ sample rate. The stapes footplate's vibrations were measured with a LDV (OHV-1000, Polytec, Waldbronn, Germany) coupled with a surgical microscope (OPMI-1, Zeiss, Oberkochen, Germany).

The model was tested with three different IE impedances. A low IE impedance was provided by leaving the IE cavity empty, a medium IE impedance was provided by a water filled IE canal with a short volume extension (approx. $20\ mm^3$) and a high IE impedance was provided by a water filled round window module with a longer volume extension

(approx. 27 mm^3).

Results of SFP's response to sound

As mentioned in the Section 1.2.2, a healthy human ME's sound transfer can be simplified to two regions: a plateau region at lower frequencies and a roll-off region at the higher frequencies. The resonance frequency marks the point, where the plateau region ends and the roll-off begins. Same two regions can be observed in the transfer function of the 3D-printed ME model. For instance, a plateau region can be observed, where the displacement of the SFP stays almost constant at lower frequencies. This constant transmission ends at a resonance frequency between 0.5 and 1 kHz and a roll-off dominates the frequencies above that. However, the roll-off slope of the ME model was steeper than the desired slope given by the ASTM standard.

Because the transmission and the resonance frequency mainly depend on the material properties of the soft tissues, different silicone rubbers were applied to the TM, ligaments, epithelium around the ossicular chain and the OW membrane. In the first model, a silicone rubber of SH $40A$ for all the soft tissues (see Table 3.2, M1). This model had a significantly higher resonance frequency (approx. 3 kHz) and a low transmission in the plateau region (approx. 20 dB below the ASTM range; see Figure 3.8). Both were indicators that the material was too stiff.

In the second attempt with M2 the material of the all soft tissues were changed to very soft silicone rubber of SH $20A$. However, these models had a significantly lower transmission. This was very likely due to the too soft coupling of ossicles, which did not transmit the sound. Because of the low transmission we have abandoned the soft ossicle epithelium.

In the next series of models (M3.1-6), a hybrid approach was taken. TM, ligaments and the OW membrane were made of a silicone rubber of SH $20A$, whereas the ossicle epithelium was made of a silicone rubber of SH $40A$. These models met the transmission requirements fairly well at the plateau region. They had a flat plateau region in the frequency range of $0.125 - 1$ kHz with an amplitude range of -36 $-$ -44 dB re μm. These values were $4 - 8$ dB lower than the ASTM reference mean values in this frequency range and within the given 95% percentile tolerance range around the mean value. Furthermore, the resonance frequency of these models laid close to 1 kHz. However, these models had two deficits: The roll-off trend was steeper than the desired ASTM reference and the vibration of the casing dominated the measurements above 3 kHz.

To fully understand how the material affected the transfer function, an even softer silicone rubber (SH $10A$) was used in the fourth version (M4.1-2) for the soft tissues except

Table 3.2.: The measurement results of the SFP's response to sound. The models (Mx.x) are categorized according to the Shore hardness A (SH A) of materials used for their TM, ligaments and OW membrane (TLO) as well as the epithelium of the ossicles (EO). It is also given, if the IE volume (IEV) was empty (IEV=0 mm^3), was filled with water in normal size ($IEV = 20\ mm^3$) or filled with water in extended volume (IEV=27 mm^3).

TLO/EO	Model	IEV [mm^3]	125 Hz	250 Hz	500 Hz	1000 Hz	2000 Hz	3000 Hz	4000 Hz	Stapes Displacement [dB re µm/Pa]
SH 40A/40A	M1	0	-50,4	-52,7	-47,5	-47,2	-58,5	-52,5	-63,5	
		20	-48,2	-50,9	-46,9	-47,5	-57,1	-53,0	-60,8	
		27	-51,2	-50,0	-48,2	-47,7	-56,9	-55,7	-65,8	
SH 20A/20A	M2	0	-63,9	-58,1	-44,1	-61,5	-69,6	-65,3	-59,6	
		20	-62,8	-56,4	-42,1	-65,0	-73,2	-65,4	-70,3	
		27	-67,5	-71,2	-52,8	-70,2	-70,4	-67,4	-64,5	
SH 20A/40A	M3.1	0	-43,3	-44,0	-37,4	-36,2	-53,9	-64,5	-53,0	
		20	-41,6	-42,1	-36,5	-35,0	-59,5	-67,4	-60,7	
		27	-41,3	-40,2	-37,1	-41,9	-64,2	-64,3	-69,8	
	M3.2	0	-36,7	-38,0	-38,1	-35,9	-50,2	-74,0	-58,5	
		20	-34,8	-36,2	-37,7	-39,6	-54,1	-75,3	-72,2	
		27	-33,3	-33,7	-31,3	-43,7	-58,2	-77,1	-68,5	
	M3.3	0	-27,9	-29,0	-28,5	-30,4	-44,7	-69,3	-63,7	
		20	-23,5	-30,0	-29,3	-29,4	-41,9	-66,8	-60,6	
		27	-23,9	-29,9	-29,2	-29,5	-41,7	-67,0	-60,2	
	M3.4	0	-46,2	-47,4	-44,1	-41,8	-58,3	-58,2	-63,5	
	M3.5	0	-47,4	-49,6	-47,1	-43,9	-51,2	-78,8	-73,6	
	M3.6	0	-36,1	-37,3	-31,4	-31,4	-60,3	-68,9	-69,8	
SH 10A/40A	M4.1	0	-28,2	-28,7	-20,8	-34,6	-49,0	-55,1	-51,2	
	M4.2	0	-20,0	-19,6	-10,6	-25,0	-45,3	-60,9	-62,6	
SH 10&20A/40A	M5.1	0	-29,6	-31,6	-24,0	-29,7	-44,6	-68,4	-70,8	
	M5.2	0	-27,1	-29,0	-19,5	-32,5	-41,3	-73,4	-66,1	

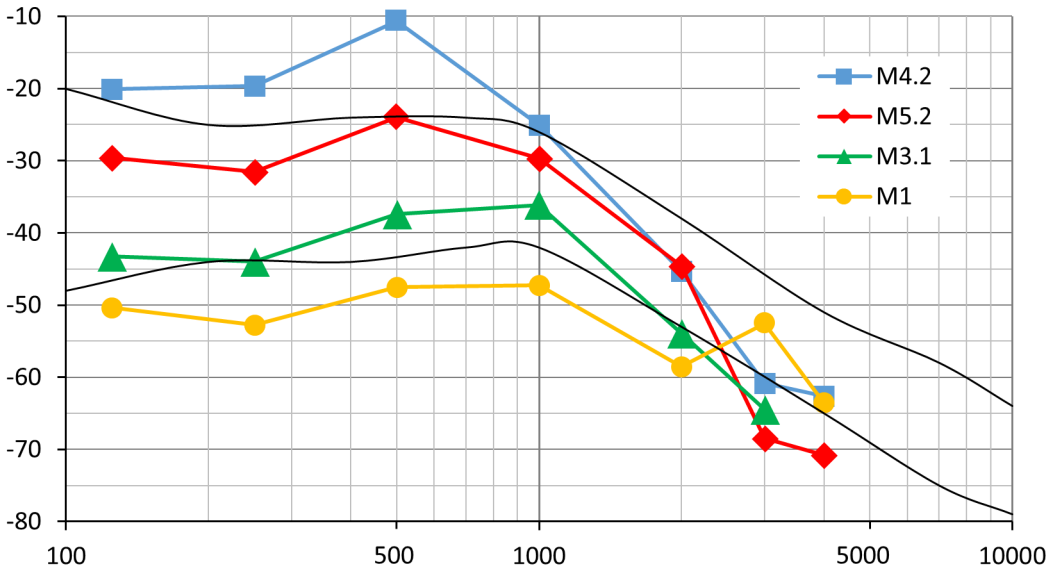

Figure 3.8.: The SFP's response to 94 dB SPL sound of four different models. The acceptance range given by ASTM is shown by the black lines. An inversely proportional correlation of the plateau region intensity and the SH of the soft tissue material could be observed. The amplitude of the transfer in the plateau region was highest for M4.2 (blue squares), second highest for M5.2 (red diamonds), third for M3.1 (green triangles) and lowest for the M1 (yellow circles). It could also be observed that the resonance frequency was higher for M1 and M3.1 with harder TM compared to M4.2 and M5.2 with softer TM. Note that the lines connecting the data points are just a visual help to visualize the trend, but they do not represent measurement results.

for the epithelium on the ossicles where we used SH $40A$. The transmission at low frequencies was even higher than the ASTM range. Possible explanations for this are the drift of the resonance frequency towards $0.5\ kHz$ due to a lower spring constant of the TM and OW as well as a better sound energy absorption at the TM due to a lower impedance difference between the TM and the air.

In the last version (M5.1-2) we have combined the silicone rubbers with SH 10A and SH 20A by mixing them in the fluid state or by making the TM with SH 20A and porosity sealing of TM with SH 10A. This attempt resulted in characteristics between a TM with SH 10A and SH 20A, however much closer to the models with SH 10A, which cannot be considered as a significant change.

Another variable to experiment with was the IE impedance, which could be changed by the size of the IEV (see Figure 3.9). For the ME models M1, M3.1 as well as M3.2, an increase in the IEV, thus the water mass inside the IE, resulted in a slight increase of the response intensity at frequencies up to 500 Hz and a slight decrease of the response intensity at frequencies above 1 kHz (see Table 3.2). However, the measurements on M3.3 showed a slight increase of the response at almost all frequencies, when extra IEV was added.

A table with the results of SFP's response to sound for all the models can be found in the appendix C.

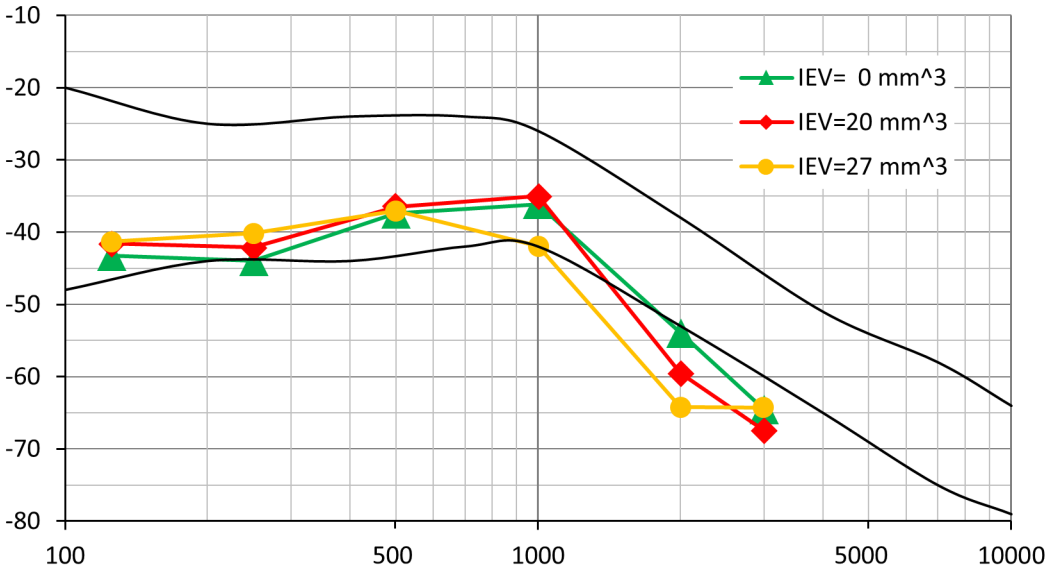

Figure 3.9.: The measurement of the SFP's response to 94 dB SPL sound on M3.1 with different IE impedances. The acceptance range given by the ASTM is shown by the black lines. The green triangles show the results for low IE impedance (IEV=0 mm^3), the red diamonds for medium IE impedance (IEV=20 mm^3) and the yellow circles for high IE impedance (IEV=27 mm^3). Note that the lines connecting the data points are just a visual help to visualize the trend, but they do not represent measurement results.

3.3.3. Tympanometry

Expected results from the tympanometry

Since the tympanometry measures the compliance, which is the inverse stiffness, the compliance of the TM and the hardness of the TM's material should show an anti-proportional correlation. Furthermore, the peak of the tympanogram should be at the $0\ dPa$ pressure difference (pressure equilibrium) and around $1.5\ ml$.

Experimental setup for Tympanometry

The tympanometry is one of the most widely used standard procedures to test the functions of a patient's ME, mainly the static functions. As mentioned in the Section 1.4 the aim of this diagnostic procedure is to find out, if the patient's TM has a healthy compliance and if the air pressure in the ME is in balance with the ambient pressure. Since the ME model was built with an airtight EC, it was possible to carry out tympanometry with a standard tympanogram to test, if it had a similar maximum compliance compared to reference value of up to $1.5\ ml$ and if it had a TM, which was free of tension under $0\ dPa$ pressure difference.

Results

The tympanometry measurements showed that the maximum compliance of the model was comparable with the normal compliance and that it had a strong correlation with the material of the TM in a similar way to the stapes' response to sound. As it can be observed in the Figure 3.10, a soft material (SH 10A) causes even an overshoot in the tympanogram. This result is consistent with our results with the stapes' response to sound, that the spring coefficient of the ME system depends primarily on the material of the soft tissue simulation.

3.3.4. Discussion of the experimental results with the middle ear model

In the very first attempt to build the ME model, which could be named M0, 3D-printed ossicles with anatomical forms and elastic silicone rubber epithelium were attached to a flat silicone rubber TM in a small aluminum half-open casing (see Figure 3.11). The ossicular chain was hanging between the TM and the OW without ligaments to support. This was more of a feasibility test than the realization of the model. Although M0 was a very primitive model, the sound transfer showed the classic plateau and roll-off regions. The

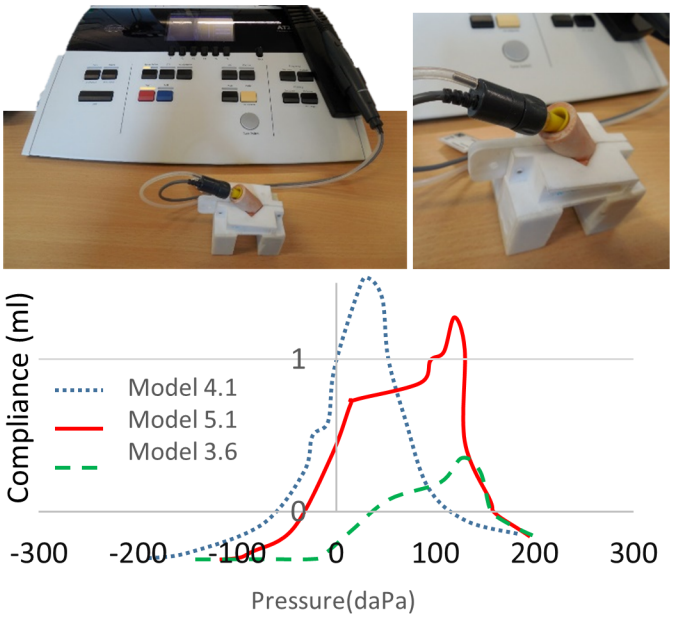

Figure 3.10.: The model attached to the tympanometer (top). The tympanograms of three different models (bottom). The models have the same shape but their TMs were made with different SHs ($10A - 20A$). An inversely proportional correlation of the compliance and the SH of the TM material can be observed: While the TM of M4.1 (SH $10A$) had the highest compliance, the TM of M5.1 (SH $10A\&20A$) and M3.6 (SH $20A$) had lower compliances.

concept was feasible, but approx. $20\ dB$ beneath the tolerance range given by the ASTM. With this motivation the improvement process had begun. From the M1 on, an anatomical TM as well as the ligaments were added to the model and the casing was designed such that the defined positions of the essential anatomical structures were maintained.

The next step was to add an airtight EC to conduct tympanometry. This step proved itself to be a very essential improvement, because the tympanometry measurements had an effect on the assembly process. During the tympanometry measurements on earlier models, the maximum compliance was at approx. $+150\ daPa$ instead of $0\ dPa$. This indicated that the TM had a built in tension during the manufacturing. The positive pressure difference indicated that the tension was pushing the TM outwards. This was possibly due to the assembly step, where the MIC was connected to the TM. During this step, the TM was positioned horizontally and the MIC rested on the TM, until the connecting silicone rubber was fully vulcanized. This positioning was probably causing a preload and

an initial deformation on the TM due to the weight of the MIC pressing down the TM. Therefore, this step was changed by connecting the MIC via the ligaments in horizontal position, then turning the TM to a vertical position and finally connecting the malleus to the TM at manubrium as described in the page 68. This way, the effect of gravitational forces was minimized during attachment of the malleus to the TM. After changing this step, the pressure at maximum compliance was decreased to a range of $0 - 50\ daPa$.

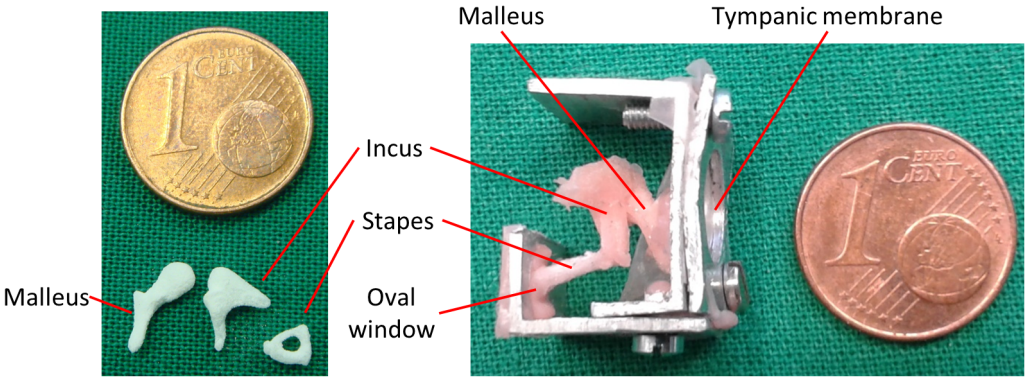

Figure 3.11.: The 3D printed ossicles on the left and the very first attempt to build the ME model on the right.

The measurement results showed that it was possible to manipulate the sound transfer behavior, so that healthy or pathological scenarios could be created. For this purpose the models were built with different mechanical properties by varying the hardness of the silicone rubber used for TM, OW, ligaments and ossicle epithelium in the range of SH $10A - 40A$. This allowed to set the transmission amplitudes in the plateau region higher, lower or within the tolerances given by the ASTM.

The experimental results showed that it was possible to build an artificial model of the human ME by using 3D-printing technology in combination with silicone rubber molding. It was possible to reproduce the anatomical shape of the ME's essential elements with high accuracy and also assemble them into a functioning ME model. The acoustic behavior of the model could be reproduced and manipulated by the choice of user.

However, the ME model had some limitations. The first limitation was the steep roll-off slope at frequencies higher than $1\ kHz$. This might be caused by the PA2200's low elastic modulus of $1.7 GPa$ compared to the ossicles' elastic modulus of approx. $14\ GPa$ and/or due to the silicone rubber with SH $40A$ (approx. $1.4\ MPa$) used for ossicle epithelium. Another limitation of our model is the reproducibility of the sound transfer. Although the characteristics are similar between individuals of the model series, the amplitudes varied

up to 21 dB at some frequencies. The manual steps of the manufacturing process might cause these variations, such as making the silicone rubber ligaments. Finally, the unwanted vibrations in the higher frequencies could not be solved entirely. By measures of installing screws to the casing and covering the casing with plasticine, the vibrations up to $4\ kHz$ could be eliminated, but the vibrations were still dominant above this frequency.

To conclude, The experiments regarding the sound transmission showed that the model has a similar behavior to a human ME. The transfer function has a resonance frequency at around 1 kHz, the SFP response is almost constant for frequencies below the resonance and a roll-off is observed above the resonance. The tympanometry results show that the compliance of the ME model is similar to the compliance of a healthy human ME.

CHAPTER 4

The Postoperative Adjustable Middle Ear Prosthesis

A new postoperative adjustable middle ear prosthesis (PAM) with a spring-damper-element (SDE) is proposed in this thesis, which mimics the static force compensation and sound conduction functions of the ossicular chain. The Chapter 2 described the theoretical background of the concept as well as a concept of a development method and the Chapter 3 described the needed tools to test the concept during the iterations of the development phase as well as during the validation. This chapter will describe the design and manufacturing processes of the PAM as well as different experiments to support the claims that PAM can offer advantages over conventional prostheses based on these two previous chapters.

The structure of this chapter will follow an iterative path as proposed in the Chapter 2, which consists of four iterations. The first iteration was a feasibility study, where a PAM was made by using preliminary tools, without biocompatible prosthesis foot or head and with an SDE made of a biocompatible but not implantable silicone. In the second iteration, more sophisticated tools were introduced for a better manufacturing quality and different SDE forms, while the SDE was made of long term implantable silicone rubber. In the third iteration, the manufacturing steps were optimized, the prosthesis head as well as foot were made of a conventional titanium prosthesis and a custom titanium part for intraoperative length adjustment was designed. In the forth and last iteration the SDE's form as well as the length adjusting part were optimized based on simulation results in order to improve the sound conduction of the PAM. The last two iterations include experiments on TB preparations according to ASTM to illustrate the sound conduction behavior of PAM.

4.1. First Iteration: A Feasibility Study

First step was to find the right materials for the prosthesis head and foot, the elastic cover as well as the fluid filling. As described in the Section 1.6.1, titanium prostheses mark a breakthrough for the ORP manufacturing. Since its advantages are also crucial for designing PAM, especially that it can be forged into delicate forms, PAM should also equip titanium for its head and foot.

The material of the elastic cover must be very elastic, must be formed into a hermetically sealed thin balloon and it must be long term implantable. For both purposes silicone rubber and gel were chosen to achieve our functional and structural goals. The silicone rubber products have an excellent elastic behavior with long term durability, which can be used for the spring element. In the gel form, they offer a great variety of materials from self-tacking to fluid, which can be used for the damper element. Furthermore, the silicone products offer a high biocompatibility and long-term implantability. They have been implanted as soft tissue prosthesis in different parts of the human body since decades (Curtis & Colas 2013). From the manufacturing point of view, the silicone rubbers and gels can be easily used for making small structures by molding, which enables building small and lightweight elastic objects.

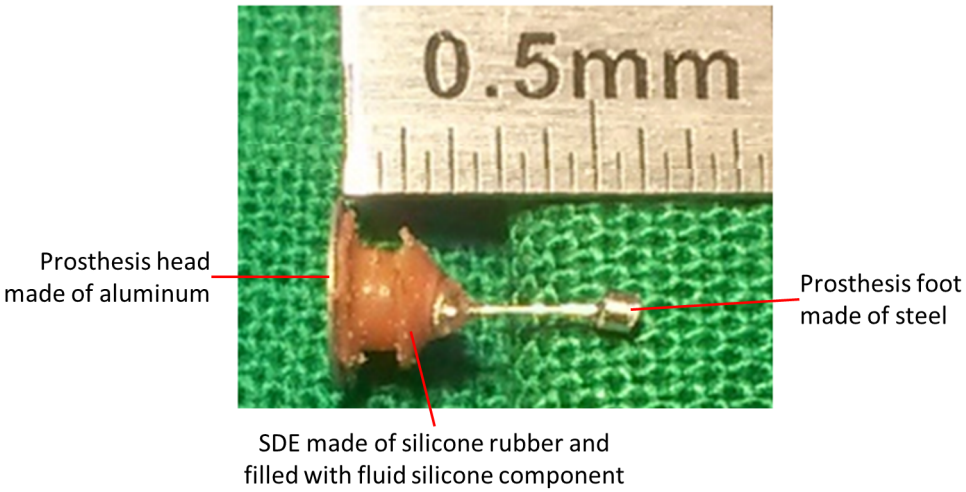

Figure 4.1.: The functioning model of PAM after first iteration.

Since the first iteration was a feasibility study of the PAM, which took functional aspects more into account than the biomedical aspects, this iteration does not include a prototype, but a functional model of PAM (see Figure 4.1). The metal parts of the functional model

were custom made, whereas its head was manufactured with aluminum and its foot with steel. The SDE was made of a silicone that was used for dentistry, which was biocompatible but not long-term implantable. Although these materials were clearly not suitable for manufacturing implants, their mechanical properties were realistic enough for the feasibility study. After the initial verification of the concept, these materials could be replaced with a long-term implantable member from the same material family.

4.1.1. Load compensation experiment in first iteration

This load compensation experiment (LCE) was carried out by López Ferrer (2015) to find out, if the prosthesis could compensate the static loads better than a conventional TORP as hypothesized in this thesis. The criteria was that if the load on the SFP was higher with the TORP than with the functional model of the PAM, when the same static load was applied to the TM by the pressure difference up to $5\ kPa$.

Experimental setup for LCE in first iteration

For this experiment, the OE was isolated from our ME model described in the Chapter 3. The OE model consisted of an anatomically shaped silicone rubber TM, an enclosed airtight EC, an air inlet for increasing the pressure in the EC and an air outlet for measuring the pressure inside the EC (see Figure 4.2). The difference between the EC pressure and the ambient pressure was measured with a differential pressure sensor HSCMRRN020ND7A3 (Honywell, Morristown, NJ, USA), which could measure a pressure difference span of $\pm 50\ cm\ H_2O$ (approx. $\pm 5000\ Pa$) with an accuracy of 0.25%. Approx. $6\ mm$ distant from the TM, a force sensor KD40s 2N (ME-Meßsysteme GmbH, Germany) was mounted, which could measure $\pm 2\ N$ with an accuracy of 0.1%. The position of the force sensor was not changed relative to the TM during the measurements.

First, the $6mm$ long functional model of PAM was placed between the TM and the force sensor. The prosthesis model was fixed to the TM with a very small amount of the same silicone rubber as the TM material, so that it did not slide and change its position during measurements. The pressure difference was set to $0,\ 1,\ 2,\ 3,\ 4$ and $5\ kPa$ and monitored with the pressure sensor. During every force measurement, first the pressure level was set, then the force sensor recorded the static load at the prosthesis foot and the pressure difference was set back to $0kPa$. For every pressure difference level 10 measurements were carried out. For the comparison, same procedure was repeated with a conventional TORP (Heinz Kurz GmbH, Germany) of $6\ mm$ length.

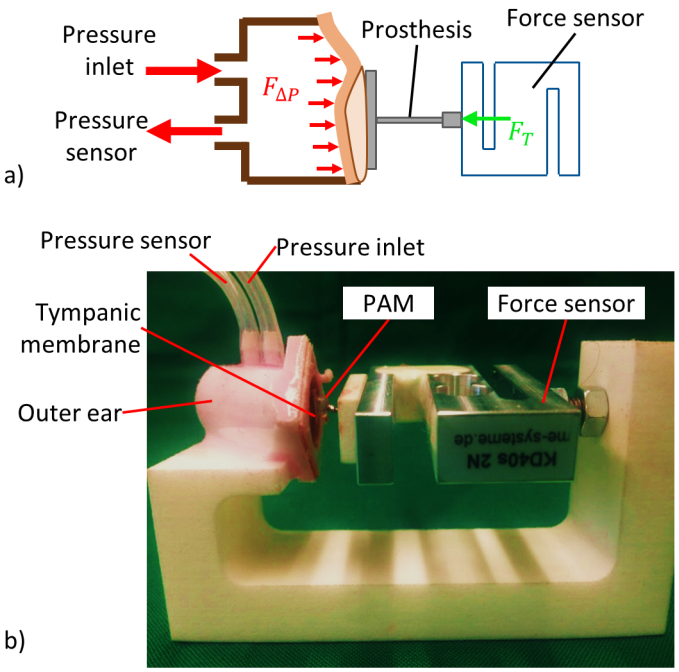

Figure 4.2.: a) schematic presentation of the experimental setup, during which a conventional TORP is pressed against a force sensor by increasing the pressure at the TM and b) footage from the actual experiment with the functional model of PAM.

Methodology for interpreting the results of LCE in first iteration

In this experiment, confidence interval of the measurements with the functional model of PAM was compared to the confidence interval of the measurements with a conventional TORP. For this, the confidence intervals were defined as a range around the mean value of the measurement that would withhold 99.9% of the data points of a normal distribution. For a data set with sample size N, the mean value $\overline{x}$ can be calculated as:

$$\overline{x} = \frac{1}{N} \sum_{i=1}^{N} x_i \tag{4.1}$$

and the standard deviation σ as:

$$\sigma = \sqrt{\sum_{i=1}^{N} \frac{(x_i - \overline{x})^2}{N}} \tag{4.2}$$

Table 4.1.: The results of the force measurements at different pressure difference levels $(1 - 5kPa)$. The mean values of 10 force measurements for TORP as well as functional model of PAM, lower endpoint (LEP) of the confidence interval for TORP measurements and upper endpoint (UEP) of the confidence interval for measurements with functional model of PAM at every pressure difference level

Parameter	$1kPa$	$2kPa$	$3kPa$	$4kPa$	$5kPa$
Mean TORP $[mN]$	117	179	217	291	347
LEP TORP $[mN]$	110	176	212	288	338
UEP PAM $[mN]$	50	124	154	188	214
Mean PAM $[mN]$	49	120	151	185	211

Since we know that the probability is $p = 0.999$ for the range of $\pm 3.3\sigma$ in a normal distribution, we can calculate the confidence interval of the data set by:

$$\overline{x} \pm \frac{(3.3 \cdot \sigma)}{\sqrt{N}} \tag{4.3}$$

where the subtraction gives us the minimum value in the confidence interval (lower endpoint) and the addition gives us the maximum value in the confidence interval (upper endpoint).

The hypothesis was supported, if the lower endpoint of the confidence interval for force measurements with TORP was greater that the upper endpoint of the confidence interval for force measurements with functional model of PAM at all five different pressure difference levels up to $5kPa$.

Results for LCE in first iteration

The measured forces with functional model of PAM were lower than the measured forces with the TORP with a confidence of 99.9%. As seen in the Table 4.1 the upper endpoints of prosthesis model measurements were below the lower endpoints of TORP measurements at every pressure difference level and as seen in the 4.3 the increase trend of the TORP is steeper than the prosthesis model.

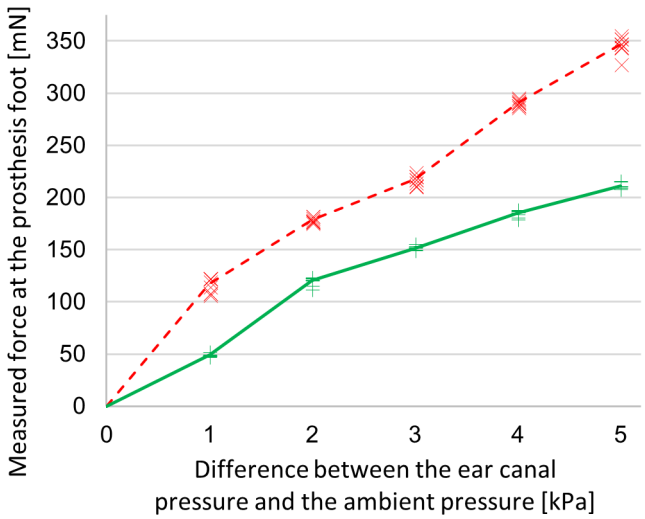

Figure 4.3.: The results of the force measurements under varying pressure difference between the EC and the surrounding of the ear. The red crosses mark the measurements with TORP and green plus symbols mark the measurements with functional model of PAM. A red dashed line connects the mean of 10 values for the TORP and the green line for the functional model of PAM.

4.1.2. Stapes' response to sound in first iteration

A second experiment of stapes' response to sound (SRS) was carried out to find out, if the functional model of PAM could conduct the sound better than a comparable conventional prosthesis, when the ossicular chain of the ME Model was reconstructed with a high tension between the TM and SFP. The hypothesis was that the functional model of PAM had a higher sound transfer, if the amplitude of the measured SFP oscillation was higher with the functional model of PAM compared with the TORP.

Experimental setup of SRS in first iteration

For this experiment, the ME model was used, which had a similar transmission characteristics compared to a human middle ear up to $3kHz$. We placed the functional model of PAM between the TM and the SFP of the ME model (see Figure 4.4). A function generator 33220A (Agilent Technologies, CA, USA) was used to generate sound waves with $1kHz$. The SFP's oscillations were measured with a LDV of type OFV-3001 (Polytech GmbH, Germany) and monitored by an oscilloscope Waverunner 6030A (Teledyne

LeCroy GmbH, Deutschland). Same procedure was carried out 10 times for the functional model of PAM and for a conventional TORP (Heinz Kurz GmbH, Germany). The distance between the TM and the SFP was approx. $4.5\ mm$. Both the model as well as the conventional TORP were $6\ mm$ long, so that they would certainly cause a high tension in the reconstruction.

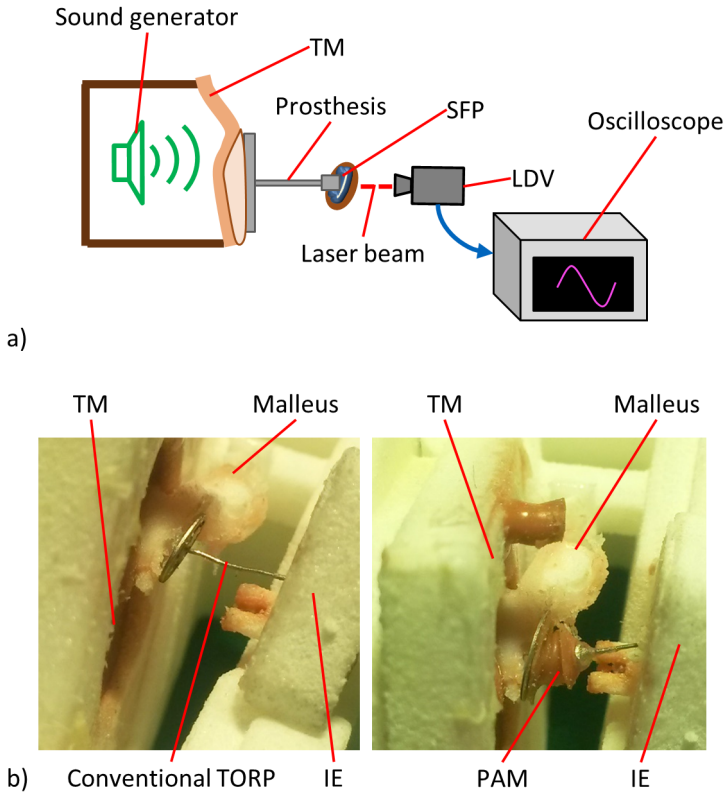

Figure 4.4.: a) Schematic presentation of the experimental setup, during which a conventional TORP is inserted into the model by placing it between the TM and SFP. b) Picture of the experiment with a conventional TORP (left) as well as with a functional model of PAM.

Methodology for interpreting the results of SRS in first iteration

Our hypothesis would be supported, if the lower endpoint of the confidence interval for amplitude measurements with the functional model of PAM was greater than the upper endpoint of the confidence interval for measurements with the TORP according to the Equation 4.3.

Table 4.2.: Results of Amplitude Measurements

Parameter	Unit	TORP	PAM
Size of sample N	$[-]$	10	10
Mean value $\overline{X}$	$[\mu m]$	0.78	2.02
Standard deviation σ	$[\mu m]$	0.18	0.31
Confidence interval	$[\mu m]$	± 0.19	± 0.32
Upper endpoint	$[\mu m]$	0.96	2.34
Lower endpoint	$[\mu m]$	0.59	1.70

Results of SRS in first iteration

As seen in the Table 4.2 the lower endpoint of measurements with prosthesis model was above the upper endpoint of measurements with TORP, which showed that the sound transfer with the functional model of PAM was higher than the sound transfer with the TORP with a confidence of 99.9%.

4.1.3. Discussion of the first iteration

The preliminary results supported that the new concept had a potential to reduce the risk of extrusion as well as luxation and enhance the sound transfer by limiting the load on the tissues. However, the results based on a single functional model and a single ME model. Especially, it was not possible to rule out that PAM could have different motion modes in the higher frequencies, which could cause sound distortion or insufficient sound transfer. Furthermore, the presented tests were carried out on a cylindrical SDE with a wall-thickness of $0.1mm$. Finally, the comparison of the sound transfer was done under high tension, which did not include the normal case. For conclusive results, different variations of PAMs should be built and tested with different ME models and TB preparations at frequencies up to $10\ kHz$, whereas different forms and wall-thicknesses as well as different materials should be tested to determine the optimal parameters for the best transfer behavior.

Overall, this iteration was a positive impulse to go on with the concept, because it acted as expected in its both static and dynamic behaviors. The functional model of PAM consisted of a rigid prosthesis head and foot such in conventional prostheses, which were coupled through a SDE made of a biocompatible silicone rubber and silicone gel. Even though these were not materials suited for implant manufacturing, there were various met-

als and silicone products with different mechanical properties, so that it was plausible to find implantable substitutes for these materials.

4.2. Second Iteration: Exploring Different Forms

As explained in the Section 2.2.4, the SDE is a combination of a spring and a damper element, which react differently to quasi-static and dynamic forces. Since the damper part is implemented as a shapeless fluid fill but the elastic cover (spring part) as a hermetically closed balloon, the elastic cover is the critical part from the manufacturing point of view. Thus, it had to be investigated precisely, if it was feasible to manufacture an elastic cover with a sufficiently low spring coefficient, while it could withstand the large deformations or local stresses and staying hermetically sealed. As a result, the realization of the elastic cover was the necessary condition and the realization of the sound conducting SDE was the sufficient condition for the overall functionality of PAM.

Therefore, the focus of this iteration was the manufacturing of the elastic cover and its evaluation by determining its behavior under quasi-static forces. In this iteration, the concept of the manufacturing process was improved by introducing a steel molding form, choosing the right silicone rubber and creating as well as validating a finite element (FE) model for early mechanical evaluation of the SDE. The focus of this iteration was more on the spring part of the SDE and the behavior under quasi-static forces, which is why this iteration does not include a sound transfer experiment but only load compensation experiment.

4.2.1. Silicone rubber molding

A translucent two component silicone rubber SILPURAN UR 7000/20 (Wacker Chemie AG, Munich, Germany) was chosen for the PAM, which had a Shore $20A$ hardness (Young's modulus of approx. $0.7MPa$), could withstand elongations up to 800% and was long term implantable. The mixture of the silicone components for the elastic cover was a very thick fluid, which could be shaped by press molding. The mixture vulcanization took approx. $2\ d$ at room temperature, but this procedure could be accelerated to approx. $10\ min$ by heating it to $70 - 80°C$. Another property of this material was that a non-vulcanized mixture fuses with an already vulcanized silicone rubber mass. This was a very essential property, because this allowed to vulcanize a balloon with an opening on one side in first step and then close this opening with a fresh mixture without additional agents (such as glues).

A steel mold was designed with three parts. The first part, interchangeable inner mold part, which shaped the inner form of the elastic cover (see Figure 4.5). This part was mounted on a second positioning part, which had aligning pins on it. The third part had a cavity, which shaped the outer form of the elastic cover. The aligning pins could position the second and the third parts very precisely. A fourth and last part was designed to enclose the SDE, which was placed in the positioning part like the interchangeable inner part. For empirical investigation of the effects of the wall thickness, the wall thickness of the elastic cover could be varied without changing the outer diameter of the SDE by replacing the inner part that was produced with different diameters.

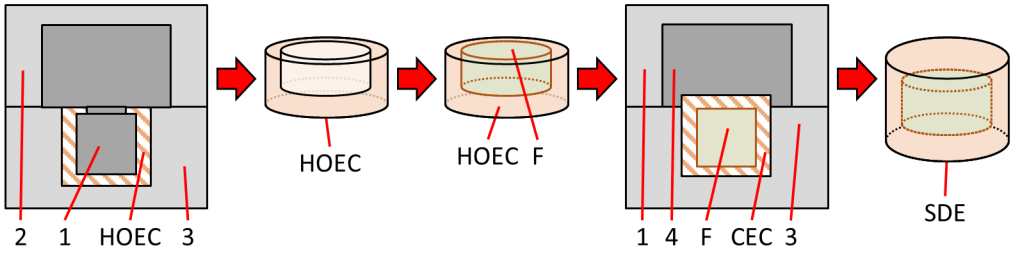

Figure 4.5.: Process of silicone rubber molding. 1: interchangeable inner mold part, 2: positioning part holding the inner mold part, 3: outer mold part, 4: SDE enclosing part, HOEC: half open elastic cover, F: fluid fill, CEC: closed elastic cover and SDE: enclosed spring-damper-element.

The silicone molding began with filling the outer mold part with the fresh mixture of silicone rubber. The inner part (mounted in the positioning part) is pressed together with the outer part and the assembly is put into oven to accelerate the vulcanization. After the vulcanization, the half open elastic cover was removed from the mold. Separating agents were not used for removing. At this stage, the top surface of the elastic cover was open, so that it could be filled with a silicone gel. The component A of the silicone rubber was used as fluid fill, because it was a very viscous and showed non-Newtonian properties.

Afterwards, the inner mold part was changed with the SDE enclosing part, which had a thin flat cavity filled with fresh silicone mixture. The filled open elastic cover was placed back into the outer mold part. The flat inner part was placed on the filled elastic cover by positioning it with the same alignment pins. As the thin silicone mixture vulcanized, it merged seamlessly with the half open elastic cover, so that the top of the elastic cover was sealed hermetically. Three sets of molds with cylindrical, conical and hemispherical forms were manufactured (see Figure 4.6).

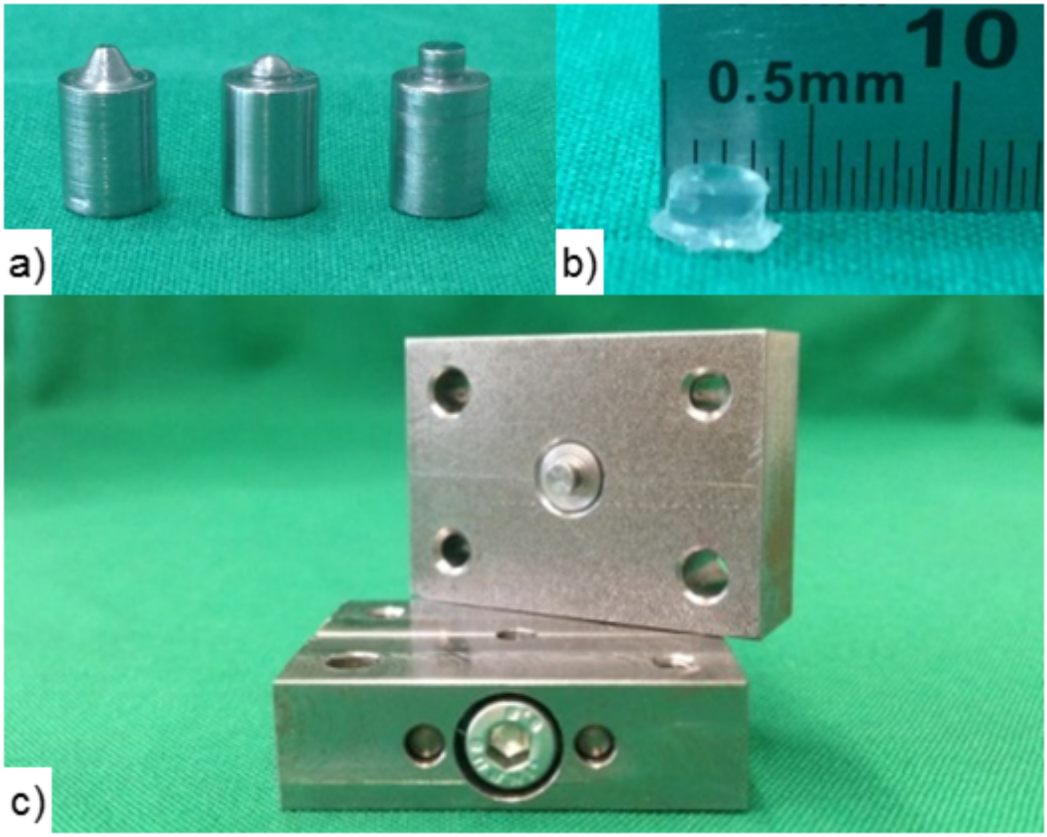

Figure 4.6.: a) The inner parts with cylindrical, conical and hemispherical forms. b) The cylindrical SDE in close caption. c) Mold set for the cylindrical SDE.

4.2.2. Load compensation experiment in second iteration

The LCE in the second iteration had the same hypothesis that the prosthesis models could compensate the static loads better than a conventional TORP, if for a probability of 99.9% the confidence interval of the force measurements on the prosthesis foot are higher with the TORP than with the SDEs. However, this iteration was not just to show that the PAM was better than the TORP, but also that the SDEs with different shapes could change the stiffness and that one of the experimented form was better than the others.

Experimental setup for LCE in second iteration

The experimental setup of the LCE in second iteration was the same experimental setup for the first iteration with two exceptions. First, the pressure difference was set to two levels

instead of 5 levels, because the second LCE relied on the strong trend observed in the first iteration. Second, the experimentation was carried out with three different SDEs instead of one. Besides these minor changes, the process was identical. First, a conventional TORP (Heinz Kurz GmbH, Germany) or one of the functional models of PAM was fixed between the TM and the force sensor(see Figure 4.7). The pressure difference was set to $0,\ 2.5$ and $5\ kPa$ under monitoring with the pressure sensor. For every force measurement, the pressure level was set, the force sensor recorded the static load and the pressure difference was set back to $0kPa$. For every pressure difference level 10 measurements were carried out. All SDEs had a wall thickness of $0.1mm$ and all probes were $6\ mm$ long.

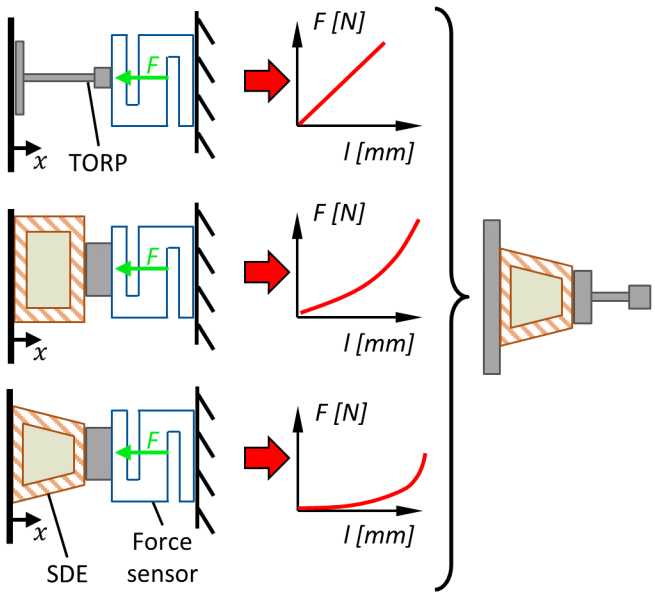

Figure 4.7.: Schematic presentation of the experimental setup, during which the functional models of PAM were pressed against a force sensor by increasing the pressure at the TM. The experiment was repeated with a conventional TORP as well as with SDEs with cylindrical, conical and hemispherical forms. Thus, the SDE with lowest stiffness could be determined

Methodology for interpreting the results of LCE in second iteration

The methodology for interpreting LCE results was same as the methodology of the first iteration. The confidence intervals for $p = 0.999$ were compared between the TORP and the functional models of the PAM at 2.5 and $5kPa$. A candidate was accepted as better than the other, if it had a lower stiffness, which meant that its UEP was lower than the LED

of all other candidates at both pressure levels.

Results for LCE in second iteration

The measured forces with the functional models of PAM were lower than the measured forces with the TORP with a confidence of 99.9%. As seen in the Table 4.3 the upper endpoints of the measurements with prosthesis models were below the lower endpoints of the TORP measurements at both pressure difference levels. Moreover, the confidence intervals of the SDEs did not overlap either, so that it could be shown that all three SDEs had significantly different stiffness.

Table 4.3.: Force Measurements Under Varying Pressure Difference. The mean values of 10 force measurements, lower endpoint (LEP) of the confidence interval and upper endpoint (UEP) of the confidence interval at two pressure difference levels (PDL) for TORP as well as functional models of PAM (PAM) with hemispherical (hem.), cylindrical (cyl.) and conical (con.) shaped SDEs. The LEP of TORP and the UEP of PAMs are marked bold for comparison.

Prosthesis type	Measurement type	Load on SFP at PDL $2.5kPa$ $[mN]$	Load on SFP at PDL $5kPa$ $[mN]$
TORP	Mean	165	257
	UEP	169	263
	LEP	**162**	**250**
PAM-Hem.	Mean	139	190
	UEP	**142**	**192**
	LEP	135	189
PAM-Cyl.	Mean	111	138
	UEP	**112**	**141**
	LEP	111	136
PAM-Con.	Mean	74	79
	UEP	**77**	**81**
	LEP	71	77

4.2.3. Verification of FEM simulation in second iteration

As mentioned in the Section 2.2.5 and Section 3.1, a virtual model was needed for the development process for early evaluation of the SDEs. Parallel to the building the physical models for the PAM, same SDEs were simulated with the FEM model. The comparison of the results from both models served as the verification of the virtual model. The simulation of the SDEs calculated the resulting force on the SFP as $0.14N$ for conical, $0.17N$ for cylindrical and $0.37N$ for hemispherical SDEs (see Figure 4.8).

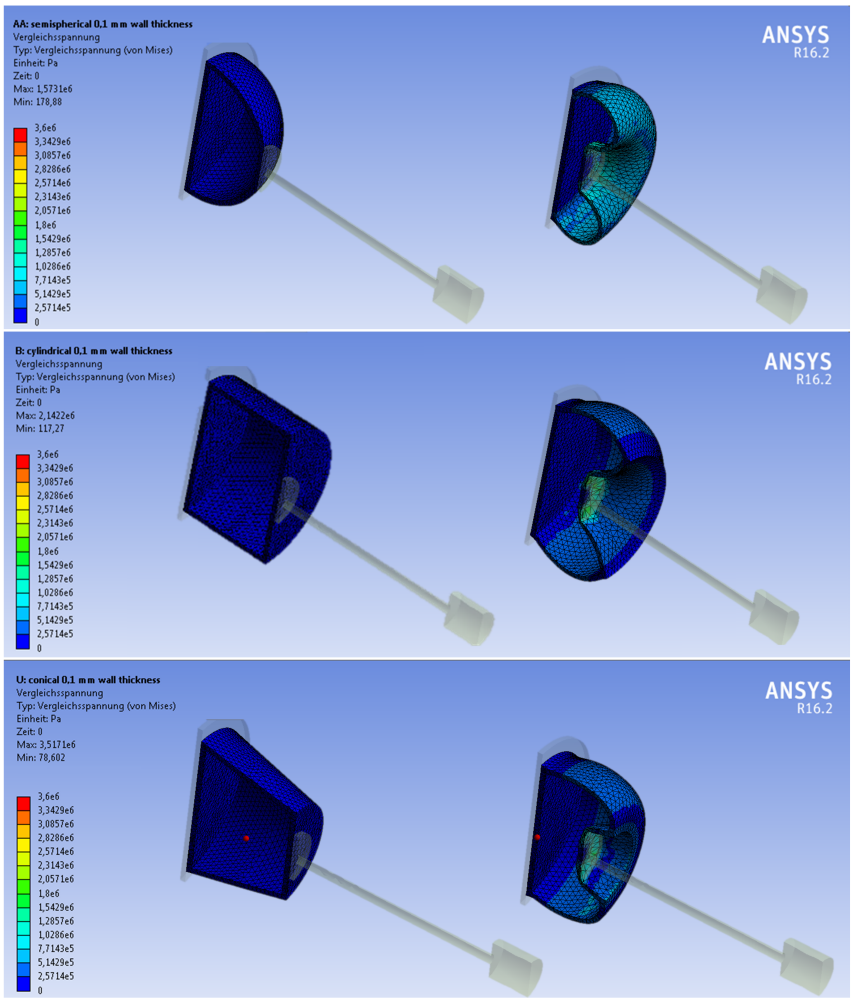

Figure 4.8.: Simulation results of three different SDEs. The blue zones show the regions with the lowest stress peaks and the red zones with the highest. The forms from top to bottom: hemispherical, cylindrical and conical.

4.2.4. Discussion of the second iteration

Three SDEs with different forms were successfully implemented in this iteration and it could be shown that the mechanical properties could be manipulated by form variations. These measurements showed that the ability to compensate the forces on SFP was best with the conical shape, then with the cylindrical shape and last with the hemispherical shape, while all SDEs could compensate force better than the conventional TORP. Furthermore, the calculations with the FEM model had the same order as the measurements. Although it could not be fully validated and the calculated values did not exactly match the measurements with physical models, it was realistic enough to make quantitative comparisons between different designs, which was sufficient for an early virtual evaluation.

There were two practical issues to manufacturing. First, the spreading of fluid filling to the edges of the elastic cover by accident made it impossible to seal the SDE hermetically. Second issue was the air bubbles that were left in the fluid filling, because the small elastic cover prevented the thick fluid to flow inside the cover freely. First issue was solved by simply letting most of the manufacturing attempts to fail and by using the ones that were sealed. The second issue was not solved per se, however it could be shown with the simulation that the air bubbles had negligible effect on the static behavior. Of course, it was probable that these air bubbles would have an effect on the dynamic behavior. These two issues had to be solved by a better manufacturing process (see next iteration for the solution), but they did not have an effect on the measurements in this iteration.

The results of the second iteration were very crucial, because they verified both the proposed development method from Section 2.2.5 and the manufacturing process for the SDE. To sum up the impact of the results, this iteration showed that it was possible to design different SDEs, evaluate them in a virtual environment, choose the best candidate, build a functional model with the long-term implantable materials and test it in reality with the aid of the physical 3D printed ME model. Since the testing of the dynamic behavior could be shown in the first iteration, at this stage it could be concluded that the proposed method was a plausible and reliable method.

4.3. Third Iteration: From Prosthesis Model to Prosthesis Prototype

In the previous iteration, the process for manufacturing the SDE was verified, the materials were chosen and the form of the SDE was selected out of the three candidates. In the third iteration, it was time to build the prototype of PAM, which could be theoreti-

cally used under real circumstances. Of course, implant manufacturing has much more requirements such as clean room conditions etc., however this thesis focuses on a concept of a development process for PAM. Therefore, the last leap from a prosthesis prototype that is theoretically implantable to a practically implantable one is out of the scope of this thesis. The aim of this iteration is to address all the requirements from manufacturing to implantation in a plausible way. That being said, the remaining two issues to address were to improve the SDE manufacturing to a reliable yet scalable process and to introduce a solution for the crucial feature of intraoperative length adjustment.

4.3.1. Improvements in third iteration

Manufacturing process

Since a reliable way of manufacturing was needed for the PAM prototype, an elaborate method with dedicated tools was implemented during this iteration. First, an advanced press molding form was designed, which eliminated the problems with hermetically sealing and which allowed to manufacture up to five SDEs at once. Then, a centrifuge was designed to get rid of the air bubbles left in the SDE. The press molding form was made of five parts: inner part for shaping the inner wall of the SDE, outer part for shaping the outer wall of the SDE, the middle part for securing the SDEs from tearing apart while separating the inner from the outer part, sheet part for keeping the sealing area clean from fluid filling and the sealing part for enclosing the SDEs' open side at the end.

The manufacturing process started by filling the outer part and the sealing part with fresh silicone rubber mixture and putting them into the custom made centrifuge under vacuum for $4\ min$ (see Figure 4.9). This step was necessary to degas all the air bubbles from the mixture that formed while mixing the silicone components, which would otherwise leave holes in the SDE walls. Afterwards, the outer, sheet, middle and inner parts were pressed together, while they were positioned by two pins. This mold form assembly for conic SDE pressed and shaped the fresh silicone mixture into the lateral surface of cone, leaving the base circle open with some skirts around its edge. In the later steps, the open base circle was enclosed around the skirts and supported by the prosthesis head. After the vulcanization of the lateral surface in an oven for $20\ min$ in $85°C$, first inner and then the middle parts were removed from assembly. While the inner part was removed from the cores of the SDEs, the middle part was holding the SDEs in place by pressing at the skirts. By this partition of the mold parts for core and skirt, the surface to separate was partitioned into two steps, so that the risk of tearing the lateral surface was minimized.

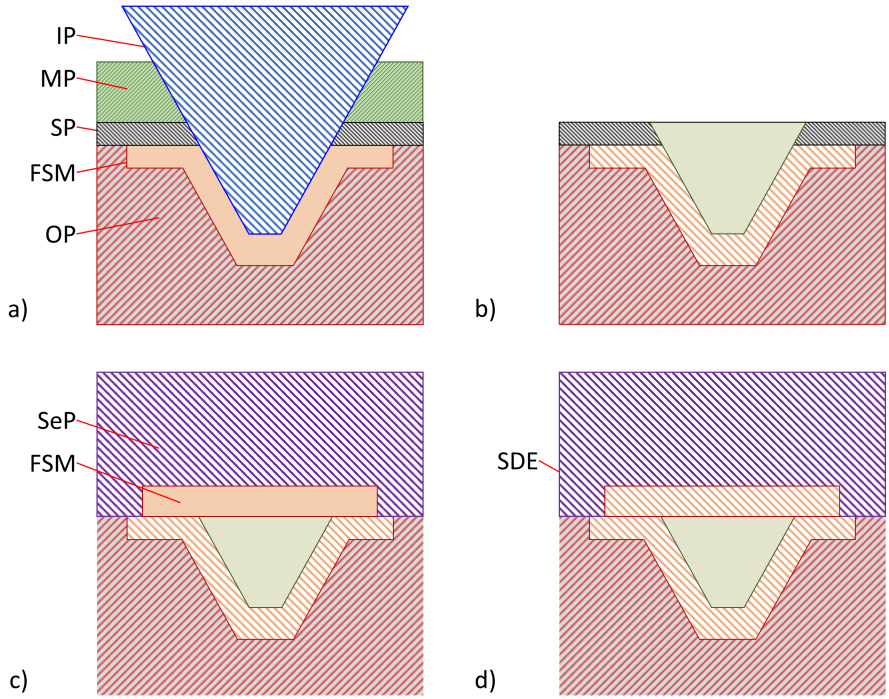

Figure 4.9.: a) the outer (OP), sheet (SP), middle (MP) and inner (IP) parts were pressed together, which shaped the degassed fresh silicone mixture (FSM) as the lateral surface of the cone. b) the IP and the MP were removed to fill the vulcanized lateral surface (VLS) with degassed fluid filling (FF) through the SP. c) the SP was removed and the half open VLS was sealed with the sealing part (SeP) that was filled with FSM. d) after the second vulcanization process the spring-damper-element (SDE) was enclosed and hermetically sealed.

While the sheet part was still adhering on the SDEs' skirts, the SDEs were filled with the silicone fluid filling through the holes in the sheet part and centrifuged under vacuum for approx. $10\ min$. After removing the remaining component A on the sheet part, the sheet part was taken off the outer part. Finally, the sealing part, still full with fresh mixture, was put on the outer part and they were placed in the oven for vulcanization again about $20\ min$ in $85°C$. After this second vulcanization, the flat membranes that were shaped by the sealing part stuck to the skirts of the SDEs in the outer part, thus sealing the SDEs permanently. Some crucial parts of the manufacturing can be seen in Figure 4.10.

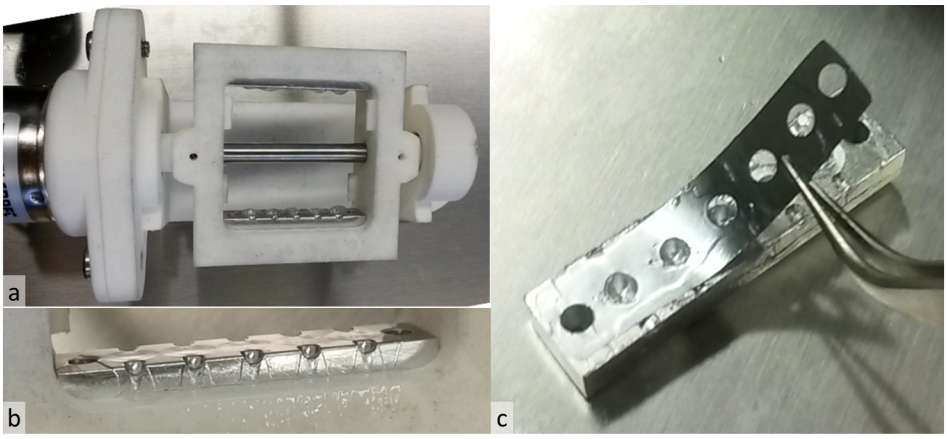

Figure 4.10.: a) the outer part (bottom) and the sealing part (top) were placed in the centrifuge prior to degassing. b) smooth surface of the fresh silicone mixture in the outer part right after the degassing in the centrifuge. c) removing the sheet part from the outer part after degassing the fluid filling in the vulcanized lateral surface.

Intraoperative length adjustment

A crucial feature for PAM to be suitable for clinical use was to realize a mechanism to adjust the initial length intraoperatively, because the SDE was designed for a postoperative length adjustment of approx. $1\ mm$ and not for the intraoperative length adjustment range of up to $3.5\ mm$. As one of the main requirements was to build the PAM in a way that its usability stays similar to the conventional solution, a clamping mechanism, a custom made crimping pliers and a sizer disc (PAM-Sizer-Disc) similar to the sizer disc of the TTP-VARIAC system were designed for intraoperative length adjustment Figure 4.11. For further simplification of the manufacturing process, the prosthesis heads and feet were taken from TTP-VARIAC Partial and Total Prostheses (Heinz Kurz GmbH, Dusslingen, Germany). This type of prosthesis was already equipped with a clamping mechanism. The clamping mechanism of the conventional prosthesis was not used for PAM, but its prosthesis head and foot were connected very loosely in its initial form. This made it easy to separate them without damaging the prosthesis.

The clamping mechanism of PAM consisted of a custom-made medical grade titanium part with a $0.25\ mm$ wide drill hole through it. While the titanium part was fixed to the SDE, the $0.2\ mm$ thick wire-like portion of the prosthesis foot was placed in the hole loosely. As seen in the Figure 4.12, PAM was placed in the PAM-Sizer-Disc, so that the prosthesis foot contacted the disk floor. The distance between the disc floor and the clamp-

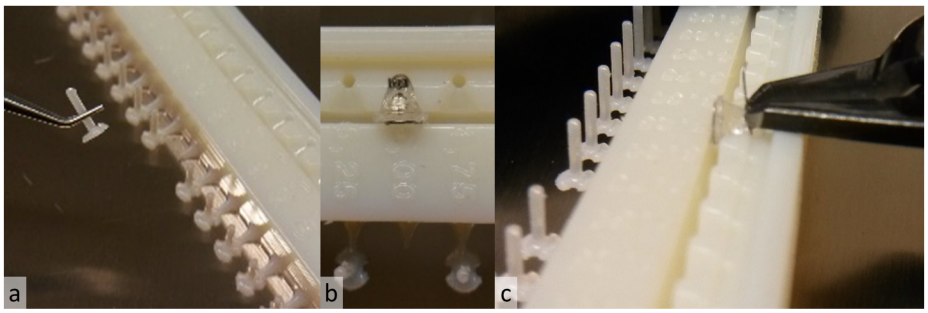

Figure 4.11.: a) the PAM-Sizer-Disc had prosthesis dummies in a range of $3.5 - 7.0\ mm$ attached to its side, which could be easily tore apart and put into the ME for measuring the right prosthesis length. b) the PAM-Sizer-Disc had dedicated spaces for different prosthesis lengths. Note that the prosthesis dummy was missing, which was used for measuring. c) the PAM could be crimped by a custom made crimping pliers.

ing mechanism was predefined to adjust the final length to a desired value. In this position, the clamping mechanism was crimped via a custom-made pliers. Thereafter, the prosthesis foot of PAM must be bent about $90°$, so that the prosthesis foot became perpendicular to the prosthesis head. Although this step of bending to right angle is not necessary for conventional prostheses, bending the conventional prostheses to adapt their shape to the anatomy of the patient is a common procedure carried out by surgeons. Finally, the wire-like portion of the prosthesis foot was cut off as usual. The final prosthesis can be seen in Figure 4.13.

4.3.2. Lifespan test in third iteration

For the measurement of the lifespan, a custom-made apparatus was built, which simultaneously compressed five conical SDEs $1\ mm$ axially and released immediately. The SDEs were placed on a flat surface and compressed by $3\ mm$ thick round stamps. The relatively large surface of the stamps ensured a maximum stress on the elastic cover. The compression-release cycle was repeated for $17\ h$ long with a cycle duration of approx. $1\ s$, thus ensuring at least $60,000$ cycles. The number of cycles was determined as the double amount of cycles, if the SDE was compressed at least 5 times a day for 15 years. After the experiment, manual or optical examining did not reveal any leakages or changes in any of the five SDEs. Thus, it could be concluded that the SDEs could endure the mechanical loads during the expected lifespan of a conventional middle ear implant.

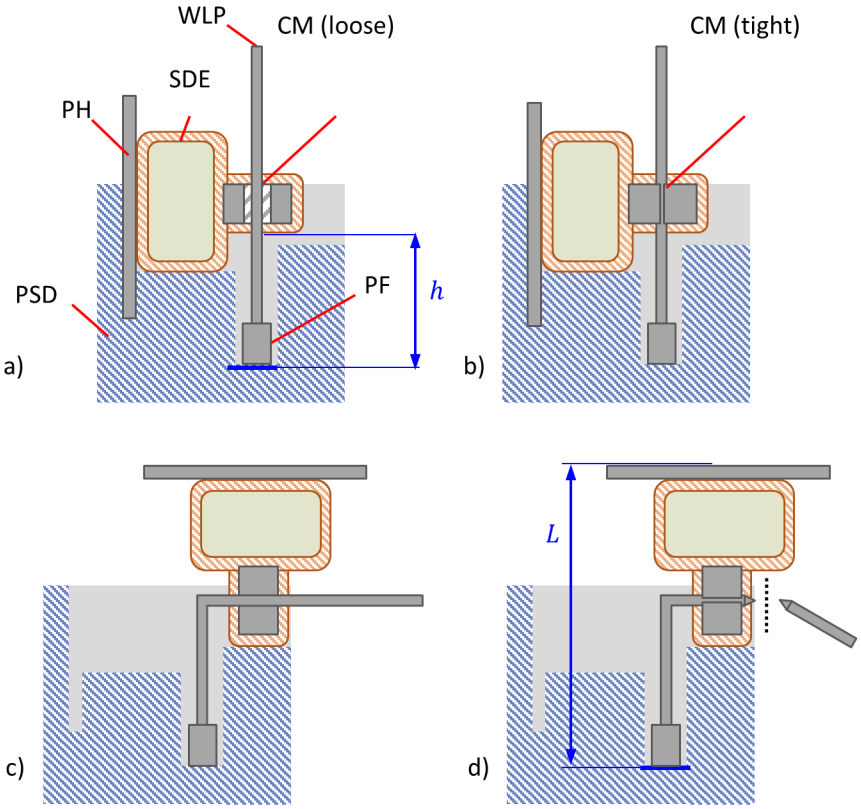

Figure 4.12.: cross-section of the PAM placed inside the PAM-Sizer-Disc (PSD). The steps of the intraoperative length adjustment of PAM were as follows: a) prior to crimping, the wire-like-portion (WLP) of the prosthesis foot (PF) could be slid in the crimping mechanism (CM, loose) until the PF touches the floor (thick blue line), b) PF could be crimped to the SDE at the CM (tight) with a defined distance of h, c) the PF was bent $90°$ at the CM and d) the WLP was cut off. The distance h between the PF and the CM defines the final length of the prosthesis L.

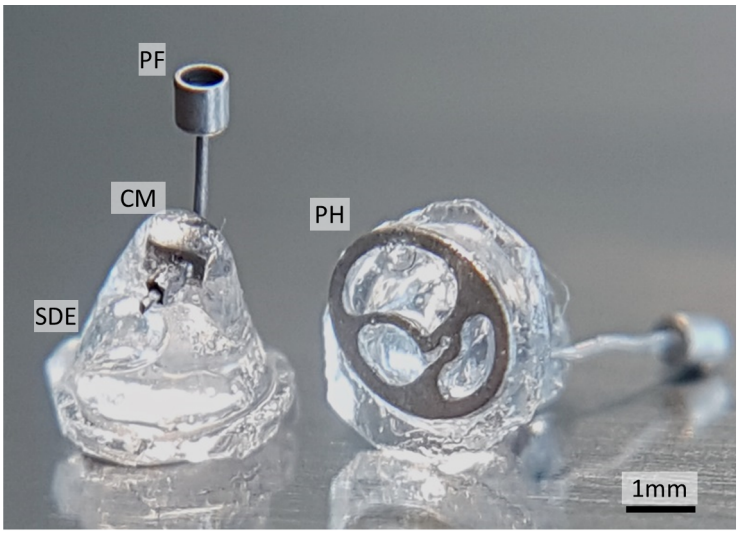

Figure 4.13.: PF: Prosthesis foot, CM: Clamping Mechanism, SDE: Spring-Damper-Element and PH: Prosthesis head. In the left PAM, the pointy end on the bottom left side of the CH is the rest of the wire-like portion of the PF that was cut off.

4.3.3. Axial and radial stiffness measurements in third iteration

The axial stiffness of PAM was measured by using an 11-bit analog-digital-converter Digiforce 9310 (burster gmbh & co kg sensors & precision measurement, Germany). The force was measured by a sensor KDs47 (ME-Meßsysteme GmbH, Germany), which could measure force range of $\pm 0.5\ N$. The elongation was measured by a potentiometric displacement sensor 8711 (burster gmbh & co kg sensors & precision measurement, Germany) with a range of $50\ mm$.

Compression-force curves were measured with a force resolution of $0.5\ mN$ and displacement resolution of 27 μm thus generating $10 - 11$ displacement-force pairs for every curve. This guaranteed at least a $250\mu m$ compression range with contact to the prosthesis. For each of four conic PAMs (PAMco1-4), whose specifications can be seen in Table 4.4, three curves were measured. Consequently, the simple linear regression was calculated for every PAM with $30 - 33$ displacement-force pairs. A table with all displacement-force pairs can be found in the appendix D.

The same procedure was used for measuring the radial stiffness. In the radial configuration, the PAMs were fixed at their prosthesis heads and the force was applied to their feet in a radial direction to their axes. Applying the force sideways resulted in a bending

deformation of the SDE, thus tilting the prosthesis foot relative to the prosthesis head.

Table 4.4.: Conic PAMs and TORPs used for experiments in the third iteration

Name	SDE-form	Length $[mm]$	Filling Component A/B	TB number
TORP1	-	5.50	-	1
TORP2	-	6.00	-	1
PAMco1	Conic	5.50	A	1
PAMco2	Conic	6.00	A	1
TORP3	-	4.00	-	2
TORP4	-	4.25	-	2
PAMco3	Conic	4.00	A	2
PAMco4	Conic	4.50	A	2

Our measurements revealed a median axial stiffness of 70 mN/mm and a median radial stiffness of 16 mN/mm for conic PAMs. The stiffness values can be seen in Table 4.5. Here, two issues must be mentioned with the measurements. First, it must be taken into account that the radial force application makes it hard to compare the radial values directly, because the bending force decreases with the increasing prosthesis length. Second, due to their long lever arm the force needed to bend PAMco1 and PAMco2 were too weak to measure. This led to unsatisfactory precision and exclusion from radial stiffness measurements.

Table 4.5.: Results for the axial and radial stiffness measurements in the third iteration

Name	Axial stiffness $[mN/mm]$	Radial stiffness $[mN/mm]$	Length $[mm]$
PAMco1	65	-	5.50
PAMco2	83	-	6.00
PAMco3	73	20	4.00
PAMco4	75	11	4.50

4.3.4. Handling test in third iteration

During the first TB experiment, a handling test was arranged in addition to the functional experiment. Two senior surgeons evaluated the conic PAMs by implanting them to the TB preparation through the EC with the aid of standard instruments. The goal was to test, if

the PAM could be implanted without the necessity of new techniques or instruments as well as within a usual frame of time and effort needed for conventional operation.

The evaluation revealed three major aspects:

1. prosthesis length adjustment
2. prosthesis geometry adjustment
3. maneuverability of the prosthesis during implantation

During the intraoperative prosthesis length adjustment of PAM, the soft SDE was not fixed properly in the PAM-Sizer-Disc. Thus, the unstable positioning of the clamping mechanism did not allow an easy length adjustment. After the length adjustment of a conventional TORP, surgeons usually bend the prosthesis by holding the prosthesis at its head and foot, in order to adapt the prosthesis geometry to patient's anatomy. This was not possible for PAM, because the prosthesis foot could not be bent by holding PAM at its head, which are connected through the elastic SDE. Also, bending the prosthesis foot of PAM alone proved problematic due to its much smaller size compared to conventional TORP. Finally, the flexible SDE proved to be useful during prosthesis manipulation through the EC and inside the tympanic cavity. Here, both rotational and translational DoF were helpful (see Figure 4.14).

As a result, both surgeons agreed that the implantation did not necessitate new instruments or techniques and that the length adjustment of PAM needed improvement. The first surgeon evaluated PAM's self adjustment sufficient enough and that the geometry adjustment by bending was not as crucial for PAM as it was crucial to the conventional TORP. The second surgeon however evaluated the lack of geometry adjustment as an obstruction. Both surgeons agreed that the maneuverability of PAM was better than conventional TORP. As to the overall clinical evaluation, first surgeon evaluated PAM better than TORP and the second surgeon evaluated PAM neither better nor worse than a conventional TORP.

4.3.5. Temporal bone experiments in third iteration

Goal and procedure for TB experiments in third iteration

The aim of the experiments with TB was to compare the sound conduction of PAM to a conventional TORP under optimal and suboptimal stress situations. The core process of the comparison was as follows: First, the stapes' response to sound (SRS) of the natural TB was measured according to ASTM Standard F2504.24930-1 to ensure that the TB preparation was within the acceptance range. Then, the incus was removed and the desired

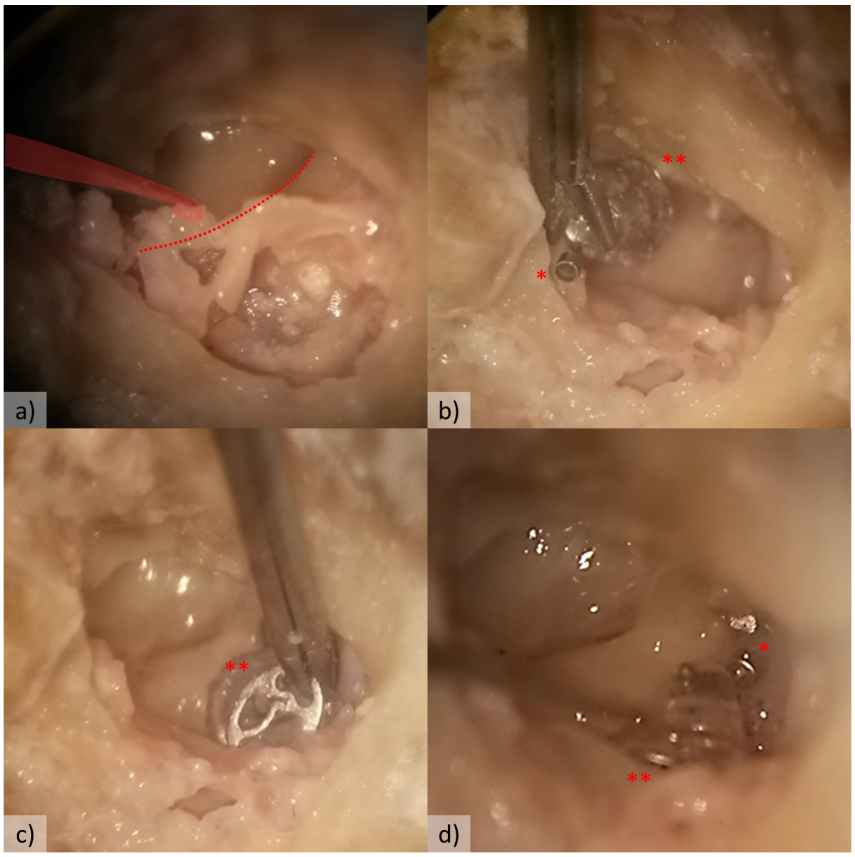

Figure 4.14.: Selected steps of the implantation of the PAM through EC as in an usual tympanoplasty. a) cutting and flapping the TM with a spoon knife (the knife is highlighted in red and the edge of the TM fold is marked with dashed line), b) introducing PAM Through the opening with standard ENT tweezers, c) placing the PAM by holding at the prosthesis head and d) PAM in its final position with a slightly angular self-adjustment. *: PAM's foot, **: PAM's head.

prosthesis length was measured by using sizers from Heinz Kurz GmbH (Dusslingen, Germany). The right length was determined by examining the prosthesis fit and by comparing the SRS measurements with different sizers.

After the measurements with the natural TB, a first conventional TORP from Heinz Kurz GmbH (Dusslingen, Germany) was set to the determined prosthesis length and implanted into the TB. The SRS of the reconstructed TB was measured. The first TORP was replaced with a first PAM of equal length and its sound conduction was measured as well. This was followed by replacing the first PAM with a second PAM, which was $0.5\ mm$ longer than the first PAM. Then, the second PAM was replaced with an equally long second TORP, which was $0.5\ mm$ longer than the first TORP. The SRS was measured after each prosthesis replacement.

While the comparison between the first TORP and the first PAM gave insight to the sound conduction under optimal tension, the comparison between the second PAM and the second TORP gave insight to suboptimal situations. A suboptimal situation could represent a too long prosthesis or a compressed ossicular chain under static pressures. In both cases, the prosthesis applies an undesired force to the IE, because the prosthesis is longer than the distance between the malleus and the SFP. Furthermore, comparison between the first and second PAM or between the first and second TORP allowed to characterize the same type of prosthesis under optimal and suboptimal tensions.

Three major results were expected from these experiments:

1. that the transmission characteristics of the first TORP and PAM would not show a significant difference under optimal tension,

2. that the second PAM would conduct sound significantly better than the second TORP under suboptimal tension and

3. that the sound conduction of first and second PAMs would not show a significant difference.

Since it was not possible to conduct enough measurements for statistical analysis, a large margin of $10\ dB$ was adopted to determine that the difference between any two measurements was significant. Furthermore, because the ex-vivo results under lab conditions are usually better than the operational outcome, a successful sound conduction was defined as an ABG less than $10\ dB$ instead of $20\ dB$.

The experimental setup for SRS measurements was the same with the SRS measurements that was described in Section 3.3.2, thus it will not be described here any further.

Experimental results for TB experiments in third iteration

As to the first step of the comparison process, it could be shown that both TB preparations were within the acceptance range of the ASTM standard. During the first experiments, two TORPs were implanted as well as four conic PAMs to two different TBs (see Table 4.4). The measurements with the sizers revealed that the optimal tension for the first TB was achieved with a prosthesis length of $5.5\ mm$ and for the second TB with $4.0\ mm$. However, there were some unforeseen problems with the experiments. First, the sound conduction with the TORP2 could not be measured on the first TB, because the SFP was ruptured during implantation. Furthermore, the TORP4 was adjusted too short ($4.25\ mm$ instead of $4.5\ mm$).

As seen in the Figure 4.15, the TORP1 and TORP3 with the right length showed smaller losses than $10\ dB$, besides at $10\ kHz$ in first TB (TORP1) and at $3\ kHz$ in second TB (TORP3). The TORP2 and TORP4 (that were too long) showed significant loss in sound conduction, but in some cases * resulted in gain. The conic PAMs exhibited higher losses than $10\ dB$, even compared to the too long TORPs. Therefore, our first expectation was only fulfilled for some parts of the frequency range and our second expectation was almost never fulfilled except at $3\ kHz$ in second TB. Fortunately, the third expectation was fulfilled in both TBs. The PAMs showed insignificant differences due to length change in 8 frequencies out of 10 with the first TB (80%) and in 9 frequencies out of 10 with second TB (90%), while all three significant differences were approx. $12\ dB$. In contrast, the comparison of the TORP 3 to TORP 4 was insignificant in 6 out of 10 cases (60%), while the significant differences were $10,\ 15,\ 15$ and $24\ dB$, which were higher than the differences between PAMs.

4.3.6. Discussion of the third iteration

This iteration was a mile stone for PAM, because all the issues concerning the manufacturing and clinical usability were addressed. The manufacturing process was improved to minimize the effects of the steps that contained manual work. Although the process was not automatized, it was precisely defined and some level of scaling up was achieved by manufacturing five SDEs at the same time. Moreover, the clinical usability was fulfilled by assembling the SDE, prosthesis foot and head to PAM as well as by introducing a clamping mechanism and dedicated tools to adjust the prosthesis length intraoperatively. The manufactured SDEs and the clinical usability of the PAM were tested both under lab

*Here, a *case* is defined as a measurement of the SRS of a prosthesis at a frequency. For example SRS measurement of TORP1 at the frequency $1\ kHz$.

conditions but also in a TB experiment, which was the closest to real conditions and which has been used for validating commercial ME prostheses.

Despite the positive results from the functional tests and handling test, which supported the applicability of the manufacturing and usability, the TB preparations showed that the sound conduction was not satisfactory. Therefore, the form of the SDE needed improvements, which could be done by analyzing the effects of the form on the static behavior of the SDE.

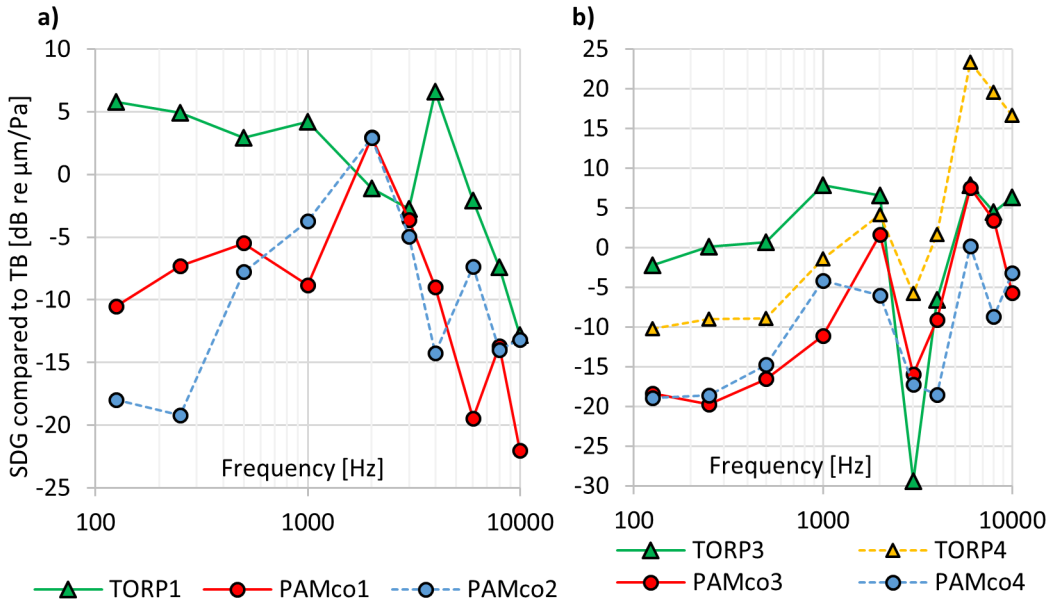

Figure 4.15.: The measurement results for the stapes' response to sound of conical PAMs (PAMco) acc. to ASTM. The dB-values do not present absolute SPLs, but the gain relative to the sound conduction of the temporal bone (TB). a) Measurements on the first temporal bone and b) measurements on the second temporal bone. SDG: stapes displacement gain

4.4. Forth Iteration: Final Prototype

4.4.1. Form optimization

The unsatisfactory experimental results from the SRS measurements of the third iteration made an improvement of the sound conduction necessary. As the hitherto forms of hemisphere, cylinder and cone that were analyzed for feasibility purposes were only selected out of common objects, it was clear that the form of the SDE must have been designed in a whole new way. This meant that the development method proposed in the Section 2.2.5 should be applied from the beginning.

As described in the Section 2.2.5, the process began with the virtual analysis of the small, flagrant and elastic structure of the SDE. Therefore, it was decided to simulate the SDE with an FEM model, which was described in the Section 3.1. While the second iteration focused on the verification of the FEM simulation, in the fourth iteration it was used for virtual evaluation of different new design concepts. Because the prosthesis head had an elliptical form and the prosthesis foot formed an axis, the concepts for SDE-design were limited to rotational symmetric forms.

Since the minimum stiffness of the SDE was aimed, the wall thickness was kept to $0.1\ mm$, thinnest wall that could be manufactured with the provided infrastructure. Another parameter was the area of the prosthesis foot. On the one hand, a larger area meant sound conduction over a bigger cross-section, but on the other hand this increased the axial stiffness of the SDE. As the form of the elastic cover was stabilized by the hydrostatic pressure, the spring stiffness depended much on the form stability. A soft spring, however, could be achieved by a unstable form. This can be clarified by referring to the three exemplary forms described in the second iteration. The hemisphere had the highest stiffness, because it was a very stable and homogenous shape, which redirected any applied force on the surface into tensile stresses around the surface, to which even thin structures can show high resistance. A simple strategy to lower the stability was to build a conical SDE, because a large buckling motion at the tip of the cone (connection to prosthesis foot) displaced a small volume of fluid, which caused limited stress by spreading to the bottom of the cone with larger cross section. In the simulations, the stiffness of the conic SDE had a stiffness around $20\ mN/mm$.

A more effective way to reduce the form stability was to add heterogeneity on the peripheral surface, which would redirect some of the force to compressive stresses, resulting with buckling and collapsing of the thin membrane. However, this heterogeneity must be in the cross-section and not along the axis. For example, a sandglass shaped SDE has a buckle

around the axis and always a circular cros-ssection along the axis. This does not reduce its form stability, because the circular cros-ssection distributes the stress evenly around the circumference. However, deviations in the cross-section perpendicular to the symmetry axis, such as a star shaped SDE, weakened the stability more effectively (see Figure 4.16). The best results were achieved with cubic shapes, because they allowed buckling of flat surfaces and the cross-section was unstable at the corners. In the simulations, this effect allowed to enlarge the area of the prosthesis foot four times, while increasing the axial stiffness to approx. $50\ mN/mm$ only 2.5 times compared to the conical SDE.

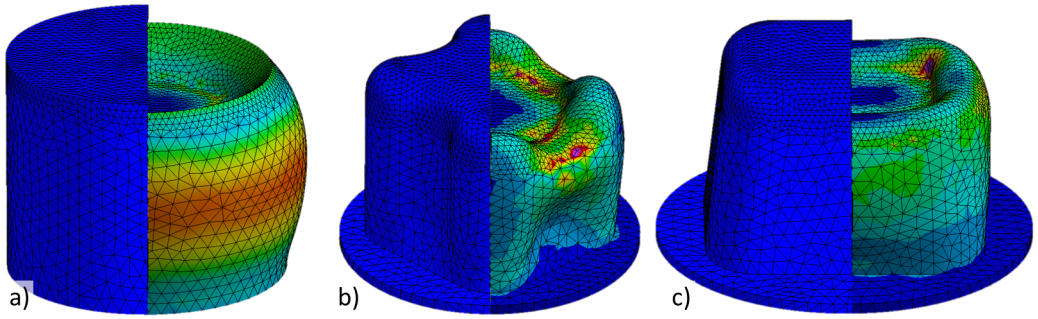

Figure 4.16.: Simulation of the considered SDE-designs: a) cylindrical, b) star shaped and c) cubic SDEs. The pictures show undeformed shapes on the left side (left half) and the shapes deformed by indentation on the right side (right half). While the uniformly distributed deformation of the cylindrical SDE makes it a stable form, the less stiff cubic SDE shows buckling formations.

The cubic PAMs were manufactured with the same method that was described in the third iteration Figure 4.17. The only difference here was that the mold parts were made of PEEK, a highly biocompatible even long-term implantable material, with the exception of the sheet part, which was still made of steel due to the required thin, elastic and durable material properties.

4.4.2. Axial and radial stiffness measurements in fourth iteration

The same experimental setup was used for these measurements that was described in Section 4.3.3. Again, three compression-force curves with a force resolution of $0.5\ mN$ and displacement resolution of $27\mu m$ with $30 - 33$ displacement-force pairs for each of three cubic PAMs (PAMcuA1-3) were measured, whose specifications can be seen in Table 4.6. A table with all displacement-force pairs can be found in the appendix D.

These measurements revealed a median axial stiffness of $150\ mN/mm$ and a median

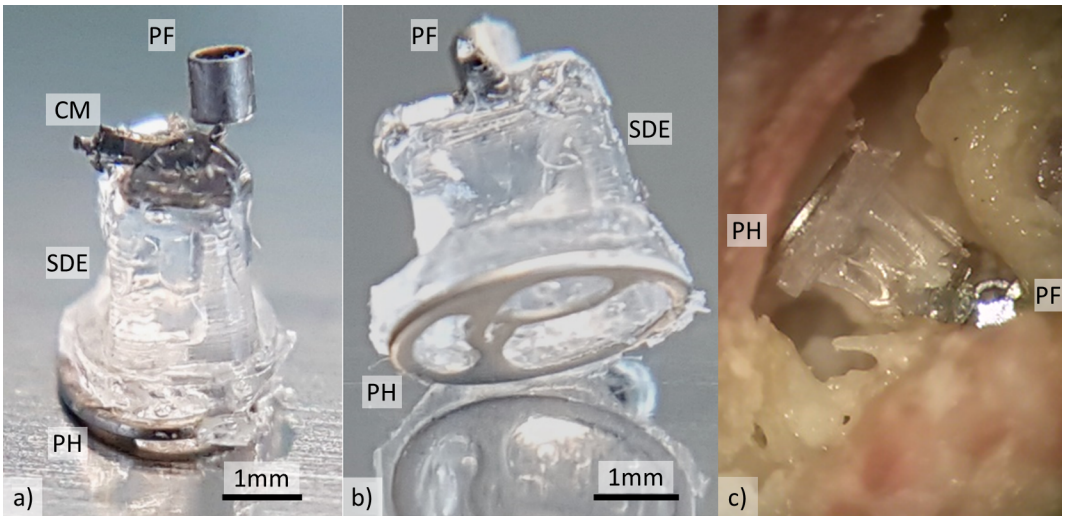

Figure 4.17.: a) cubic PAM, the pointy end on the bottom left side of the CH is the rest of the wire-like portion of the PF that was cut off. b) a different view of the PAM showing the PH. c) cubic PAM implanted into the TB preparation. The shiny square at PF was the reflector for LDV. PF: Prosthesis foot, CM: Clamping Mechanism, SDE: Spring-Damper-Element and PH: Prosthesis head.

radial stiffness of 12 mN/mm. The stiffness values can be seen in Table 4.7. Here, it must be taken into account that the radial force application made it hard to compare the radial values directly, because the bending force decreased with the increasing prosthesis length. Furthermore, the stiffness of the PAMs with the silicone component B as filling could not measured, because it was observed that this filling kept on vulcanizing, which transformed the SDE into a simple spring element made of a block of silicone rubber. This vulcanization was much slower than the vulcanization of the fresh mixture and had no effect on the SRS measurements, because the stiffness measurements took place several weeks after the TB experiments.

4.4.3. TB experiments in fourth iteration

Goal and procedure of the TB experiments in fourth iteration

The aim of the second TB experiment and the followed procedure was the same as the first TB experiment described in Section 4.3.5. SRS of the first PAM and first conventional TORP with optimal lengths as well as the SRS of the second TORP and second PAM with extended lengths were measured to find out, if the three expected results were achieved

Table 4.6.: Cubic PAMs and TORPs used for experiments in the fourth iteration

Name	SDE-form	Length $[mm]$	Filling Component A/B	TB number
TORP5	-	4.00	-	3
TORP6	-	4.25	-	3
PAMcuA1	Cubic	4.50	A	3
PAMcuA2	Cubic	4.50	A	3
PAMcuA3	Cubic	5.00	A	3
PAMcuB1	Cubic	4.50	B	3
PAMcuB2	Cubic	4.25	B	3
PAMcuB3	Cubic	4.50	B	3

Table 4.7.: Results for the axial and radial stiffness measurements in the fourth iteration

Name	Axial stiffness $[mN/mm]$	Radial stiffness $[mN/mm]$	Length $[mm]$
PAMcuA1	150	18	4.50
PAMcuA2	168	12	4.50
PAMcuA3	98	27	5.00

with the cubic PAMs. As a reminder, a measurement difference was significant, if it was higher than $10\ dB$ and it was expected from the experimental results...

1. that the transmission characteristics of the first TORP and PAM would not show a significant difference under optimal tension,
2. that the second PAM would conduct sound significantly better than the second TORP under suboptimal tension and
3. that the sound conduction of first and second PAMs would not show a significant difference.

Experimental results for TB experiments in fourth iteration

Measurements on the third TB preparation showed that it was too within the acceptance range of the ASTM standard. In this experiment two TORPs as well as six cubic PAMs were implanted to the third TB (see Table 4.6). Measurements with the sizers revealed that the optimal tension for this TB was achieved with a prosthesis length of $4.0\ mm$. However, because the cubic PAMs could not be adjusted as short as $4.0\ mm$, it was not possible to compare TORP5 and cubic PAMs with the desired length. Nevertheless, enough measurements to highlight significant cases could be gathered.

As seen in the Figure 4.18, the TORP5 with the right length showed no losses greater than $10\ dB$ besides at $10\ kHz$. The TORP6, which was $0.5\ mm$ too long, showed significant loss in sound conduction, but in some cases resulted in gain. Although the first expectation could not be tested in the second TB experiment, it could be shown that the cubic PAMs were more successful in fulfilling the second expectation. In the whole frequency range with 60 cases, cubic PAMs conducted sound significantly better than TORP6 in 8 cases (13%) and slightly better in 14 cases (24%), slightly lower in 15 (25%) cases and significantly lower in 23 cases (38%). Comparing PAMcu to PAMco reveals that this was a significant improvement in sound conduction. Out of 40 cases, too long conic PAMs could conduct sound significantly better in no cases (0%), slightly better in 2 cases (5%), slightly worse in 17 cases (42.5%) and significantly worse in 21 cases (52.5%). An unnegligible observation in this picture is that the cubic PAMs conducted sound significantly lower than TORP6 in all 18 cases at the frequencies 0.125, 0.25 and $0.5\ kHz$ without exception. This leaves only 5 cases with significantly lower conduction for the frequencies $1\ kHz$ and above out of 42 cases.

For testing the third expectation, the PAMcuA3 could be compared with the other PAMs, which was $0.5\ mm$ longer than the PAMcuA1, A2, B1 and B3. This comparison revealed

that in 29 out of 40 cases (72.5%), prosthesis length difference of PAMcu did not cause a significant change of sound conduction. An unexpected result was that in contrast to the conical PAMs, cubic PAMs showed a very high deviation up to 27 dB. In comparison, the TORP5 and TORP6 showed a similar deviation similar to the other TORPs with insignificant differences in 4 cases 40% and 6 significant differences up to 20 dB in 10 cases.

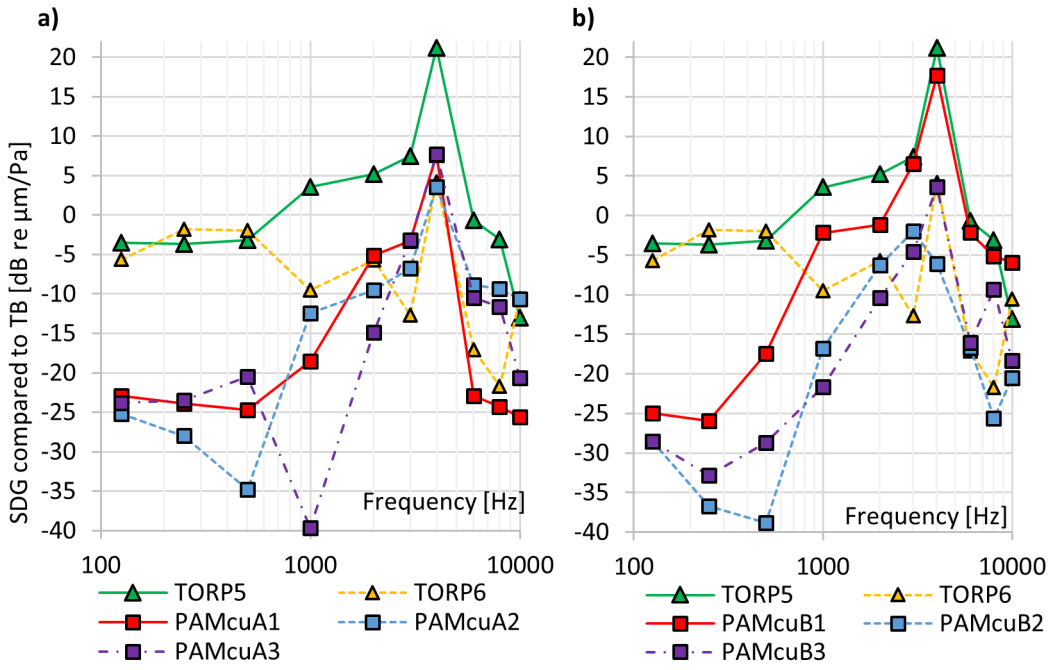

Figure 4.18.: The measurement results for the stapes' response to sound of two TORPs and six cubic PAMs (PAMcu) acc. to ASTM. The dB-values do not present absolute SPLs, but the gain relative to the sound conduction of the temporal bone (TB). a) Measurements with PAMcu filled with component A and b) Measurements with PAMcu filled with component B. SDG: stapes displacement gain

4.4.4. Discussion of the fourth iteration

This final iteration was the completion of the development method. The virtual SDE model was used to analyze the effects of SDE form on the final static behavior, a promising SDE with cubic form was built by using the manufacturing tools and verified with the testing tools introduced in the prior iterations, it was assembled to cubic PAM and finally cubic

PAM was tested on TB preparation. This iteration was initiated with the aim to improve the sound conduction without making the SDE significantly stiffer and this aim was achieved by applying the proposed development method in this thesis.

Despite the positive results, this iteration showed that some issues could not be investigated thoroughly. Although the SRS results of the cubic PAMs were better than the conical PAMs, a significant frequency dependence was observable. Cubic PAMs failed in the lower frequencies without exception and showed a very high deviation when they were compared to each other, especially at $1\ kHz$. This might be an indication that the cubic PAMs have frequency modes, which could not be simulated beforehand and whose cause could not be clarified sufficiently.

4.5. Discussion

The novelty of PAM is not the idea of using a mechanical element with viscoelastic or spring-damper properties for middle ear prostheses. Its novelty lies in the integrity of its development method for testing and realizing a new SDE, while fulfilling requirements and avoiding restrictions dictated by the anatomical and clinical circumstances. Precisely because this is a novel solution, PAM has some drawbacks at present that could not be solved or some that could not be even investigated properly.

First and most importantly, the sound conduction of PAM was only acceptable for a limited range of frequencies. Therefore, it must be improved to meet the required levels in all frequencies. Second, the intraoperative length and geometry adjustments could be done in a similar way to conventional procedure, but not as easy due to the loose connection between the head and the foot of the prosthesis via elastic SDE. Furthermore, the sterility and biocompatibility were missing from the tests of usability. In theory, PAM was made of materials that were proved to be biocompatible and that could withstand the typical temperatures for autoclave, but neither could not be validated in this work.

Finally, the long-term effects must be investigated thoroughly. To eliminate such risks, a long-term implantable silicone rubber was selected, the deformations were limited to less than the quarter of the rupture elongation of the silicone rubber and the mechanical durability was verified for $60,000$ cycles. However, the middle ear environment can still cause changes or malfunctions in PAM, despite its capsular design. For example, the thin walls of the elastic cover may not be able to block the diffusion of the fluid filling, which might drain the elastic cover and reduce the damping property to a critical value.

Finally, the initial length of PAM was not solved properly. Compared to the conventional system, it was not easy to adjust the length of the PAM and in some cases the length was

adjusted wrong. Also, the minimum initial length of PAM was too long. Although the PAM was built with a partial prosthesis foot for tympanometry IIIA, it was too long to implant it between the malleus and stapes. Even the PAM with total prosthesis foot was too long for the third TB. So the initial length adjustment is an open issue, which must be improved by another iteration. A shorter SDE for a shorter initial length could be achieved by an SDE that has sharper corners.

The accomplishments of PAM were nonetheless significant. First, PAM was exclusively made of long-term implantable biocompatible materials using conventional manufacturing techniques. While it provided multiple DoF including rotation as well as translation, it did not have a structure consisting of classical mechanic components, which would necessitate a complicated manufacturing process. The SDE improved the prosthesis from a technical standpoint, although the handling of PAM remained the same or even better maneuverable than the conventional prosthesis by integrating it into one of the most preferred commercially available TORPs. Furthermore, it was anticipated that PAM could reduce the risk of extrusion without risking a migration by limiting the tension on the tissues to a predefined value in every direction.

CHAPTER 5

Conclusion and Outlook

5.1. Summary

The middle ear is a complex mechanical structure, whose most important members are the tympanic membrane, malleus, incus, stapes and the ligaments that combines the three ossicles to an ossicular chain. The main functions of the middle ear are the protection of the inner ear against external conditions and sound conduction from the outer ear to inner ear. Thanks to its superior mechanic formation, middle ear can carry out its both functions under extreme conditions. However, the complex and delicate structures of the middle ear make it prone to different injuries caused by diseases, degeneration and trauma. In some cases these injuries are irreversible and the middle ear loses its ability to conduct sound, which is called conductive hearing loss. There are numerous methods to diagnose the different causes of the conductive hearing loss varying from simple hearing tests to electronic pure tone audiometry and to cure these distinct causes there are many methods and devices varying from the conservative hearing aids to surgically inserted middle ear implants accordingly.

Two of the most common conductive hearing loss cases are the missing parts of the ossicles or immovable ossicles that fuse to the middle ear walls. In these cases the ossicles can be replaced with ossicular replacement prostheses by a tympanoplasty type IIIA or IIIB surgery. Since the natural ossicular chain moves as one piece during the sound conduction, the replacement of the ossicular chain with a monolithic prosthesis reconstructs the sound conduction mostly sufficient. Nevertheless, changes in external conditions are compensated by relative motions in the elastic ossicular chain, which cannot be reproduced by monolithic commercial prostheses. Therefore, the intraoperative length adjustment be-

comes a very challenging step during the tympanoplasty. If the prosthesis length was not set correctly, the prosthesis may migrate, extrude through the tympanic membrane as well as the stapes and/or block the stapes motion. In all cases the Air-Bone-Gap stays higher than 20 dB and patient must go under a revision operation without the guarantee of a better outcome than the first surgery.

To solve this issue, a new kind of ossicular replacement prosthesis is needed, which can adapt its length postoperatively. Indeed, many researchers proposed ossicular replacement prostheses with postoperative length adjustment function, however, these concepts are mostly stayed just as ideas, while only few of them were tested in laboratories and none of them made it to clinical studies. One of the main reasons for that is the lack of experimental environments that provide realistic and reproducible testing conditions without costing too much time and effort, in order to investigate and optimize the parameters of the ossicular replacement prosthesis in development. Another reason is that it is very hard to estimate the long term effects of the biological mechanisms in middle ear, in order to exclude the new causes of complications that could occur after a long time posterior to the surgery (e. g. extrusion).

Having this background in mind, this work started by gathering the requirements for building a new PAM that originated from the anatomy and physiology of the middle ear as well as the clinical usability of the conventional ossicular replacement prostheses. The mechanical analysis of the middle ear revealed that it operates under two major modes. In the static mode, it is a kinematic system that transforms the large motions of the tympanic membrane into smaller tilting motions at the stapes, which protects the inner ear from excessive static forces. In the dynamic mode, its viscoelastic properties transform small tympanic membrane vibrations into even smaller but stronger stapes foot plate vibrations, which constitutes the sound conduction. When the number of links and joints are reduced by tympanoplasty type III, in order to bridge the tympanic membrane directly to stapes foot plate, the sound conduction is maintained to a larger portion, but the static force compensation gets canceled out almost entirely. Therefore, reconstructions with PORPs need at least one extra DoF and reconstructions with TORPs need at least two extra DoF. Other crucial properties of PAM were determined based on the literature, such as the motion range of 1 mm and maximum weight of 50 mg. Also some design limits were set based on the clinical use and literature, such as using exclusively long-term implantable materials, limiting the prosthesis size as well as the handling to commercial prostheses and limiting the invasiveness of the procedure.

Next, different concepts were gathered and classified. Especially different mechanical elements such as springs, dampers and flexure hinges were analyzed in detail. Based on

the previously determined requirements and limits, many of these solution concepts were eliminated, for example all active implant solutions or mechanisms containing friction elements. This elimination narrowed down the scope of solutions to viscoelastic mechanisms. Here some more detailed analysis steered the search for a solution to an spring-damper-element, which had to be able to bend, twist and stretch in all spatial directions. The most promising concept to achieve these requirements was an elastic balloon that was filled with a viscose fluid. Furthermore, a new iterative ossicular replacement prosthesis development method was proposed, which would utilize virtual and physical test environments to minimize the time and effort needed for development.

To be able to follow the proposed development method, different novel test environments had to be implemented first. For this purpose an FEM simulation was developed for virtual analysis and testing of the viscoelastic spring-damper-element. Furthermore, a new functional 3D printed anatomical middle ear model was developed in this thesis. The tympanic membrane's and ossicles' anatomical forms were reproduced by segmenting them from μCT-data of a cadaver and by 3D printing them or by silicone rubber molding with 3D printed mold parts. To enable the relative motions between the ossicles, the ossicles were 3D printed separately and attached together with elastic joints by casting them into an epithelium made of silicone rubber. The structures were positioned by a casing, whose form was not anatomical but artificially designed based on the μCT-data.

The 3D printed middle ear model's acoustic behavior in dynamic mode was tested by measuring its stapes's response to sound according to the ASTM standard and its quasi-static behavior in static mode was tested with tympanometry. Although the transfer function was not in the ASTM tolerances for the entire frequency range, its dynamic characteristics were close enough to a human middle ear to proceed with experiments. Also, the tympanometry results demonstrated that the compliance of the tympanic membrane was comparable to a human tympanic membrane. Furthermore, both dynamic and quasi-static behavior could be manipulated by using different materials. This supported that the presented model was a plausible way to build a middle ear model not only for regular, but also for pathological scenarios.

The PAM was developed in an iterative way according to the development method while using the aid of the dedicated testing tools. In the first iteration, the feasibility of the PAM was analyzed. A PAM was built using preliminary tools and easily accessible materials. The prosthesis head and foot were made of metal and the spring-damper-element was made of silicone rubber, which could be changed afterwards with implantable materials with similar chemical and mechanical properties. This iteration was finalized with preliminary experiments on middle ear model that supported the potential of both force compensation

and the sound conduction in one prosthesis.

In the second iteration, the manufacturing quality was improved by more sophisticated tools and a spring-damper-element was made of a long-term implantable silicone rubber, which was used for the rest of this work. Different spring-damper-element forms were tested and it could be shown that all the spring-damper-elements could compensate forces better than a commercial prosthesis. A conical spring-damper-element form was chosen for further development because of its superior force compensation. Simultaneously, these experimental results were used for verifying the proposed FEM model.

The third iteration was the transition from building functional models to building a prototype. The manufacturing process was optimized and scaled up with improved tools. Also, the prosthesis head and foot were made of a conventional titanium prosthesis. Finally, a custom-made titanium part and a special sizer-disc were designed for intraoperative length adjustment. With the completion of the concept, an experiment was carried out using two human temporal bone preparations to compare the proposed PAM to a conventional TORP. Although the sound conduction was not fully satisfactory, two senior surgeons approved that the proposed concept was fit for its surgical application.

The last and forth iteration was the showdown of the whole development process and the PAM concept. The spring-damper-element's form was designed in a new way by applying the proposed method from the beginning. This time, the FEM simulation was used to analyze the effects of the form on the stiffness and a cubic form was selected as the most promising one. The chosen cubic spring-damper-element was designed and manufactured, which had a larger sound conducting cross-section but whose stiffness was not significantly higher than the conical spring-damper-element. The cubical PAM was also tested on a human temporal bone preparation for its sound conduction.

To conclude, a new PAM concept and a new method for developing PAM were introduced and successfully implemented in this thesis. The measurement results showed that the proposed PAM was very elastic and it could withstand $60,000$ cycles of extension, equivalent to a 30 years of lifespan. The evaluations showed that PAM did not necessitate any additional instrument or surgical procedures for its surgical insertion and the effort needed for handling PAM was definitely not higher than the effort needed for a conventional TORP. The human temporal bone experiments showed that the PAM could conduct sound even better than a conventional TORP in some cases and that the variations in its length had a minor effect on its sound conduction characteristics. Finally, it could be shown that the sound conduction of the PAM could be significantly improved by applying the proposed development method.

5.2. Future Work

This thesis presents a work of four years. Considering the vast variety of aspects to develop a new postoperative adjustable middle ear prosthesis, which needed a whole new method for developing including dedicated testing tools, this span of time was only enough to create the concept and to conduct tests to present the possibilities, but it was not enough to bring its full potential into action. Therefore, both the testing environments and the PAM have a long leeway of improvement in multiple directions. Some of these improvements were implemented to some degree without reaching a level that they could be included in this thesis, some were addressed in theory and some could not be addressed at all. Of course, if these improvements could be implemented, more aspects would come to daylight, which were not even considered yet.

First of all, the simulation tool had a systematic error that had to be corrected by an additional coefficient depending on the wall thickness. This systematic error may be depending on the material model, which should be improved to match the real material. Furthermore, the hydrostatic pressure was implemented without taking the fluid properties (e. g. viscosity) into account. Therefore, the spring-damper-element's sound conduction could not be simulated digitally. A simulation that could give some insight to the dynamic behavior of the spring-damper-element would accelerate the iterations immensely and it could even help optimize the spring-damper-element form in an unforeseen way.

As to the middle ear Model, to the author's best knowledge, this was the first 3D printed anatomical and functional middle ear model ever presented. Of course, there were some issues, which could not be overcome during this work. First of all, the model's transfer function should be improved to meet the ASTM standards at higher frequencies. New 3D printing techniques and materials should be tested for this purpose. For example, the ossicles could be made of a more bone-like material than the PA2200. Furthermore, the tympanic membrane should be built with its typical fiber structure instead of the plain homogeneous silicone rubber. Another issue was the insufficient reproducibility of the model that way clearly caused by the assembly steps with manual work. This shall be improved by changing assembly to a more automatic process with dedicated tools such as anatomically adapted positioning apparatus. Another improvement could be to build an inner ear with its characteristic spiral form and with a perilymph substitute that has sufficient viscoelastic properties for the inner ear. The model should include generally more anatomically reproduced middle ear structures in the future and even active functions such as Valsalva maneuver. Also, anatomic pathologies such as alterations and degenerations should be mimicked. Finally, the model should be evaluated by surgeons by reconstruct-

ing the middle ear functionality with different types of implants on middle ear models with different anatomies.

Another point that would be essential for testing environments would be an equipment that would allow to change the pressure on the tympanic membrane while measuring the stapes's response to sound. A student project by Grün (2017) was initiated to address this need. Although the experimental setup with the middle ear model delivered promising results at our labs, time constraints did not allow to use this setup with the calibrated equipment for stapes's response to sound measurement during human temporal bone experiments.

Again to the best of author's knowledge, proposed PAM was the first realized TORP that was equipped with an spring-damper-element. Therefore, the effects of spring and damper properties on the sound conduction could not be clarified yet. Parametrization and test series are needed for understanding and optimizing these properties for both a better sound conduction and a better static force compensation. The sound conduction of PAM should be tested under positive, negative and neutral pressure differences on different middle ear models and on temporal bone preparations. Here, the doctoral thesis of Sauer (2016) would be a great example for such experiments. The geometry of the elastic cover should be parametrized to optimize the spring properties.

Also, varying filling materials should be tested for optimization of damping properties. The optimizations of filling is of great interest, because temporal bone experiments indicate a weak sound conduction in the lower frequencies. This could be solved by a hybrid solution, which combines the proposed elastic SDE and the sound conduction through contact proposed by Hüttenbrink et al. (2005). For example loose titanium spheres in the elastic cover, which could move freely within the viscose filling, could conduct forces through direct contact without the need of a mechanic joint.

Finally, PAM may have some potential advantages, which we could not investigate so far. The assembly of an elastic cover and a fluid fill enables parametrization of damping and spring properties independently. Thus, this could be used to optimize PAM for particular anatomical or pathological cases.

Bibliography

Abel, E. & Abraham, F. (2011), 'Ossicular replacement prosthesis'. US 12/529,461.

Ahmad, N. & Wright, A. (2014), 'Three-dimensional temporal bone reconstruction from histological sections', *The Journal of laryngology and otology* **128**(5), 416.

ASTM (2005), 'Practice for describing system output of implantable middle ear hearing devices'. ASTM F2504.24930-1.

Austin, D. (1963), 'Vein graft tympanoplasty: two-year report.', *Transactions-American Academy of Ophthalmology and Otolaryngology. American Academy of Ophthalmology and Otolaryngology* **67**, 198.

Bhansali, S. A. (2012), 'Dynamic ossicular prosthesis'. US 8262729 B2.

Bornitz, M., Hardtke, H. J. & Zahnert, T. (2010), 'Evaluation of implantable actuators by means of a middle ear simulation model.', *Hearing research* **263**(1-2), 145–51.

Bornitz, M., Zahnert, T., Hüttenbrink, K. & Hardtke, H. (2004), Design considerations for length variable prostheses finite element model simulations, *in* 'Middle ear mechanics in research and otology', World Scientific, pp. 153–160.

Buytaert, J., Goyens, J., De Greef, D., Aerts, P. & Dirckx, J. (2014), 'Volume shrinkage of bone, brain and muscle tissue in sample preparation for micro-ct and light sheet fluorescence microscopy (lsfm)', *Microscopy and Microanalysis* **20**(4), 1208–1217.

Cai, H., Jackson, R., Steele, C. & Puria, S. (2010), A biological gear in the human middle ear, *in* 'Proc. COMSOL Conf', Vol. 28, p. 46.

Cheng, J. T., Aarnisalo, A. A., Harrington, E., del Socorro Hernandez-Montes, M., Furlong, C., Merchant, S. N. & Rosowski, J. J. (2010), 'Motion of the surface of the human tympanic membrane measured with stroboscopic holography', *Hearing Research* **263**(1), 66 – 77.

Cheng, J. T., Ravicz, M., Guignard, J., Furlong, C. & Rosowski, J. J. (2015), 'The Effect of Ear Canal Orientation on Tympanic Membrane Motion and the Sound Field Near the Tympanic Membrane.', *Journal of the Association for Research in Otolaryngology : JARO* **16**(4), 413–32.

Curtis, J. & Colas, A. (2013), Chapter ii.5.18 - medical applications of silicones, *in* B. D. R. S. H. J. S. E. Lemons, ed., 'Biomaterials Science (Third Edition)', third edition edn, Academic Press, pp. 1106 – 1116.

Dalchow, C., Grün, D. & Stupp, H. (2001), 'Reconstruction of the ossicular chain with titanium implants', *Otolaryngology-Head and Neck Surgery* **125**(6), 628–630.

Dirckx, J. J. & Decraemer, W. F. (1991), 'Human tympanic membrane deformation under static pressure', *Hearing Research* **51**(1), 93–105.

Directive, C. (1993), '93/42/eec of 14 june 1993 concerning medical devices'.

Eiber, A. (1999), 'Mechanical Modeling and Dynamical Behavior of the Human Middle Ear', *Audiology and Neuro-Otology* **4**(3-4), 170–177.

Emmett, J. R. (1989), 'Biocompatible implants in tympanoplasty.', *Otology & Neurotology* **10**(3).

Ferris, P. & Prendergast, P. (2000), 'Middle-ear dynamics before and after ossicular replacement', *Journal of Biomechanics* **33**(5), 581–590.

Fisch, U., May, J., Linder, T. & Naumann, I. C. (2004), 'A new l-shaped titanium prosthesis for total reconstruction of the ossicular chain', *Otology & Neurotology* **25**(6), 891–902.

Funnell, W. R. J. & Laszlo, C. A. (1978), 'Modeling of the cat eardrum as a thin shell using the finite-element method', *The Journal of the Acoustical Society of America* **63**(5), 1461–1467.

Gan, R. Z., Yang, F., Zhang, X. & Nakmali, D. (2011), 'Mechanical properties of stapedial annular ligament', *Medical Engineering & Physics* **33**(3), 330–339.

Grote, J. (1984), 'Tympanoplasty with calcium phosphate', *Archives of Otolaryngology* **110**(3), 197–199.

Grün, A. (2017), 'Ein messaufbau zur messung der übertragungseigenschaften einer mittelohrprothese unter variierendem umgebungsdruck', Term paper (Semesterarbeit), Technische Universität München.

Helmholtz, H. (1868), 'Die Mechanik der Gehörknöchelchen und des Trommelfells', *Pflüger, Archiv für die Gesammte Physiologie des Menschen und der Thiere* pp. 1–60.

Hess-Erga, J., Moller, P. & Vassbotn, F. S. (2013), 'Long-term hearing result using Kurz titanium ossicular implants.', *European archives of oto-rhino-laryngology : official journal of the European Federation of Oto-Rhino-Laryngological Societies (EUFOS) : affiliated with the German Society for Oto-Rhino-Laryngology - Head and Neck Surgery* **270**(6), 1817–21.

Hildmann, H. & Sudhoff, H. (2006), *Middle Ear Surgery*, Springer Science & Business Media.

Hoffstetter, M. (2011), 'Ability to Adjust in Length and Damping: Missing Features in Middle Ear Implants?', *Recent Patents on Biomedical Engineering* **4**(1), 20–25.

Huber, A., Linder, T., Ferrazzini, M., Schmid, S., Dillier, N., Stoeckli, S. & Fisch, U. (2001), 'Intraoperative assessment of stapes movement.', *The Annals of otology rhinology and laryngology* **110**(1), 31–35.

Huber, A. M. & Eiber, A. (2011), 'Vibration properties of the ossicle and cochlea and their importance for our hearing system', *HNO* **59**(3), 255–60.

Hurst, H. (1973), 'Ossicle replacement prosthesis'. US 3,710,399.

Hüttenbrink, K. B. (1988), 'The mechanics of the middle-ear at static air pressures: the role of the ossicular joints, the function of the middle-ear muscles and the behaviour of stapedial prostheses.', *Acta Oto-Laryngologica* **105**(sup451), 1–35.

Hüttenbrink, K., Zahnert, T., Hofmann, G. & Bornitz, M. (2005), 'Flexible ossicular prosthesis'. EP 1,498,088.

Jahnke, K., Plester, D. & Heimke, G. (1979), 'Aluminiumoxid-keramik, ein bioinertes material für die mittelohrchirurgie', *European Archives of Oto-Rhino-Laryngology* **223**(2), 373–376.

Kim, N.-H. (2014), *Introduction to Nonlinear Finite Element Analysis*, Vol. 21, Springer Science & Business Media.

Kohl, M. (2002), *Entwicklung von mikroaktoren aus formgedächtnislegierungen*, Forschungszentrum Karlsruhe.

Koike, T., Wada, H. & Kobayashi, T. (2002), 'Modeling of the human middle ear using the finite-element method', *The Journal of the Acoustical Society of America* **111**(3), 1306.

Kraus, E. (2011), 'Ossicular prosthesis having helical coil'. US Patent 8,057,542.

Kuru, I., Maier, H., Müller, M., Lenarz, T. & Lueth, T. C. (2016a), 'A 3D-printed functioning anatomical human middle ear model', *Hearing Research* **340**(October), 204–213.

Kuru, I., Muller, M., Entsfellner, K., Lenarz, T., Maier, H. & Lueth, T. (2014), A new human middle ear model for the biomechanical evaluation of a prosthesis for the ossicular chain reconstruction, *in* 'Robotics and Biomimetics (ROBIO), 2014 IEEE International Conference on', pp. 613–618.

Lenarz, T. & Boenninghaus, H.-G. (2012), *Hals-Nasen-Ohren-Heilkunde*, Springer-Lehrbuch, 14 edn, Springer Berlin Heidelberg, Berlin, Heidelberg.

Lenkauskas, E. (1990), 'Wire spring prosthesis for ossicular reconstruction'. US 4,957,507.

Letens, U. (1988), Über die Interpretation von Impedanzmessungen im Gehörgang anhand von Mittelohr-Modellen, PhD thesis, Ruhr-Universität Bochum.

Leysieffer, H., Baumann, J. W., Müller, G. & Zenner, H. P. (1997), 'Ein implantierbarer piezoelektrischer Hörgerätewandler für Innenohrschwerhörige', *HNO* **45**(10), 801–815.

López Ferrer, F. (2015), 'Empirical determination of the optimal shape of a spring-damper-element for a postoperative adjustable middle ear prosthesis', Bachelor's Thesis, Technische Universität München.

Magnan, J., Giquel, L. & Prandi, B. (2001), 'Middle ear prosthesis'. US 6,203,571.

Mankekar, G., ed. (2014), *Implantable Hearing Devices other than Cochlear Implants*, Springer India, New Delhi.

Mardassi, A., Deveze, A., Sanjuan, M., Mancini, J., Parikh, B., Elbedeiwy, A., Magnan, J. & Lavieille, J. (2011), 'Titanium ossicular chain replacement prostheses: prognostic

factors and preliminary functional results.', *European annals of otorhinolaryngology, head and neck diseases* **128**(2), 53–8.

McGrew, R. (1986), 'Telescoping self-adjusting ossicular prostheses'. US 4,601,723.

Meister, H., Stennert, E., Walger, M., Klünter, H.-D. & Mickenhagen, A. (1997), 'Ein Meßsystem zur Überprüfung des akustomechanischen Übertragungsverhaltens von Mittelohrimplantaten', *HNO* **45**(2), 81–85.

Meulemans, J., Wuyts, F. L. & Forton, G. E. J. (2013), 'Middle ear reconstruction using the titanium Kurz Variac partial ossicular replacement prosthesis: functional results.', *JAMA otolaryngology– head & neck surgery* **139**(10), 1017–25.

Mojallal, H., Stieve, M., Krueger, I., Behrens, P., Mueller, P. P. & Lenarz, T. (2009), 'A biomechanical ear model to evaluate middle-ear reconstruction', *International journal of audiology* **48**(12), 876–884.

Møller, A. R. (1961), 'Network Model of the Middle Ear', *The Journal of the Acoustical Society of America* **33**(2), 168–176.

Monasta, L., Ronfani, L., Marchetti, F., Montico, M., Vecchi Brumatti, L., Bavcar, A., Grasso, D., Barbiero, C. & Tamburlini, G. (2012), 'Burden of disease caused by otitis media: systematic review and global estimates', *PLoS One* **7**(4), e36226.

Morris, D. P., Bance, M., van Wijhe, R. G., Kiefte, M. & Smith, R. (2004), 'Optimum tension for partial ossicular replacement prosthesis reconstruction in the human middle ear.', *The Laryngoscope* **114**(2), 305–8.

Nishihara, S. & Goode, R. (1994), 'EXPERIMENTAL STUDY OF THE ACOUSTIC PROPERTIES OF INCUS REPLACEMENT PROSTHESES IN A HUMAN TEMPORAL BONE MODEL.', *Otology & Neurotology* **15**(4).

Offergeld, C. (2013), 'Qualitatssicherung nach rekonstruktiver Mittelohrchirurgie', *HNO* **61**(12), 1011–6.

Palva, T., Palva, A. & Karja, J. (1971), 'Results with 2- or 3-legged wire columellization in chronic ear surgery', *Annals of Otology, Rhinology & Laryngology* **80**(5), 760–765.

Reck, R. (1983), 'Bioactive glass ceramic: a new material in tympanoplasty', *The Laryngoscope* **93**(2), 196–199.

Rosowski, J. J., Cheng, J. T., Ravicz, M. E., Hulli, N., Hernandez-Montes, M., Harrington, E. & Furlong, C. (2009), 'Computer-assisted time-averaged holograms of the motion of the surface of the mammalian tympanic membrane with sound stimuli of 0.4–25khz', *Hearing research* **253**(1), 83–96.

Rosowski, J. J., Davis, P. J., Merchant, S. N., Donahue, K. M. & Coltrera, M. D. (1990), 'Cadaver middle ears as models for living ears: comparisons of middle ear input immittance.', *The Annals of otology, rhinology, and laryngology* **99**(5 Pt 1), 403–12.

Roth, M. (2016), Development of a finite element model for a postoperative adaptable middle ear prosthesis, Master's thesis, Technische Universität München.

Sauer, K. (2016), Dynamische und statische Funktionalität einer neuartigen Mittelohrprothese mit integriertem silikongestützten Gelenk, PhD thesis, Technische Universität Dresden.

Schmerber, S., Troussier, J., Dumas, G., Lavieille, J.-P. & Nguyen, D.-q. (2006), 'Hearing results with the titanium ossicular replacement prostheses.', *European archives of oto-rhino-laryngology : official journal of the European Federation of Oto-Rhino-Laryngological Societies (EUFOS) : affiliated with the German Society for Oto-Rhino-Laryngology - Head and Neck Surgery* **263**(4), 347–54.

Schünke, M., Schulte, E., Schumacher, U., Voll, M. & Wesker, K. (20006), *Prometheus LernAtlas der Anatomie: Kopf und Neuroanatomie.*, Thieme.

Sennaroglu, L. (2016), 'Using cements for ossiculoplasty', *The Journal of Laryngology & Otology* **130**(S3), S28.

Shea, J. (1958*a*), 'Fenestration of the oval window', *Annals of Otology, Rhinology & Laryngology* **67**(4), 932–951.

Shea, J. (1958*b*), 'Tympanoplasty in chronic right otitis media: a case report', *Memphis Med* **33**, 271–275.

Shea, J. (1976), 'Plastipore total ossicular replacement prosthesis', *The Laryngoscope* **86**(2), 239–240.

Statistisches Bundesamt (2014), Operationen und Prozeduren der vollstationären Patientinnen und Patienten der Krankenhäuser - 2013, Technical report, Statistisches Bundesamt, Wiesbaden.

Stieger, C., Bernhard, H., Waeckerlin, D., Kompis, M., Burger, J. & Haeusler, R. (2007), 'Human temporal bones versus mechanical model to evaluate three middle ear transducers.', *Journal of rehabilitation research and development* **44**(3), 407–15.

Strutz, J. & Mann, W. (2017), *Praxis der HNO-Heilkunde, Kopf- und Halschirurgie*, Thieme.

Taschke, H., Weistenhöfer, C. & Hudde, H. (2000), 'A Full-Size Physical Model of the Human Middle Ear', *Acta Acustica united with Acustica* **86**(1), 103–116.

Theissing, J., Rettinger, G. & Werner, J. A. (2006), *HNO-Operationslehre: mit allen wichtigen Eingriffen*, 4 edn, Georg Thieme Verlag, Stuttgart.

Tonndorf, J. & Khanna, S. M. (1972), 'Tympanic-Membrane Vibrations in Human Cadaver Ears Studied by Time-Averaged Holography', *The Journal of the Acoustical Society of America* **52**(4B), 1221–1233.

Vassbotn, F. S., Mø ller, P. & Silvola, J. (2007), 'Short-term results using Kurz titanium ossicular implants.', *European archives of oto-rhino-laryngology : official journal of the European Federation of Oto-Rhino-Laryngological Societies (EUFOS) : affiliated with the German Society for Oto-Rhino-Laryngology - Head and Neck Surgery* **264**(1), 21–5.

Wiens, G., Antonelli, P., Rippere, T. & Rao, K. (2013), 'Method and apparatus for in-situ adjustability of a middle ear prosthesis'. US 8,435,291.

Wullstein, H. (1952), 'Operationen am mittelohr mit hilfe des freien spaltlappentransplantates', *Arch Otorhinolarynol* **161**, 422–435.

Wullstein, H. (1956), 'Theory and practice of tympanoplasty', *The Laryngoscope* **66**(8), 1076–1093.

Yamada, H. & Goode, R. L. (2010), 'A self-adjusting ossicular prosthesis containing polyurethane sponge', *Otology & Neurotology* **31**(9), 1404–1408.

Yu, H., He, Y., Ni, Y., Wang, Y., Lu, N. & Li, H. (2013), 'PORP vs. TORP: a meta-analysis.', *European archives of oto-rhino-laryngology : official journal of the European Federation of Oto-Rhino-Laryngological Societies (EUFOS) : affiliated with the German Society for Oto-Rhino-Laryngology - Head and Neck Surgery* **270**(12), 3005–17.

Zahnert, T. (2003), 'Lasers in ear research', *Laryngo- rhino- otologie* **82 Suppl 1**(S 1), S157–80.

Zahnert, T. (2011), 'Rekonstruktion der Ossikelkette mit passiven Implantaten', *HNO* **59**(10), 964–973.

Zwicker, E. & Fastl, H. (2013), *Psychoacoustics: Facts and Models*, Springer Series in Information Sciences, Springer Berlin Heidelberg.

Zwislocki, J. (1962), 'Analysis of the Middle-Ear Function. Part I: Input Impedance', *The Journal of the Acoustical Society of America* **34**(9B), 1514.

Appendix

APPENDIX A

Acronyms

2D Two Dimensional

3D Three Dimensional

ABG Air-Bone-Gap

ASTM American Society for Testing and Materials

CHL Conductive Hearing Loss

CT Computed Tomography

μCT Micro Computed Tomography

CWD Canal-Wall-Down

CWU Canal-Wall-Up

DoF Degrees of Freedom

DICOM Digital Imaging and Communications in Medicine

GUI Graphical User Interface

HA Hydroxyapatite

ICW Intact-Canal-Wall

IMEHD Implantable Middle Ear Hearing Device

IMJ Incudomalleolar Joint

ISJ Incudostapedial Joint

IE Inner Ear

LCE Load Compensation Experiment

LDV Laser-Doppler-Velocimeter

MIC Malleus-Incus-Complex

ME Middle Ear

OE Outer Ear

ORP Ossicular Replacement Prosthesis

OW Oval Window

PAM Postoperative Adjustable Middle Ear Prosthesis

PORP Partial Ossicular Replacement Prosthesis

PTA Pure Tone Audiometry

PTFE Polytetrafluoroethylene

RW Round Window

SFP Stapes Footplate

SLS Selective Laser Sintering

SNHL Sensorineural Hearing Loss

SRS Stapes' Response to Sound

SSS Stapes Superstructure

SI International System of Units

SP Sound Pressure

SPL Sound Pressure Level

TB Temporal Bone

TORP Total Ossicular Replacement Prosthesis

TM Tympanic Membrane

VOI Volume of interest

APPENDIX B

List of Publications

Kuru, I., Gonenc, B., Balicki, M., Handa, J., Gehlbach, P., Taylor, R. H. and Iordachita, I. (2012), 'Force sensing micro-forceps for robot assisted retinal surgery', in *Annual International Conference of the IEEE Engineering in Medicine and Biology Society (EMBC)*, 2012 IEEE International Conference, p. 1401.

Entsfellner, K., **Kuru, I.**, Maier, T., Gumprecht, J. D. J. and Lueth, T. C. (2014), 'First 3D printed medical robot for ENT surgery-Application specific manufacturing of laser sintered disposable manipulators', *in Intelligent Robots and Systems (IROS)*, 2014 IEEE/RSJ International Conference on, p. 4278-4283.

Kuru, I., Müller, M., Entsfellner, K., Lenarz, T., Maier, H. and Lueth, T.C. (2014), 'A new human middle ear model for the biomechanical evaluation of a prosthesis for the ossicular chain reconstruction', *in Robotics and Biomimetics (ROBIO)*, 2014 IEEE International Conference on, p. 613-618.

Kuru, I., Coy, J., and López Ferrer, F., Lenarz, T., Maier, H. and Lueth, T. C. (2015), 'A new postoperative adjustable prosthesis for ossicular chain reconstructions, *in Robotics and Biomimetics (ROBIO)*, 2015 IEEE International Conference on, p. 385-390.

Entsfellner, K., **Kuru, I.**, Strauss, G. and Lueth, T. C. (2015), 'A new physical temporal bone and middle ear model with complete ossicular chain for simulating surgical procedures, *in Robotics and Biomimetics (ROBIO)*, 2015 IEEE International Conference on, p. 1654-1659.

Kuru, I., Maier, H., Müller, M., Lenarz, T. and Lüth, T. C. (2015), 'A new 3D printed functional human middle ear model', *in 7th International Symposium on Middle Ear Mechanics in Research and Otology*.

Kuru, I., Maier, H., Müller, M., Lenarz, T. and Lueth, T. C. (2016), 'A 3D-printed functioning anatomical human middle ear model', *Hearing research* **340** (October), 204-213.

Maier, H., **Kuru, I.**, Lueth, T. C. and Lenarz, T (2016), 'A Functional 3D Printed Human Middle Ear Model', *The Journal of Laryngology & Otology* **130** (S3), p. S92.

Kuru, I., Maier, H., Lenarz, T., and Lueth, T. C. (2016), 'A New Postoperative Adjustable Middle Ear Prosthesis', *The Journal of Laryngology & Otology* **130** (S3), p.S1173.

Kuru, I., Roth, M., López Ferrer, F., Krieger, Y. S., Lenarz, T., Maier, H. and Lueth, T. C. (2016), 'Design and manufacturing concept of a postoperative adjustable prosthesis for ossicular chain reconstructions', *in Biomedical Robotics and Biomechatronics (BioRob)*, 2016 6th IEEE International Conference on, p. 1035-1040.

Krieger, Y., Brecht, S. V., Roppenecker, D. B., **Kuru, I.**, and Lueth, T. C. (2016), 'First Approach towards a Manipulator System for Single-Incision Laparoscopic Surgery Using Rapid Manufacturing', in *CURAC*, p. 111-116.

Krieger, Y. S., Roppenecker, D. B., **Kuru, I.** and Lueth, T. C. (2017), 'Multi-arm snake-like robot', *Robotics and Automation (ICRA)*, 2017 IEEE International Conference on, p. 2490-2495.

APPENDIX C

Measurement Results with the 3D Printed Middle Ear Model

Table C.1.: All results for the transfer function measurements with the middle ear models. The green cells show a sound-noise-ratio (SNR) lower than 6dB, the yellow cells show SNR between 6-12 dB and the red cells show SNR higher than 12 dB for that measurement.

Freq. [Hz]	Model 1	Model 1 (2 Rings)	Model 1 (6 Rings)	Model 2	Model 2 (2 Rings)	Model 2 (6 Rings)
125	-50.4	-48.2	-51.1	-63.9	-62.7	-67.5
250	-52.7	-50.9	-50.0	-58.1	-56.4	-71.1
500	-47.5	-46.9	-48.2	-44.1	-42.1	-52.9
1000	-47.2	-47.5	-47.7	-61.5	-65.0	-70.2
2000	-58.5	-57.1	-57.0	-69.6	-73.2	-70.4
3000	-52.5	-53.0	-55.7	-65.3	-65.3	-67.4
4000	-63.5	-60.8	-65.8	-59.6	-70.3	-64.5
6000	-81.0	-79.0	-77.5	-80.7	-87.4	-87.4
8000	-85.1	-84.7	-79.1	-76.2	-79.8	-71.3
10000	-89.0	-84.8	-83.6	-63.7	-84.5	-77.9

Freq. [Hz]	Model 3.1	Model 3.1 (2 Rings)	Model 3.1 (6 Rings)	Model 3.2	Model 3.2 (2 Rings)	Model 3.2 (6 Rings)	Model 3.3	Model 3.3 (2 Rings)	Model 3.3 (6 Rings)
125	-43.3	-41.6	-41.3	-36.7	-34.8	-33.3	-27.9	-23.5	-23.9
250	-44.0	-42.1	-40.2	-38.0	-36.2	-33.6	-29.0	-30.0	-29.9
500	-37.4	-36.5	-37.0	-38.1	-37.7	-31.3	-28.5	-29.3	-29.2
1000	-36.2	-35.0	-41.9	-35.9	-39.6	-43.7	-30.4	-29.4	-29.5
2000	-53.9	-59.5	-64.2	-50.2	-54.1	-58.2	-44.7	-41.8	-41.7
3000	-64.5	-67.4	-64.3	-74.0	-75.2	-77.1	-69.3	-66.8	-67.0
4000	-53.0	-60.7	-69.7	-58.5	-72.2	-68.4	-63.7	-60.6	-60.2
6000	-68.0	-78.1	-81.8	-70.3	-73.2	-74.9	-77.6	-75.2	-76.0
8000	-79.5	-73.8	-71.3	-78.3	-84.2	-93.8	-77.9	-80.2	-79.1
10000	-74.6	-79.7		-79.9	-81.7	-81.5	-74.6	-81.9	-83.6

Freq. [Hz]	Model 3.4	Model 3.5	Model 3.6	Model 4.1	Model 4.2	Model 5.1	Model 5.2
125	-46.2	-47.4	-36.1	-28.2	-20.1	-29.6	-27.1
250	-47.4	-49.6	-37.3	-28.7	-19.6	-31.6	-29.0
500	-44.1	-47.1	-31.4	-20.8	-10.6	-24.0	-19.5
1000	-41.8	-43.9	-31.4	-34.5	-25.0	-29.7	-32.5
2000	-58.3	-51.2	-60.3	-49.0	-45.3	-44.6	-41.3
3000	-58.2	-78.8	-68.8	-55.1	-60.9	-68.4	-73.4
4000	-63.4	-73.5	-69.7	-51.2	-62.6	-70.8	-66.1
6000	-86.1	-82.5	-83.2	-87.4	-82.3	-81.1	-72.3
8000	-65.1	-79.1	-80.3	-96.0	-101.9	-93.6	-90.4
10000	-76.6	-78.2	-62.4	-85.6	-107.8	-92.4	-84.6

APPENDIX D

Axial and Radial Stiffness Measurements

Table D.1.: The results of the axial and radial stiffness measurements for conic PAM.

	Axial								Radial			
	PAMco-4.0		PAMco-4.5		PAMco-5.5		PAMco-6.0		PAMco-4.0		PAMco-4.5	
Nr.	X [mm]	F [N]	X [mm]	F [N]	X [mm]	F [N]	X [mm]	F [N]	X [mm]	F [N]	X [mm]	F [N]
1	0.027	0.006	0.026	0.001	0.026	0.002	0.027	0.002	0.027	0.001	0.027	0.001
	0.054	0.009	0.053	0.006	0.053	0.006	0.054	0.009	0.054	0.003	0.054	0.001
	0.081	0.012	0.080	0.009	0.080	0.008	0.081	0.012	0.081	0.002	0.081	0.001
	0.107	0.014	0.107	0.011	0.107	0.007	0.108	0.014	0.108	0.002	0.108	0.001
	0.134	0.013	0.134	0.010	0.134	0.012	0.135	0.014	0.135	0.003	0.135	0.002
	0.161	0.018	0.161	0.014	0.161	0.014	0.162	0.016	0.162	0.003	0.161	0.003
	0.188	0.021	0.188	0.016	0.188	0.012	0.189	0.021	0.188	0.004	0.188	0.003
	0.215	0.024	0.215	0.019	0.214	0.018	0.215	0.021	0.215	0.005	0.215	0.003
	0.242	0.025	0.241	0.020	0.241	0.021	0.242	0.024	0.242	0.006	0.242	0.003
	0.269	0.026	0.268	0.021	0.268	0.022	0.269	0.026	0.269	0.004	0.269	0.003
	0.295	0.023	0.295	0.015	0.295	0.020	0.296	0.023				
2	0.027	0.002	0.027	0.001	0.026	0.001	0.027	0.002	0.027	0.001	0.027	0.001
	0.054	0.005	0.054	0.002	0.053	0.004	0.054	0.007	0.054	0.002	0.054	0.001
	0.081	0.007	0.081	0.004	0.080	0.005	0.081	0.009	0.081	0.002	0.081	0.001
	0.108	0.008	0.108	0.002	0.107	0.007	0.108	0.013	0.108	0.002	0.108	0.001
	0.135	0.011	0.135	0.004	0.134	0.009	0.135	0.018	0.134	0.003	0.135	0.001
	0.162	0.012	0.162	0.008	0.161	0.011	0.162	0.021	0.161	0.003	0.162	0.001
	0.189	0.014	0.189	0.008	0.188	0.011	0.188	0.022	0.188	0.004	0.188	0.002
	0.215	0.014	0.215	0.014	0.214	0.012	0.215	0.023	0.215	0.006	0.215	0.002
	0.242	0.014	0.242	0.018	0.241	0.015	0.242	0.018	0.242	0.006	0.242	0.002
	0.269	0.018	0.269	0.021	0.268	0.016	0.269	0.024	0.269	0.007	0.269	0.002
	0.296	0.019	0.296	0.023	0.295	0.017	0.296	0.029				
3	0.027	0.004	0.027	0.002	0.026	0.002	0.027	0.002	0.027	0.002	0.027	0.001
	0.054	0.006	0.054	0.005	0.053	0.004	0.054	0.007	0.054	0.002	0.054	0.001
	0.081	0.009	0.081	0.008	0.080	0.006	0.081	0.009	0.081	0.002	0.08	0.002
	0.108	0.011	0.108	0.007	0.107	0.008	0.108	0.013	0.107	0.003	0.107	0.002
	0.135	0.008	0.135	0.013	0.134	0.010	0.135	0.018	0.134	0.004	0.134	0.002
	0.161	0.012	0.162	0.016	0.161	0.012	0.162	0.021	0.161	0.004	0.161	0.002
	0.188	0.016	0.189	0.018	0.188	0.014	0.188	0.022	0.188	0.004	0.188	0.003
	0.215	0.018	0.215	0.020	0.214	0.015	0.215	0.023	0.215	0.005	0.215	0.004
	0.242	0.019	0.242	0.021	0.241	0.018	0.242	0.018	0.242	0.004	0.242	0.004
	0.269	0.016	0.269	0.020	0.268	0.018	0.269	0.024	0.269	0.006	0.268	0.004
	0.296	0.020	0.296	0.021	0.295	0.019	0.296	0.029				

Table D.2.: The results of the axial and radial stiffness measurements for cubic PAM

	Axial						Radial					
	PAMcu-4.0		PAMcu-4.5		PAMcu-5.5		PAMcu-4.0		PAMcu-4.5		PAMcu-5.5	
Nr.	X [mm]	F [N]	X [mm]	F [N]	X [mm]	F [N]	X [mm]	F [N]	X [mm]	F [N]	X [mm]	F [N]
1	0.027	0.010	0.027	0.011	0.026	0.001	0.026	0.001	0.027	0.001	0.027	0.001
	0.054	0.018	0.054	0.016	0.053	0.004	0.053	0.002	0.053	0.002	0.054	0.001
	0.081	0.023	0.081	0.019	0.080	0.007	0.080	0.004	0.080	0.002	0.081	0.002
	0.107	0.024	0.108	0.028	0.107	0.009	0.107	0.004	0.107	0.003	0.108	0.002
	0.134	0.030	0.135	0.030	0.134	0.009	0.134	0.004	0.134	0.003	0.135	0.002
	0.161	0.035	0.162	0.032	0.161	0.018	0.161	0.005	0.161	0.004	0.162	0.002
	0.188	0.036	0.188	0.037	0.188	0.019	0.188	0.004	0.188	0.005	0.188	0.002
	0.215	0.039	0.215	0.043	0.215	0.024	0.215	0.005	0.215	0.004	0.215	0.002
	0.242	0.044	0.242	0.048	0.241	0.028	0.241	0.006	0.242	0.004	0.242	0.002
	0.269	0.048	0.269	0.046	0.268	0.030	0.268	0.007	0.268	0.004	0.269	0.002
	0.296	0.047	0.296	0.050	0.295	0.030	0.295	0.007	0.295	0.005		
2	0.027	0.001	0.027	0.006	0.027	0.001	0.027	0.002	0.026	0.001	0.027	0.002
	0.054	0.010	0.054	0.019	0.054	0.010	0.054	0.002	0.053	0.002	0.054	0.002
	0.081	0.018	0.081	0.026	0.081	0.013	0.081	0.002	0.080	0.002	0.081	0.002
	0.108	0.021	0.108	0.031	0.108	0.011	0.108	0.003	0.107	0.002	0.108	0.001
	0.135	0.023	0.135	0.033	0.135	0.018	0.134	0.004	0.134	0.003	0.134	0.002
	0.161	0.030	0.162	0.039	0.162	0.023	0.161	0.004	0.161	0.003	0.161	0.003
	0.188	0.037	0.189	0.045	0.188	0.027	0.188	0.004	0.188	0.003	0.188	0.002
	0.215	0.042	0.215	0.052	0.215	0.030	0.215	0.004	0.215	0.003	0.215	0.003
	0.242	0.046	0.242	0.055	0.242	0.028	0.242	0.005	0.241	0.004	0.242	0.003
	0.269	0.046	0.269	0.043	0.269	0.025	0.269	0.005	0.268	0.004	0.269	0.003
			0.296	0.059	0.296	0.030	0.296	0.005	0.295	0.004		
3	0.027	0.008	0.027	0.002	0.027	0.003	0.027	0.002	0.027	0.002	0.027	0.001
	0.054	0.014	0.054	0.013	0.054	0.011	0.054	0.002	0.053	0.002	0.054	0.002
	0.081	0.014	0.081	0.019	0.081	0.016	0.081	0.002	0.080	0.003	0.081	0.002
	0.108	0.025	0.108	0.025	0.108	0.020	0.108	0.004	0.107	0.003	0.107	0.002
	0.134	0.030	0.134	0.030	0.135	0.022	0.135	0.004	0.134	0.004	0.134	0.002
	0.161	0.035	0.161	0.032	0.162	0.017	0.162	0.004	0.161	0.004	0.161	0.002
	0.188	0.037	0.188	0.033	0.188	0.023	0.188	0.004	0.188	0.004	0.188	0.004
	0.215	0.033	0.215	0.039	0.215	0.026	0.215	0.007	0.215	0.004	0.215	0.004
	0.242	0.040	0.242	0.045	0.242	0.026	0.242	0.007	0.242	0.005	0.242	0.004
	0.269	0.043	0.269	0.050	0.269	0.023	0.269	0.007	0.268	0.005	0.269	0.004
	0.296	0.043	0.296	0.053	0.296	0.028	0.296	0.007	0.295	0.005		